

UC Irvine

UC Irvine Electronic Theses and Dissertations

Title

Epigenetic control of medial habenula function in cocaine-associated behaviors

Permalink

<https://escholarship.org/uc/item/5mq6p0k4>

Author

Lopez, Alberto

Publication Date

2018

Copyright Information

This work is made available under the terms of a Creative Commons Attribution License, available at <https://creativecommons.org/licenses/by/4.0/>

Peer reviewed|Thesis/dissertation

UNIVERSITY OF CALIFORNIA,
IRVINE

Epigenetic control of medial habenula function in cocaine-associated behaviors

DISSERTATION

submitted in partial satisfaction of the requirements
for the degree of

DOCTOR OF PHILOSOPHY

in Biological Sciences

by

Alberto J. López

Dissertation Committee:

Professor Marcelo A. Wood, Chair
Assistant Professor Christie D. Fowler
Assistant Professor Stephen V. Mahler

2018

© 2018 Alberto J. López
Portion of Chapters 1 & 3 © 2018 John Wiley & Sons, Inc.
Portion of Chapter 2 © 2016 The Journal of Neuroscience

Dedicatoria

A mi Abuelita Ethel

quien me mostró lo que es ser fuerte, valiente, e inteligente

To my wife Christina López

of whom I am completely undeserving. Your love and support are the only reasons I've made it this far and I'm so incredibly lucky to have a true equal with whom to share this adventure. One sky, one destiny.

To my family, Lorna, Jaime, Jaime Salvador, Cecilia, Elena, and the Burgarts

who have all helped provide me with opportunities they never had.

To the friends I've made along the way (including Drs. Andre White, Janine Kwapis, and Thekla Hemstedt, & Matt Saucedo, Rianne Campbell, Amni Al-Kachak, Matt Kwapis, Sarah Cross, and the Maddi)

who have always provided incredible, and often thankless, support.

To my various sources of caffeine throughout the Southland

that have stimulated my life and work.

“Simple, maybe, but not easy. There’s nothing easy about two men sharing one life...You see, sacrifice - that’s the price of a good trick.”

Alfred Borden, *The Prestige*¹

Contents

List of Figures iv

Acknowledgments..... v

Curriculum Vitae vi

Abstract of the Dissertation xii

Introduction..... 1

 Substance Use Disorders, Drug-Induced Adaptations, & Cocaine-Associated Memories 1

 A Brief History of Epigenetics..... 7

 Epigenetics in Learning & Memory..... 12

 Epigenetic Regulation of Reward Circuitry and Response to Drugs of Abuse 17

 Structure and Function of the Medial Habenula 22

 Circuitry and Organization..... 22

 Role in Behavior 25

Chapter 1: Functional Adaptations of the Medial Habenula During Reinstatement of Conditioned Place Preference..... 35

Chapter 2: Controlling Neuronal Function Through Chemogenetics..... 43

Chapter 3: Medial Habenula Cholinergic Neurons Regulate Cocaine-primed Reinstatement..... 64

Chapter 4: Epigenetic Control of Habenula-mediated Cocaine-associated Behaviors..... 77

Chapter 5: Conclusions and Moving Forward 96

References 103

List of Figures

Figure 0.1 Ramon y Cajal drawing of the epithalamus	23
Figure 1.1 The MHb responds to cocaine re-exposure.	38
Figure 1.2 The MHb is engaged by cocaine-primed reinstatement of CPP.	40-41
Figure 1.3 Cocaine does not directly alter vMHb activity.	42
Figure 2.1 Bidirectional modulation of dorsal hippocampus via hSyn-DREADDs affects long-term memory processes.	52
Figure 2.2 Characterization of baseline synaptic transmission in hippocampal slices expressing hSyn-driven excitatory and inhibitory DREADD receptors.	55
Figure 2.3 Long-term plasticity changes associated with hSyn-driven DREADD receptor expression in adult hippocampal slices.	56
Figure 2.4 Promotor-specific effects of CaMKII α DREADD receptors on synaptic transmission and long-term plasticity.	57
Figure 2.5 Modulation of dorsal hippocampus via CaMKII α -DREADDs leads to bidirectional changes in long-term memory processes.	60
Figure 3.1 Combinatorial approach using Cre-dependent DREADD in Cre-drive line.	68
Figure 3.2 Chemogenetic activation of MHb ^{ChAT} artificially induces reinstatement of CPP.	70
Figure 3.3 CNO-priming does not induce reinstatement of CPP in DREADD-free animals.	72
Figure 4.1 Use of TdTomato ^{+/-} ::ChAT-Cre ^{Cre/+} reporter mice to isolate MHb neurons.	85
Figure 4.2 HDAC3 occupancy is altered in the MHb in response to cocaine-primed reinstatement.	86
Figure 4.3 Expression of DIO-HDAC3 ^{W.T.} and -HDAC3 ^{Y298H} is limited to Cre-expressing cell populations.	87
Figure 4.4 Loss of HDAC3 deacetylase activity generates an extinction-resistant CPP.	88
Figure 4.5 HDAC3 ^{W.T.} in the MHb does not affect cocaine-associated behaviors.	89
Figure 4.6 Expression of DIO-Nurr2c in the vMHb alters cocaine-primed reinstatement behavior.	90

Acknowledgments

I would like to thank my mentors, Drs. Marcelo Wood, Dina Matheos, and Thomas Kash, who gave me a chance and helped mold me into the scientist I am today.

I would like to thank my committee members, Drs. Christie Fowler and Steve Mahler for consistently challenging me to grow intellectually.

I would like to acknowledge various collaborators for their contributions to my work and would like to thank: Dr. Eniko Kramar for providing electrophysiological recordings of the hippocampus, Dr. Vanessa Scarfone for technical assistance conducting FACS experiments, Yousheng Jia and Dr. Gary Lynch for providing whole-cell recordings of the MHb and intellectual input on vMHb function, and various members of the Wood lab for assistance on conducting experiments including Drs. Andre White, Janine Kwapis, Annie Vogel-Ciernia, and Yasaman Alagband & Keith Sakata, Monica Espinoza, Amni Al-Kachak, Philip Hwang, Rianne Campbell, and Om Chitnis.

Permission to use copyrighted material has been granted by the Society for Neuroscience Central Office and by John Wiley and Sons.

Curriculum Vitae

Alberto J. López

ajlopez1@uci.edu

Current Position: Doctoral Candidate

University of California, Irvine
Department of Neurobiology and Behavior
Center for the Neurobiology of Learning & Memory
Wood Lab

Education

2013-Present *University of California, Irvine, Irvine, CA*
Biological Sciences, Ph.D. Candidate
Wood Lab
Cumulative G.P.A.: 3.99

2007-2011 *Duke University, Durham, NC*
Neuroscience, B.S.
Minors: Chemistry, Classical Studies (Concentration in Classical Civilizations)

Research and Work Experience

2013-Present *Doctoral Candidate, Dr. Marcelo Wood Laboratory, University of California, Irvine*

2011-2013 *Laboratory Technician and Laboratory Animal Coordinator, Dr. Thomas Kash Laboratory, UNC Chapel Hill*

2008-2011 *Undergraduate Research Assistant, Dr. Henry Yin Laboratory, Duke University*

2007-2011 *Student Athletic Trainer and Head Student Trainer, Duke University Football*

Funding

2017-Present *NIH Blueprint Diversity Specialized Individual Predoctoral to Postdoctoral Advancement in Neuroscience (D-SPAN) Award (F99/K00)*
National Institute of Neurological Disorders and Stroke: F99NS105217
“Role of a medial habenula circuit and Nr4a2 in regulating cocaine action during reinstatement”
Submitted: 4/2017; Funded: 9/2017
Impact Score: 18
PI: López

2017 *Ruth L. Kirschstein National Research Service Award Individual Predoctoral Fellowship to Promote Diversity in Health-Related Research (F31-Diversity)*
National Institute on Drug Abuse: F31DA041838
“Role of a medial habenula circuit and Nr4a2 in cocaine-induced reinstatement”
Submitted: 4/2016; Funded: 2/2017
Impact Score: 19; Percentile: 4
PI: López

2016-2017 *Diversity Supplement NIMH R01MH101491: Role of neuron-specific nucleosome remodeling in intellectual disability*
National Institute on Mental Health
PI: Wood

- 2014-2016 *Initiative for Maximizing Student Development (MBRS-IMSD) Program Fellowship Training Grant: GM055246*
Ayala School of Biological Sciences, University of California, Irvine
- 2014-2015 *Graduate Assistance in Areas of National Need (GAANN) Fellowship*
Ayala School of Biological Sciences, University of California, Irvine

Honors and Awards

- 2018 *Roger W. Russell Scholar's Award – Recipient: \$1000*
Center for the Neurobiology of Learning & Memory, University of California, Irvine
- 2017 *NIDA Diversity Scholar Travel Award – Recipient: \$1000*
National Institute on Drug Abuse, NIH
- 2017 *Howard A. Schneiderman Award – Recipient: \$5000*
Ayala School of Biological Sciences, University of California, Irvine
- 2017 *Ford Foundation Dissertation Fellowship – Honorable Mention*
Ford Foundation
- 2016 *CSHL Cellular Biology of Addiction Course – Attendee*
CSHL Travel Award: \$1500
Cold Spring Harbor Laboratory
- 2016 *Fine Science Tools Graduate Travel Award in Neurobiology – Recipient: \$500*
Ayala School of Biological Sciences, University of California, Irvine
- 2016 *Renee Harwick Advanced Graduate Student Award: \$1000*
CNLM, University of California, Irvine
- 2015 *Graduate Fellowship Award – Recipient: \$1000*
Ayala School of Biological Sciences, University of California, Irvine
- 2015 *Fine Science Tools Graduate Travel Award in Neurobiology – Recipient: \$500*
Ayala School of Biological Sciences, University of California, Irvine
- 2015 *CNLM Data Blitz – First Prize: \$100*
CNLM Conference on the Neurobiology of Learning and Memory, University of California, Irvine
- 2015 *Ford Foundation Predoctoral Fellowship – Honorable Mention*
Ford Foundation
- 2015 *NSF Graduate Research Fellowship Program – Honorable Mention*
National Science Foundation
- 2015 *REMIND Outstanding Poster Presentation – First Prize: \$100*
Emerging Scientists Symposium, UCI MIND, University of California, Irvine
- 2014-2016 *Neuroscience Scholars Program, Associate;*
Society for Neuroscience
- 2014 *NSF Graduate Research Fellowship Program – Honorable Mention*
National Science Foundation
- 2014 *Ford Foundation Predoctoral Fellowship – Honorable Mention*
Ford Foundation
- 2013 *Graduate Dean's Recruitment Fellowship – Recipient: \$10,000*
University of California, Irvine

Accepted Peer-Reviewed Publications

1. **López AJ**, Gia Y, White AO, Kwapis JL, Espinoza ME, Hwang PH, Campbell R, Alaghband Y, Chitnis O, Matheos DP, Lynch G, Wood MA (2018) Medial habenula cholinergic signaling regulates cocaine-associated relapse-like behavior. *Addiction Biology*, doi: 10.1111/adb12605
2. Shu G, Kramár EA, **López AJ**, Huynh G, Wood MA, Kwapis JL (2018) Deleting HDAC3 rescues long-term memory impairments induced by disruption of the neuron-specific chromatin remodeling subunit BAF53b. *Learning & Memory* 25:109-114
3. Alaghband Y, Kwapis JL, **López AJ**, White AO, Aimiwu OA, Al-Kachak A, Bodinayake KK, Dang R, Astarabadi M, Matheos DP, Wood MA (2017) Distinct roles for the deacetylase domain of HDAC3 in the hippocampus and medial prefrontal cortex in the formation and extinction of memory. *Neurobiology of Learning and Memory* 145:94-104
4. Vogel Ciernia A, ..., **Lopez A**, ..., Wood MA (2017) Mutation of neuron-specific chromatin remodeling subunit BAF53b: rescue of plasticity and memory by manipulating acting remodeling. *Learning and Memory* 24:199-209
5. Kwapis JL, Alaghband Y, **López AJ**, White AO, Campbell RR, Dang RT, Rhee D, Tran AV, Carl AE, Matheos DP, Wood MA (2016) Context and Auditory Fear are Differentially Regulated by HDAC3 Activity in the Lateral and Basal Subnuclei of the Amygdale. *Neuropsychopharmacology* 42: 1284-1294
6. **Lopez AJ**, Kramar E, Matheos D, Kwapis JL, White AO, Vogel-Ciernia A, Wood MA (2016) Promoter specific effects of DREADD modulation on synaptic plasticity and hippocampal learning. *Journal of Neuroscience* 36(12):3588-99
7. White A.O., Kramár E.A., **Lopez A.J.**, Kwapis J.L., Doan J., Saldana D., Davatolhagh M.F., Matheos D.P., and Wood M.A. (2016). The role of neuron-specific nucleosome remodeling in cocaine-associated memories. *Nature Communications* 7: 11725
8. Li C., ..., **Lopez AJ**, ..., Thomas L. Kash (2016) Mu opioid receptor modulation of dopamine neurons in the periaqueductal gray/dorsal raphe: A role in regulation of pain. *Neuropsychopharmacology*. doi: 10.1038/npp2016.12
9. Marcinkiewicz CA, Dorrier CE, **Lopez AJ**, Thomas L. Kash (2014) Ethanol induced adaptations in 5-HT_{2c} receptor signaling in the bed nucleus of stria terminalis: Implications for anxiety during ethanol withdrawal. *Neuropharmacology*. S0028-3908(14)00309-8

10. Li C., McCall N.M., **Lopez A.J.**, Thomas L. Kash (2013) Alcohol effects on synaptic transmission in periaqueductal gray dopamine neurons. *Alcohol*. 47(4): 279-287
11. Pleil K.E., **Lopez A.**, McCall N., Jijon A.M., Bravo J.P., Kash T.L. (2012). Chronic stress alters neuropeptide Y signaling in the bed nucleus of the stria terminalis in DBA/2J but not C57BL/6J mice. *Neuropharmacology*. 62(4): 1777-86
12. Yu C, Fan D, **Lopez A**, Yin HH. (2012) Dynamic changes in single unit activity and γ oscillations in a thalamocortical circuit during rapid instrumental learning. *PLoS One*. 7(11):e50578
13. Fan D.,..., **Lopez, A.**,...Yin, H.H. (2011). A wireless multi-channel recording system for freely behaving mice and rats. *PLoS One*. 6(7):e22033

Published Reviews

14. Xu X, Sun Y, Holmes T, **López AJ** (2016) Non-canonical connections between the subiculum and hippocampal CA1. *Journal of Comparative Neurology*
15. **Lopez AJ** and Wood MA (2015) Role of nucleosome remodeling in neurodevelopmental and intellectual disability disorders. *Frontiers in Behavioral Neuroscience*, 9:100. Doi:10.3389/fnbeh.2015.00100

In Prep and Submitted Publications

1. Kwapis JL, Alagband Y, Kramár EA, Matheos DP, Rhee D, **López AJ**, Wood MA (2017) HDAC3 contributions to age-related impairments in long-term memory and synaptic plasticity. *Submitted at Neuron*
2. **López AJ**, Hemstедt T, Campbell R, Kwapis J, Hwang P, Chitnis O, Matheos DP, Wood MA. Epigenetic control of habenula circuitry regulates cocaine-associated behaviors. *In Prep*.
3. Alagband Y, Kwapis JL, Kramár EA, Al-Kachak A, Bodinayake KK, **López, AJ**, White AO, Lattal KM, Matheos DP, Wood MA. A novel neuron-specific nBAF subunit is required for the acquisition of cocaine-cue memory. *In Prep*

Abridged Conference Presentations and Abstracts

*Indicates presenter

- A1. **López A.J.***, P. H. Hwang, O. Chitnis, R. R. Campbell, J. L. Kwapis, Y. Alagband, T. Hemstедt, D. P. Matheos, M. A. Wood. Nr4a2 in the medial habenula is a molecular regulator of cocaine reinstatement behaviors. Abstract submission for poster presentation, Society for Neuroscience, Washington D.C., CA, November 2017
- A2. **Alberto J. López***, Espinoza ME, Sakata KM, White AO, Kwapis JL, Al-Kachak A, Alagband Y, Dina P. Matheos, and Dr. Marcelo Wood. Chemogenetic modulation of the medial habenula during cocaine action. Abstract submission for poster presentation,

Society of Neuroscience, San Diego, CA, November 2016

- A3. **Lopez A.J.***, Kramar E., Kwapis J., White A.O., Matheos D., Vogel-Ciernia A., Wood M.A. Promoter specific effects of DREADD modulation on synaptic plasticity and hippocampal learning. Abstract submission for poster presentation, Society for Neuroscience, Chicago, IL, October 2015
- A4. **Lopez, A.J.***, White A.O., Vogel-Ciernia A., Wood, M.A. Bi-directional pharmacogenetic manipulation of the CA1 using DREADDs leads to modulation in object location memory, but not object recognition memory. Abstract submission for poster presentation, Society for Neuroscience, Washington D.C. November 2014.
- A5. **Lopez, A.J.***, Vetreno, R., Crews, F.T., Kash, T.L. Adolescent binge-like ethanol exposure and its effect on the infralimbic prefrontal cortex's role in fear learning. Abstract for poster presentation, Society for Neuroscience, San Diego, CA. November 2013

Invited Seminars and Conference Presentations

- 2018 International Conference on Learning & Memory (Huntington Beach, CA)
2017 Icahn School of Medicine at Mount Sinai; Hurd Lab (New York, NY)
2017 University of California, Los Angeles Brain Research Institute; Wassum Lab (Los Angeles, CA)

Teaching Experience

- 2018 *Guest Lecture* N156: Molecular Mechanisms of Memory
2014-2017 *Administrative Teaching Assistant*, Department of Neurobiology and Behavior, University of California, Irvine
BIO93: From DNA to Organisms; Fall 2014
BIO93: From DNA to Organisms; Fall 2015
N173: Human Neuropsychology; Winter 2017

Student Mentorship

- 2012-2013 **UNC Chapel Hill: Alexis Kendra**
- 2013-2015 **UC Irvine: Keith Sakata**
Excellence in Research – Recipient
Robert Ernst Prize for Excellence in Research in the Biological Sciences - Recipient
Laurence J. Mehlman Memorial Scholarship – Recipient
- 2014-2016 **UC Irvine: Monica Espinoza**
Minority Science Program
Undergraduate Research Opportunities Program
Minority Science Program “Best Presentation”
Annual Biomedical Conference for Minority Students “Best Presentation”
Excellence in Research: *Recipient and Finalist for Further Awards*

Minority Access to Research Careers Scholar
Current: Ph.D. Student Quantitative Biomedical Sciences, Dartmouth

2016-Present **UC Irvine: Philip Hwang**
Excellence in Research: *Recipient and Finalist for Further Awards*

2016-Present **UC Irvine: Om Chitniss**
Undergraduate Research Opportunities Program

Academic Service and Community Outreach

2018 *Program Committee Member*, International Conference on Learning & Memory
2016 *Neurobiology and Behavior Faculty Search Committee*, University of California, Irvine; Department of Neurobiology and Behavior
2014-2015 *Co-coordinator*, Graduate Seminar Series: Neuroblitz, University of California, Irvine; Department of Neurobiology and Behavior
2012-2014 *Founder*, Skype-with-a-Neuroscientist
2009-2011 *Project Leader and Secretary*, Manna Project International Duke Chapter, Duke University
2009 *Mentor*, bSmart, Duke University

Language Skills: Fluent in Spanish

Abstract of the Dissertation

Molecular adaptations within the medial habenula circuitry regulate cocaine-associated behaviors.

By
Alberto J. López

Doctor of Philosophy in Biological Sciences
University of California, Irvine, 2018
Professor Marcelo Wood, Chair

Drugs of abuse, such as cocaine, are known to cause long-term changes in reward circuitry and, ultimately, persistent changes in behavior. Although many critical nodes in the neural circuitry contributing to relapse of drug-seeking behavior have been identified and studied, a full characterization of the networks driving reinstatement of cocaine-seeking remains lacking. One area that may provide further insight to the mechanisms of relapse is the habenula complex, an epithalamic region composed of lateral (LHb) and medial (MHb) substructures. Recent research has demonstrated a role for the MHb in regulating drug-associated behavior; specifically, the MHb has been shown to be a regulator of nicotine-seeking behavior and nicotine withdrawal. Though there is mounting evidence suggesting the MHb is responsible for various behavioral responses to various drugs of abuse, the position of the MHb in regulating relapse-like behaviors remains tenuous. The present dissertation examined the role of the MHb in regulating reinstatement of cocaine-associated behavior. We demonstrate MHb activity is engaged during relapse of cocaine-associated behavior and driving activity in a subset of the MHb population mimics the reinstatement response. Moreover, we identify a unique epigenetic signature at transcription factor *Nr4a2* that is critical for the reinstatement of cocaine-associated behaviors. My studies provide new insight into the role of molecular adaptations within the MHb in regulating substance use disorders.

Introduction

Substance Use Disorders, Drug-Induced Adaptations, & Cocaine-Associated Memories

Substance use disorder (SUD) is a complex chronic neuropsychiatric disease with a dramatic prevalence, both globally and within the United States. As of 2014, the United States is estimated to spend over \$600 billion annually in addressing the health and societal impacts of substance abuse²⁻⁴. SUD has several defining features outlined in the DSM-5, hallmarked by progressive increases in drug-taking behavior, even in the face of adverse consequences⁵. Repeated exposure to drugs of abuse is known to cause long-lasting changes to the neural circuitry underlying memory, reward, and motivated behaviors. These changes are thought to provide the characteristic resilience and persistence of drug-seeking behavior, even following long periods of abstinence. Identifying the neural pathways and molecular mechanisms targeted by drugs of abuse has the potential to significantly alter our understanding and improve treatment of SUD.

Drugs of abuse have been coarsely divided into various subclasses such as psychostimulants (e.g., cocaine, methamphetamine, nicotine, ecstasy), depressants (e.g., alcohol, cannabis, opiates), and hallucinogens (e.g., lysergic acid diethylamide [LSD], mescaline, psilocybin) based on their subjective effects. It is important to note, however, that this categorization does not provide sufficient insight into the functional mechanisms by which each drug operates. Nevertheless, while the somatic effects of each drug of abuse may vary, they all converge in their ability to induce dopamine (DA) release in the mesolimbic pathway; dopaminergic neurons of the ventral tegmental area (VTA) release DA (among other neurotransmitters such as GABA and glutamate) onto the medium spiny neurons (MSNs) of the nucleus accumbens (NAc) (among several other regions including the prefrontal cortex and dorsal striatum). Morphine, for example, is a potent agonist to the G_i-coupled μ -opioid receptor (MOR1), leading to disinhibition of VTA DA neurons, further driving DA release⁶. Alternatively, cocaine

functions primarily as an antagonist to the dopamine transporter (DAT; although it also blocks the serotonin and norepinephrine transporters^{7,8}), leading to increased synaptic DA⁹. Due to its unique pharmacology, cocaine generates a specific molecular and synaptic profile throughout the central nervous system (CNS).

As a result of the dense dopaminergic projection from the VTA to the NAc, the mesoaccumbal pathway is particularly susceptible to changes induced by acute and repeated cocaine exposures. Chronic cocaine has been shown to increase the expression and enzymatic activity of tyrosine hydroxylase (TH), the rate limiting enzyme in DA synthesis, in the VTA, while decreased TH enzymatic activity was measured in the NAc^{10,11}. In addition, chronic cocaine leads to the accumulation of Δ FosB and *Cdk5* in the NAc, believed to be a key compensatory adaptation to the chronic effects of cocaine administration¹²⁻¹⁴. Additionally, the accumulation of Δ FosB coincides with the dysregulation of several CREB-regulated genes, such as *Nr4a2*. In post-mortem tissue of human chronic cocaine users, NR4A2 is downregulated in both the VTA and ventral striatum¹⁵⁻¹⁷. Also known as NURR1, NR4A2 is a nuclear orphan receptor, whose endogenous ligand remains undiscovered. However, it functions as an immediate early gene (IEG) and transcription factor that is of particular importance to the mesolimbic DA pathway and necessary for DA-neuronal development¹⁸⁻²¹. Moreover, while the full range of NR4A2 gene targets is unknown, several genes involved in plasticity and DA signaling that are dysregulated following cocaine are known to be downstream of NR4A2 and include *Bdnf*, *Cebpb*, *Dat*, *Th*, and *Egr1*²²⁻²⁴. Changes to NR4A2 levels could be a byproduct of this compensatory Δ FosB in response to the altered DA reuptake caused by chronic cocaine exposure; NR4A2 effects on DA transmission are likely to be upstream of DAT, as NR4A2 is not known to interact with DAT directly. Outside of the mesolimbic pathway, NR4A2 is a key regulator of memory and plasticity and its importance

in various neurobiological processes will be periodically highlighted throughout the introduction to this dissertation²⁵⁻²⁸.

Nevertheless, it is important to note that many of the cocaine-induced adaptations in gene expression do not occur globally throughout the mesolimbic pathway. Cocaine-mediated dopamine release in the NAc, simultaneously hyperpolarizes D2-receptor expressing MSNs (D2-MSN) and depolarizes D1-receptor expressing MSNs²⁹. This bidirectional response to dopamine is mediated by the opposing G-proteins in the D1- and D2-G-protein coupled receptors: D1-receptors are G_{s/a} coupled while D2-receptors are G_i coupled, leading to activation or inhibition of PKA upon activation by dopamine, respectively^{29,30}. As a result, long-lasting cocaine-mediated changes to the molecular mechanisms within the mesoaccumbal pathway, including unique gene induction and the upstream regulatory mechanisms, often diverge based on these cell-types. For example, while CREB phosphorylation (pCREB) has been shown to occur throughout the NAc in response to cocaine³¹, cocaine exposure significantly upregulates several CREB-regulated plasticity genes in NAc D1-MSNs including *CamkIIa*, *Creb*, *Fosb*, *Sirt1*, and *Nr4a2*, and downregulates these same genes in D2-MSNs³². One mechanism which may mediate these changes in plasticity and gene expression is the bidirectional phosphorylation of the 32kd-dopamine and cAMP response protein phosphatase (DARPP-32). In response to acute cocaine, D1-MSNs enrich with T34-phosphorylated DARPP-32 (pT34), D2-MSNs, conversely, become enriched with T75-phosphorylated DARPP-32^{33,34}. When phosphorylated at Thr34 (pT34), DARPP-32 potently inhibits protein phosphatase 1 (PP1) and enables cAMP-facilitated gene expression; however, when phosphorylated at T75 (pT75), DARPP-32 inhibits PKA signaling cascades^{35,36}. Following prolonged cocaine exposure, D1-MSNs become enriched with pT75-DARPP-32 and D2-MSNs enrich with pT34-DARPP-32³⁷. The cell-type specific balance of

DARPP-32 phosphorylation is a critical mediator of cocaine-associated behaviors and its role in regulating gene expression will be further discussed below.

Ultimately, these cell-type specific changes to gene expression and to the molecular regulators of transcription lead to changes in the mechanisms regulating associative memory, such as synaptic plasticity. Long-term potentiation (LTP; an in-vitro assay often described as a correlate to memory) and synaptic strength are increased in the VTA following various cocaine regimens^{38,39}. However, increased DA signaling from the VTA causes inhibition of D2-MSNs and excitation of D1-MSNs. D2-MSN inhibition blunts LTP and global excitability in response to acute and chronic cocaine in the NAc⁴⁰⁻⁴³. This divergent response is necessary for the rewarding properties of cocaine. Alternatively, cocaine withdrawal is associated with enhanced glutamatergic strength in the NAc that is subsequently blunted by cocaine re-exposure⁴³.

All this to say, the adaptations to cocaine exposures are extensive and fundamentally alter the endogenous function within the VTA-NAc pathway. However, while acute activation of the canonical “reward circuits” (e.g. the mesolimbic dopamine pathway) plays a major role in the rewarding properties of drugs of abuse, activity in this pathway alone fails to encapsulate the gamut of phenotypes in SUD, particularly the propensity to relapse in response to drug-associated cues, even following long periods of abstinence. As such, researchers have focused on identifying not only the mechanisms within the mesolimbic pathway that are engaged during relapse, but also characterizing the various regions that project into and throughout the mesolimbic pathway to regulate the chronic relapsing nature of SUD.

An early observation of human SUD patients is the ability of drug-associated cues to elicit cravings and, ultimately, relapse of drug-seeking behavior^{44,45}. Positive hedonic state and rewarding properties of drugs of abuse, such as cocaine, become associated with the cues and

context of drug exposure. Human imaging studies have shown drug-associated cues or drug re-exposures are able to reengage the neural circuitry activated by the initial drug experience, including hippocampal, prefrontal cortical, and mesolimbic brain regions^{44,46-49}. This phenotype has been reproduced in various animal models of cocaine-associated behaviors, including self-administration and conditioned place preference (CPP). For example, fast scan cyclic voltammetry and GCaMP mediated fiber photometry (both *in vivo* techniques for monitoring neuronal activity in near real-time) have demonstrated increased dopamine release, increased D1-MSN activity, and suppressed D2-MSN activity in response to cocaine predictive cues^{42,50} in the ventral striatum. Moreover, cocaine-induced CPP potentiates NAc-projecting hippocampus neurons that encode the cocaine-paired spatial environment⁵¹. Re-exposure to cocaine-paired cues also replicates several of the molecular phenotypes induced by cocaine, including increased pT34-DARPP-32 and pCREB in the NAc⁵². As with the circuit activity induced by drug-associated cues, several molecular signatures are regenerated in other whose signaling converges into the NAc, including the infra- and prelimbic prefrontal cortices, basolateral- and central amygdalae, dorsal striatum, and hippocampus, among many others. For example, the dorsal hippocampus shows cocaine-paired cue-induced increases in pGluR1, pERK2, and pCREB⁵². It appears that these various brain regions respond not only to the direct pharmacological effects of cocaine, but also generate molecular and cellular memories for the environmental predictors of cocaine experience.

In both human and rodent models of SUD, drug-associated cues re-illicit drug-seeking behavior by mimicking the neurological effects induced by the drug itself, including neural circuit activation. As such, work from several groups have identified a core structure of the circuitry mediating relapse of cocaine-seeking behavior. Specifically, both cue and cocaine-primed reinstatement engage glutamatergic mGluR5-dependent inputs from the prefrontal cortex (PFC),

hippocampus, and amygdala that converge onto ventral pallidum (VP)-projecting NAc neurons⁵³⁻
⁵⁷. Nevertheless, a direct link between the specific molecular and synaptic mechanisms altered by drug exposure (both acute and chronic) that lead to repetitive drug use and relapse remains yet to be clearly established. Repeated exposure to cocaine induces changes throughout the various levels of neuronal function, including gene expression and synaptic plasticity. These underlying molecular adaptations, ultimately, cause long-lasting changes in the pathways regulating memory and motivation to form strong associative memories that underlie SUD. Reengagement of these associations subsequently re-activate these adapted circuits to drive cravings and relapse of drug-seeking behavior.

The author would like to note that an equally long discussion can be had characterizing the phenotypes of each drug of abuse, but for the sake of “brevity” discussions throughout this dissertation will focus primarily on the effects of cocaine and cocaine-associated behaviors. Moreover, the goal of this introduction is not to encapsulate the entirety of research in the SUD field, nor fully describe the various aspects of drug associated phenomena, but to merely demonstrate that the molecular adaptations throughout various neural pathways in SUD form a mosaic that is as complex as the behavioral phenotypes they underlie. Due to the long-lasting and often robust changes in gene expression and plasticity in the neural circuitry regulating SUD, neuroepigenetics is now being pursued to better understand the changes caused by drugs of abuse.

A Brief History of Epigenetics

It is well established that targeted changes in gene expression are required for long-lasting forms of synaptic plasticity and long-term memory formation. Given the persistence of long-term changes in both gene expression and cell signaling in SUD, studies have now focused on epigenetic mechanisms in mediating the effects of drugs of abuse.

Conrad Waddington coined and defined the term ‘epigenetics’ as: “the branch of biology which studies the causal interactions between genes and their products [proteins; i.e. transcription factors], which bring the phenotype into being.”⁵⁸ While the mechanisms driving cellular differentiation are seemingly intuitive in retrospect, the goal of understanding how multi-cellular organisms are generated from a single template is astounding given the biological and historical context. During the inception of Waddington’s epigenetics (1942), the discovery of DNA’s structure had not yet been stolen from Rosalind Franklin (1953^{59–61}), Hershey and Chase had not yet officially confirmed DNA as the hereditary unit of information across cellular generations (1952⁶²), and the first transcription factor had yet to be identified (1978⁶³; the author would like to note that the discovery of the first transcription factor coincided closer in time with the revelation of Darth Vader being Luke Skywalker’s father than with Waddington’s hypothetical epigenetic regulation⁶⁴). Yet, somehow Waddington understood there must be underlying mechanisms with which cells are able to generate a cell fate and that this supergenetic programming could be carried in a heritable fashion.

Epigenetics, as a field, has had a major influence throughout biology; it would be an easier task to list the branches of biology *without* a major epigenetic component than to list those that do. Nevertheless, although epigenetics has traditionally focused on the determining of cell fate, the term has evolved alongside biology’s understanding of the underlying mechanisms driving genetic regulation. Currently, epigenetics generally refers to the study of changes in gene expression

independent from changes in the DNA sequence itself. DNA is organized into nucleosomes-repeating units of 147 base pairs of DNA spooled around a histone octamer⁶⁵. Typically, epigenetic machinery regulates transcription by altering the structure of nucleosomes and, ultimately, access to genomic DNA. Epigenetic modifiers do so through four major families of modifications: 1) DNA methylation, 2) nucleosome remodeling (the sliding of nucleosomes by large super-complexes called nucleosome remodeling complexes) 3) several RNA mechanisms, and 4) histone modifications (also referred to as chromatin modifications, and incorrectly referred to as chromatin remodeling)⁶⁶⁻⁷³. Although all four modifications have critical roles in the regulation of gene expression, post-translational modifications to histone tails are by far the most extensively studied in the field of neuroepigenetics and will be the focus of this dissertation.

The histone octamer is composed of four essential histone proteins, H2A, H2B, H3, and H4, each with variants that can be exchanged and each with positively charged N-terminal tails that interact tightly with the negatively charged DNA backbone. It is this interaction between the histone tail and spooled DNA that is sensitive to the covalent post-translational modifications that are present on the histone tail⁶⁵. The list of post-translational modifications is extensive (and includes but is not limited to acetylation, phosphorylation, ubiquitination, methylation, dopaminylation, and serotinylation); each is governed by a unique set of enzymes and each modification uniquely alters chromatin state and DNA accessibility^{65,74,75}. For example, histone acetylation is generally considered a mark permissive for gene expression as the addition of a negatively charged acetyl group to the positively charged histone tail allows for the relaxation of chromatin structure and loosens spooled DNA. Two major classes of enzymes have a critical role in modifying histone acetylation in an activity-dependent manner: histone deacetylases (HDACs) and histone acetyltransferases (HATs). The known HDACs are subdivided into four classes based

on shared families of protein domains; the most commonly studied are the Class I HDACs (HDACs -1, -2, -3, & -8) and Class 2 HDACs (HDACs -4, -5, -6, -7, & -9)⁷⁶. The HAT families, on the other hand, are far more extensive, with CREB Binding Protein (CBP)/p300 and GCN5 being the most commonly studied⁷⁷. Both HDACs and HATs operate in concert with other transcriptional repressors and activators, respectively. For example, HDAC3 is known to form a complex with HDAC4, HDAC5, N-COR, and SMRT. Because HDACs do not in and of themselves have bromodomains (domains that read the current acetylation state of a histone tail) or DNA-binding domains, targeting of deacetylase activity depends upon on its interaction with N-COR and SMRT^{78,79}. HATs, too, form large complexes of transcriptional activators. As its name implies, CBP is a protein that binds CREB and, in conjunction with other transactivators, is able to target particular gene loci^{77,80}. HDAC activity typically leads to a more compressed chromatin structure generally associated with gene silencing (due to removal of histone acetyl groups and strengthening of the positive tail/negative DNA interaction). Conversely, HATs add acetyl groups to histone tails and their activity typically leads to a more relaxed chromatin structure generally associated with gene activation. Due to this interaction, HDACs are believed to serve as a molecular brake pad, repressing gene expression until disengaged by an activity-dependent event permitting HAT-mediated gene expression.

In addition to directly competing for real estate in the histone code, histone modifications function in a combinatorial fashion. For example, phosphorylation of Histone 3 Serine 10 (pH3S10) not only prevents methylation from occurring at the same site, but also serves as a docking point for HATs, such as KAT2A; thus, pH3S10 preferentially leads to KAT2A-mediated acetylation at H3K9, H3K14, and H3K27 (and, again, preventing methylation to occur at these same residues⁸¹⁻⁸⁴). This process, known as phosphoacetylation, is critical throughout

development⁸⁵ and recent work suggests a role for phosphoacetylation in the gene expression necessary for memory formation and drug-associated behaviors and will be further discussed later⁸⁵⁻⁸⁷. Moreover, not only do interactions within a single family of histone modifications occur, but these interactions are known to occur across families of epigenetic mechanisms as well. As a brief example, proteins within the neuronal Brg1/hBrm-Associated Factor (nBAF) nucleosome remodeling complex contain histone-reading bromodomains. These bromodomains read the histone-modification state and alter large scale chromatin structure, providing another layer of DNA accessibility and gene regulation⁶⁶. Also, while RNA products, such as long non-coders and microRNAs, have been known to disrupt gene expression (one of many violations to the fundamental dogma of biology discovered by epigeneticists), recent work has demonstrated that RNAs directly interact with, and alter the function of epigenetic writers; enhancer RNA (eRNA) binding to CBP activates CBP-mediated histone acetylation and gene expression in a targeted manner⁸⁸. All this to say that while the field of epigenetics has made critical advances (and often revisions) to our understanding of the neuron, there exists a far more complex story than the early work describing HDAC:HAT interactions.

The collection of covalent modifications and altered chromatin structure provide a signal integration platform that guides transcriptional protein complexes to ultimately regulate specific gene expression profiles. As Waddington predicted, the collection of these epigenetic mechanisms is causal in targeted transcription. Epigenetic modifiers function as the heritable programming for cellular development and differentiation. As such, their role in transforming stem cell to cell fate has been well established. Yet, do these epigenetic modifiers continue to function once cell fate is established? What is their function in a post-mitotic cell population, such as neurons? Discoveries

in the learning and memory field have recognized the retrofitting of these epigenetic modifications in controlling the gene expression required for neuronal plasticity.

Epigenetics in Learning & Memory

The generation of plasticity and long-term memory is known to require a complex cascade of molecular and cellular adaptations in response to stimuli, including (but not limited to) NMDA receptor activation, Ca²⁺ influx, protein kinase cascades, and CREB phosphorylation. However, one common feature of these adaptations is their convergence on generating activity-dependent gene expression. One of the earliest demonstrations that gene expression is required for long-term memory formation came from using transcription-specific blockers following training in goldfish⁸⁹⁻⁹¹. Transcription dependence of long-term memory formation has subsequently been demonstrated to be well conserved across species, from fish to crustaceans to rodents to primates. Since this early work, the role of activity-dependent expression of IEGs and related transcription factors in learning processes has been extensively discussed, studied, reviewed, characterized, detailed, and evaluated elsewhere and will not be a major focus of this discussion. However, the epigenetic regulation of IEGs and their products (aligning with Waddington's original definition of epigenetics) during learning events has been rediscovered and provides a beachhead for understanding the role of the epigenome in memory processes. The earliest evidence that the epigenome in adult neurons responds to learning events came in 1979. Schmitt and Matthies demonstrated a training event can induce histone acetylation in the hippocampus⁹². Shockingly, it took nearly three decades for the role of histone modifications in learning to be rediscovered as several groups, nearly simultaneously, demonstrated targeted task and region-specific histone modifications⁹³⁻⁹⁶. As a direct result, these changes to histone state were discovered to be a necessary component for the gene expression required in long-term memory formation and have become a major focus of neuroepigenetics since^{74,86,95,97-99}.

HATs and HDACs, the enzymes regulating histone acetylation, are one of many key activity-dependent epigenetic modifiers. And, since the rediscovery of learning-dependent histone

acetylation, memory researchers have focused on HAT and HDAC families as modulators of memory. Various forms of HAT inhibition have been shown to impair associative processes that rely on activity-dependent gene expression. Mice with conditional CaMKII α -driven deletion of *Kat2a* (HAT formerly known as *Gcn5*) show deficits in hippocampal LTP¹⁰⁰. Similarly, loss of CBP function in the hippocampus disrupts the maintenance of LTP^{101,102}. As is often the case (though not always) these deficits in LTP are also reflected in failures in long-term memory formation. KAT2A KO animals show deficits in hippocampus-dependent memory formation, aligning with the loss in LTP¹⁰⁰. Loss of CBP activity in the dorsal hippocampus also generates memory impairments in various hippocampal tasks including contextual fear conditioning, inhibitory avoidance, novel object recognition, and the Morris water maze; when disrupted in the amygdala complex, animals display deficits in the acquisition of cued fear conditioning^{93,101–108}. Similar memory deficits were seen in transgenic mice with loss of HATs p300 or PCAF function^{109,110}. Consistent with this, pharmacological inhibition of class I HDACs (which includes HDAC3) and genetic deletion of HDAC3 not only generate enhancements to LTP but also generate profound enhancements to memory formation in various tasks, including novel object recognition, fear learning, and Morris water maze^{94,108,111–116}. Work from the Wood lab has demonstrated that it is the loss of deacetylase function (not necessarily disruption of any HDAC3-containing complex) mediating these memory enhancements. A histidine point mutation at tyrosine 298 (Y298H) generates a deacetylase dead dominant-negative HDAC3¹¹⁷; overexpression in the dorsal hippocampus blocks memory formation in the object location task and contextual fear, while overexpression in the amygdala blocks formation of cued fear¹¹⁸. These series of experiments provide evidence for epigenetic modifiers as powerful regulators of plasticity and plasticity, but also raise the question of how HATs and HDACs interact to regulate memory formation.

Loss of CBP and HDAC3 function impairs and enhances memory, respectively, through changes in the histone acetylation state and subsequent gene expression. The molecular brake pad hypothesis posits that HDACs and their associated complexes function as transcriptional repressors, preventing acetylation and subsequent gene expression until sufficient stimulation disengages these repressive complexes. Indeed, CBP deletion in the hippocampus blunts acetylation of known CBP histone targets, H4K8, H2BK12, and H3K14^{65,102}. Moreover, loss of CBP prevents the induction of training-induced histone acetylation at several IEGs, including *FosB*, *Bdnf*, *Zif268*, *Cebp*, *Nfkb*, and *Nr4a2*. This gene-specific loss of histone acetylation correlates with decreased activity-dependent expression at these same target genes^{93,95,102,119,120}. Conversely, manipulations that generate an HDAC3 loss of function (including genetic deletion, pharmacological inhibition, and dominant-negative over-expression) enable hyperacetylation throughout several H3 and H4 residues. As with CBP deletion, these changes in acetylation are targeted to, and correlate, with training-induced increases in IEGs necessary for learning and memory including *Bdnf*, *Nr4a1*, *cfos*, and *Nr4a2*^{94,108,112,115,118}. Unsurprisingly, HDAC3 and CBP appear to compete for epigenetic antagonistic influence at the same histone residues and gene loci.

Even though there are vast global changes to histone state following CBP:HDAC3 deletions, of particular note are the changes that occur at the promoter of *Nr4a2*. Learning events (such as training in water maze, conditioned fear, or object location) disengage HDAC3 from the *Nr4a2* promoter, recruit HATs (such as CBP) to acetylate the same loci, and drive *Nr4a2* gene expression^{25,26,118,121}. As previously described, HDAC3 disruption can artificially generate enhancements to learning by generating a permissive transcriptional environment. However, these memory enhancements are dependent on acetylation at the *Nr4a2* promoter and subsequent increase in *Nr4a2* expression. Several studies have shown HDAC3 functions as a brake pad on

memory through its negative regulation of *Nr4a2* where loss of HDAC3 fails to generate memory enhancements when *Nr4a2* is knocked down simultaneously^{27,112,121}. This unique relationship between HDAC3 and *Nr4a2* will be further explored throughout this dissertation.

Although this dissertation will focus on the role of histone acetylation in regulation of gene expression and neuronal function, other families of epigenetic mechanisms play key roles in adult cognition. For example, Vogel-Ciernia et al. have demonstrated that a neuron-specific subunit BAF53B, within the nucleosome remodeling complex nBAF is necessary for long-term memory¹²². Disruption of BAF53B (either in mice with heterozygous deletion of *Baf53b* or transgenic overexpression of a dominant-negative splice variant) leads to deficits in LTP in the hippocampus and loss of hippocampal long-term memory formation in object location and contextual fear conditioning tasks. These memory impairments can be restored with overexpression of wild-type BAF53B^{122,123}. Surprisingly, recent work has demonstrated that deletion of HDAC3 in the dorsal hippocampus is also able to restore synaptic plasticity and spatial memory in animals with BAF53B disruption¹²⁴, providing further evidence for the combinatorial nature of these molecular mechanisms.

The above is not meant to serve as an exhaustive review of the role of epigenetic mechanisms in learning and memory, but merely to provide examples of how epigenetic modifiers (particularly HDAC3 and competing HATs) are able to confer changes to histone state, gene expression, associative processes, and, ultimately, behavior. Specifically, HDAC3 inhibition disengages the molecular brake pad allowing for HAT-mediated acetylation and generation of a more permissive environment for the gene expression necessary for long-term memory formation. Conversely, inhibition of HATs (such as CBP) leads to a more compressed chromatin structure that inhibits the gene expression necessary for memory formation. There are various HDACs and

HATs that operate independently and concurrently with each other, HDAC3 and CBP are merely two canonical examples. It is important to be aware that this is a simplistic description of the key mechanisms regulating transcription; changes to histone state are permissive, but not instructive to the molecular cascades culminating in the gene expression required for learning and memory. For example, simultaneous deletion of HDAC3 and CBP is unable to generate the memory enhancements seen with HDAC3 deletions alone, demonstrating that loss of deacetylase activity is insufficient to recruit the totality of transcriptional machinery¹¹³. However, these epigenetic mechanisms have now been established as upstream regulators of the gene expression needed for synaptic plasticity. Researchers in the learning and memory field have shown that these enzymes are powerful regulators of memory formation and associative processes which can be artificially manipulated to either block or enhance memory. Given the long-lasting nature of the changes seen in SUD (particularly in mechanisms regulating gene expression and plasticity), are drugs of abuse able to tap into these epigenetic mechanisms to provide the resilience of drug-seeking behavior?

Epigenetic Regulation of Reward Circuitry and Response to Drugs of Abuse

Drugs of abuse cause long-lasting changes in plasticity and behavior. Due to the enduring nature of these changes, addiction researchers have hypothesized that epigenetic machinery is engaged to drive the neural circuitry changes seen in SUD. Indeed, several groups have characterized the epigenetic response to both acute and chronic drug exposures. While no single drug or drug class is unique in its ability to alter the epigenome, each generates a unique signature across the epigenome and neural circuitry underlying motivated behaviors. Similar to the neuroepigenetics of learning and memory, the epigenetic adaptations seen in response to the various drugs of abuse also accumulate in a targeted fashion. For example, adolescent rats chronically treated with ethanol show dramatic increases in H3 and H4 acetylation at *Fosb*, *cFos*, and *Cdk5*, whereas adult-treated animals show a hypermethylation in the prefrontal cortex and dysregulation at several genes involved in neurotransmission including *Syt2*^{125,126}. Conversely, opioids (such as heroin and morphine) enrich the striatum with repressive histone methylation and blunt permissive histone acetylation, particularly at the promoters of *Bdnf* and *Nr4a2*¹²⁷. The observed changes to histone methylation have been observed through withdrawal and appear to mediate the incubatory effects on heroin seeking. These results highlight the long-lasting effects of these epigenetic changes and the subsequent influence on behavior.

Regarding epigenetic effects of cocaine use disorder, there is an abundance of research on the adaptations within the striatum^{81,128-131}. Several studies have shown the accumulation of permissive histone marks in NAc D1-MSNs in response to both acute cocaine and cocaine re-exposures, including pH3, H3K14Ac, H3K18Ac, H4K5Ac, H4K8Ac, H3K12Ac and the combinatorial phosphoacetylation at H3S10/K14; these histone marks are enriched at the promoters of various genes involved in NAc plasticity, including *Fosb*, *cFos*, *Cdk5*, *Bdnf*, *Nr4a2* and correlate with their increased expression^{12,87,132-135}. However, although both acute and cocaine

re-exposures induce several phosphoacetyl marks in D1-MSNs, the accumulation occurs significantly more in acute treatments compared to re-exposed animals. Recent work identifying unique transcription profiles during cocaine re-exposures vs. acute cocaine¹³⁶ would suggest that this is not necessarily a blunted response to cocaine re-exposure, but a selective recruitment of these epigenetic mechanisms to novel gene targets. Similarly, chronic cocaine induces various changes in histone modifications overlapping with those seen in acute cocaine, such as increases in H3K9me3 and H4K5Ac¹³³. Due to the significant non-overlapping nature it is more likely that chronic cocaine exposure is generating an epigenetic environment unto itself¹³⁷⁻¹³⁹ than a degradation of the environment generated by acute cocaine.

These drastic changes have further led researchers to study the impact of cocaine on the various enzymes that are known upstream regulators of these modifications to the histone code. The observed increase in phosphoacetylation is likely mediated by the convergence of pMSK1, pERK, and P-Thr34-DARPP-32 as these post-translational modifications accumulate in the nucleus of D1-MSN following acute cocaine, catalyze H3 phosphorylation, and simultaneously protect pH3 through inhibition of PP1^{34,134,140}. Both acute and chronic cocaine also target more canonical epigenetic enzymes, such as HDACs and HATs. Cocaine exposure results in the recruitment of CBP to the *Fosb* and *Nr4a2* promoters, correlating with the described increases in loci-specific histone acetylation and gene expression^{132,141}, and induce the nuclear export and gene-specific disengagement of HDACs 3 and 5^{135,142}. To be clear, this is only a sampling of the various resulting effects drugs of abuse have on the epigenome (the full extent of epigenetics research in SUD has been reviewed extensively elsewhere), it is clear drugs of abuse profoundly alter the epigenome, often, in concert with the previously discovered mechanisms necessary for the

addictive phenotype. Researchers now look to reverse these drug-induced changes to the epigenome as a means of reversing long-lasting drug-associated behaviors.

Since drugs of abuse, in particular cocaine, are able to affect endogenous epigenetic function, several studies have targeted epigenetic regulating enzymes. As in the learning and memory field, studies focusing on the upstream regulators of histone acetylation have demonstrated that HATs and HDACs appear to be positive and negative regulators, respectively, of cocaine-associated behaviors. Overexpression of HDACs (such as HDAC4 and -5) or loss of HAT function (such as CBP) prevent cocaine-induced CPP and changes in cocaine-induced gene expression, particularly at *Nr4a2*^{12,132,141-143}. Conversely, Class 1 HDAC inhibition or deletion (including HDAC3) enhances cocaine-associated behavior, including sensitization and CPP^{12,135,141}. Most of this work has centered on balancing HAT and HDAC activity, although studies have also characterized the role of nucleosome remodeling in cocaine-associated behaviors. Animals with loss of function mutations to BAF53B show deficits in cocaine-induced CPP and LTP that is restored with targeted overexpression of *Bdnf* to the NAc¹⁴⁴. *Baz1a*, a member of the ISWI nucleosome remodelers, is induced by acute cocaine and, when overexpressed in the NAc, blocks cocaine-induced CPP¹⁴⁵. This body of work demonstrates that drugs of abuse tap into the endogenous molecular machinery, in particular the machinery that provides epigenetic regulation to gene expression, and researchers are able to likewise tap into these mechanisms to reverse the effects of drugs of abuse. The advent of CRISPR-dCas9 will allow for gene loci-specific targeting of epigenetic modifications to provide further specificity to these manipulations and identify drug-induced changes susceptible to future therapeutics.

The growing field of addiction epigenetics has fundamentally changed our understanding of SUD. It has provided further evidence of SUD being a neurobiological disease, not a behavioral

flaw in individuals lacking will power. However, it has also provided a stronger understanding of the biological mechanisms that drugs of abuse recruit and modify, often in a combinatorial fashion (often referred to as the gateway hypothesis). While the ideas that cannabis provides the only path to SUD or use of a legal drug is a prerequisite for subsequent dependence to an illicit drug are completely absurd (and travel with a rather large suitcase of racial bigotry), there is accumulating evidence that long term exposure to one drug of abuse can leave individuals susceptible to the subsequent neurobiological effects of others, via both epigenetic and non-epigenetic mechanisms. For example, nicotine and alcohol pretreatment enhances subsequent cocaine-induced CPP and self-administration, respectively. In the case of nicotine, this enhancement to cocaine associated behavior is likely mediated by nicotine's ability to increase H3/H4 acetylation through degradation of HDAC4/5 and enhance LTP in the amygdala and NAc^{41,146,147}. Moreover, early life cannabis exposure generates long lasting changes in histone methylation throughout the striatum, leading to increased sensitivity to rewarding properties of opioids (such as heroin)¹⁴⁸⁻¹⁵⁰. These cannabis-induced effects on opioid sensitivity have (alarming) been shown to be transferred across generations, as offspring of cannabis exposed animals have increased neurobiological responses to acute heroin exposure^{151,152}. Each drug of abuse creates a unique epigenetic signature and these changes to the epigenome are what leave the neural circuitry susceptible to the effects of other substances.

Still, the bulk of the neuroepigenetics research has focused on the core circuitry known to regulate reward, motivation, and learning (such as the PFC, NAc, dorsal striatum, and VTA). In the same fashion that no single Deathly Hallow makes one the Master of Death, no single brain region, neural circuit, cell-type, receptor, kinase, or transcription factor is likely to provide the cure to SUD. It will take a *nearly* complete understanding of drug-induced dysfunctions to yield a path

towards comprehensive therapeutics, neither of which neuroscientists currently wield. While there are volumes of research investigating the mechanisms and effects of cocaine exposure, the field unfortunately has not yet generated an effective therapeutic for cocaine use disorder. As such, it is critical that as the field continues its depth of understanding in these aforementioned brain regions, it also expands its breadth to include the other neural pathways critical to the drug response including the raphe nuclei, ventral pallidum, and habenula.

Structure and Function of the Medial Habenula Circuitry and Organization

The habenula is an evolutionarily conserved epithalamic complex present from zebrafish to primates. In zebrafish, the habenula complex is made up of dorsal and ventral subregions; the mammalian correlates of these substructures are the medial (MHb) and lateral (LHb) habenula, respectively¹⁵³. Of these substructures, disproportionate research has focused on understanding LHb function and circuitry. Recent work has characterized the LHb as a reward prediction error locus. LHb glutamatergic projections to the GABAergic rostral medial tegmental grey (RMTg) generate inhibition of VTA DA neurons and serve as a signal for aversive (or, more accurately, reward-omitted) states¹⁵⁴. As such, its role in regulating motivated behaviors has become clearer over recent decades. On the other hand, the MHb has been relatively neglected by the majority of neuroscience and is often excluded from even the most inclusive addiction-related diagrams. One of the earliest descriptions of the MHb came from Santiago Ramón y Cajal in 1911. Ramón y Cajal provided detailed drawings of the dense input of the stria medullaris to the MHb and the dense output to the interpeduncular nucleus (IPN) via the fasciculus retroflexus (See **Fig. 0.1**)¹⁵⁵. The MHb, however, was neglected for the better half of the 20th century despite this pioneering work.

Renewed interest in the habenula complex has continued Ramón y Cajal's early work in attempts to provide a definitive function for this small evolutionarily conserved region. With the advent of advanced genetic and tracing techniques, the internal structure and cellular properties of the MHb are now better known despite its small size (in humans, the complete habenula complex is ~30mm³, about the size of a grain of rice^{156,157}). It is important to note that within the gross organization of the MHb exists a more refined subcircuitry in the MHb-IPN pathway. Five major substructures have been identified within the MHb: Superior, Intermediate, Central, Medial and

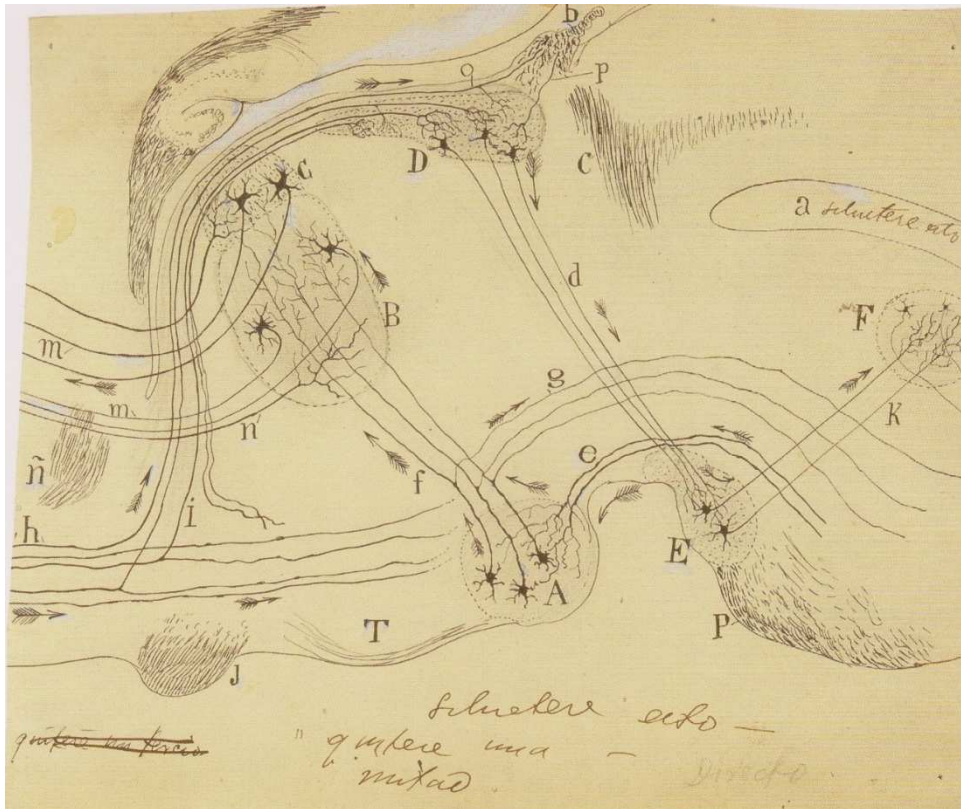


Figure 0.1: Ramon y Cajal drawing of the epithalamus. Sketch includes one of the first descriptions of the (D) MHb and its projection to the (E) IPN via the (d) fasciculus retroflexus

¹Lateral nuclei. Nevertheless, the MHb most commonly is divided into Substance P-rich dorsal (dM Hb) and cholinergic ventral (vMHb) subregions, both of which co-release glutamate¹⁵⁸. Although superficial, this first-level organization is convenient, functionally relevant, and will be further explored and employed throughout this dissertation.

Primary MHb inputs from the medial septum (triangular nucleus) and the diagonal band of Broca converge via the stria medullaris and are comprised of various neurotransmitters such as glutamate, ATP, acetylcholine, and, of particular interest, an *excitatory* GABAergic input (the MHb has low levels of KCC2, the transporter responsible for generating a low intracellular [Cl⁻]; as a result, the activation of GABA_A receptors causes Cl⁻ efflux and subsequent depolarization)¹⁵⁹. The balance of these varying inputs provides the tonic baseline firing rate (~4Hz) seen in both the

¹ Adapted from ¹⁵⁵

dMHb and vMHb^{159–162}. Moreover, a dense serotonergic input to the MHb of unknown origin has been described¹⁶³. Common sense would suggest that this serotonergic input originates from either the dorsal raphe (DRN) or median raphe nuclei (MRN), but recent tracing studies have negated this possibility¹⁶³. Although the median raphe has been shown to project to the MHb, this projection is likely GABA-ergic¹⁶⁴. One potential, yet unverified, source of this serotonergic input is the serotonergic population of IPN¹⁶⁵, which likely receive direct innervation from the cholinergic neurons of the vMHb.

Nevertheless, these signals converge on the MHb where projections diverge via the internal portion of the fasciculus retroflexus, sending the vast majority of axons to the IPN. The subregion projections from the MHb to the subregions of the IPN have been shown to be non-overlapping: the dMHb sends outputs to the lateral subnucleus (IPL), whereas the vMHb sends outputs to the rostral, caudal, intermediate and dorsolateral subnuclei of the IPN (IPR, IPC, IPI, and IPDL, respectively). Furthermore, recent circuit tracing experiments identified the targets of dMHb- and vMHb-innervated IPN neurons. vMHb-innervated IPN neurons (mainly IPR and IPC) send GABAergic projections to the median raphe and dorsal raphe nuclei^{164,166}. As such, the MHb functions as a potential brake pad to serotonergic signaling¹⁶⁷. In addition, studies using early tracing techniques identified sparse projections from the MHb to the LHb, VTA, and MRN, among others, but have not been extensively characterized or studied compared to the MHb-IPN pathway¹⁶⁸. Due to the positioning of this circuitry, the MHb is considered a key hub in the dorsal diencephalic pathway linking forebrain and midbrain circuitry, providing an alternate to the median forebrain bundle. The characterization of this circuitry provides the foundation for understanding the systems level effects of MHb function and, ultimately, its contributions to behavioral outcomes.

Role in Behavior

Even though evolutionarily conserved across vertebrate species, the totality of MHB functions are not well understood. The heterogeneous cellular organization within the MHB is incredibly intricate despite its small size. Several groups have sought to fully describe the unique transcriptome within the habenula complex^{169,170}. Doing so may provide further insight into not only how the MHB generates behavioral outcomes, but also provide an avenue for targeted therapeutics. The vMHB has a perplexing (and often frustrating) gene expression profile which makes conceptualizing its function difficult. A cursory glance at the MHB transcriptome would lead one to believe MHB neurons occupy a pivotal space in the mesolimbic DA pathway; for example, the vMHB is enriched with DARPP-32^{171,172} (often inaccurately described as a marker for medium-spiny neurons); rich in *Th*, but lacking tyrosine hydroxylase protein, and rich in NR4A2¹⁷³. In addition, the vMHB is also enriched with various serotonin receptors (*Htr3a*, *Htr4*, *Htr5a*, and *Htr5b*^{170,174–176}) coinciding with the dense serotonergic innervation, is one of the few regions in the CNS expressing the kisspeptin1 receptor^{177,178}, and, most often studied, the vMHB-IPN pathway has the densest expression of nicotinic acetylcholine receptors (nAChRs; specifically, the $\alpha3$ - $\beta4$ - $\alpha5$ cluster)^{169,179,180}. These unique properties of the vMHB provide a unique challenge in understanding its function, but the field at large has now dedicated significant attention to this goal.

From a systems level perspective, it is important to note that various regions of the CNS have dichotomous structures which function in parallel, albeit often opposing, fashion; for example, pre-limbic vs infralimbic prefrontal cortex, NAc core vs. NAc shell, and dorsal lateral vs. dorsal medial striatum, all have roles in overlapping behaviors, yet often compete for generating behavioral outcomes. Similarly, the LHb provides feed-forward inhibition of VTA DA neurons (through excitation of the GABA-rich RMTg) and the MHB seems to provide feed-

forward inhibition of the raphe nuclei (through excitation of the GABA-rich IPN). These tripartite pathways do receive external innervation to modulate their overall function and MHb/LHb function are not so easily distinguished. Nevertheless, the habenula complex appears to fit this dichotomous mold and this perspective can provide a framework for identifying habenula function.

In Adaptive Responses to Aversive States

The LHb has had significant research dedicated to describing its function. Work from various groups has developed a sophisticated understanding of the LHb's influence over the mesolimbic DA system; the LHb receives input from the lateral septum, basal ganglia, and the accumbens and primarily inhibits dopaminergic release through activation of the GABAergic RMTg^{181,182}. LHb activity has been shown to increase when animals are exposed to a cue-predictive reward, but the reward is withheld. Conversely, inputs from the pallidum suppress LHb firing in response to reward-predictive cues¹⁸³⁻¹⁸⁵. LHb activity is also induced by onset of punishment and, when stimulated, LHb functions to generate behavioral avoidance phenotypes^{154,186}. Activity in the LHb can be regulated in a biphasic manner, activity suppressed with the onset of reward (or reward-predictive cues) and upregulated in response to reward-withholding or punishment onset.

More recently, LHb dysfunction has been implicated in the onset of depressive-like phenotypes. In rodent models of depression (e.g.; learned helplessness), there is a loss of LHb volume (accounted for by a loss in glial cell count), increased glutamatergic synaptic input, and increased LHb metabolic activity that, as the circuitry would predict, inversely correlates with metabolic activity in the VTA¹⁸⁷⁻¹⁸⁹. Furthermore, this tonic increase in LHb activity has been linked causally to the onset and progression of depressive phenotypes. Lesions of either the Hb complex (which include both the MHb and LHb; a caveat which will be further discussed below)

or the LHb alone prevent the induction of learned helplessness (measured by latency to escape a shock-paired chamber), forced swim test, and tail suspension test^{190,191}. Electrical (via deep brain stimulation) and pharmacological inhibition of the LHb has also been shown to improve measures of learned helplessness^{192,193}. In humans, functional imaging has shown Hb dysfunction in patients with major depressive disorder (MDD); MDD patients are known to have increased activity in the Hb complex and inhibition of the LHb via deep brain stimulation can successfully alleviate depressive symptoms in patients of therapeutic-resistant MDD^{156,157,194,195}. Due to this volume of work, the habenula complex is characterized as an aversive, anti-reward structure. But, it remains unclear if the MHb serves a role redundant to the LHb in regulating aversive and depressive-like states.

As seen in the LHb, animal models of MDD show decreased MHb neuronal volume, but increased baseline activity (which as the circuitry would predict, is positively correlated with increased IPN activity)^{187,188,196}. However, more recent work suggests that the MHb is responding to conditioned stressors, not necessarily exposure to acute stressors themselves. The MHb is activated during the consolidation of cued fear conditioning and has been shown to increase expression of various IEGs (including *Nr4a2*) in the vMHb. However, this vMHb engagement was not seen in animals that received unpaired shocks in a familiar context¹⁹⁷, suggesting that aversive stimuli alone are unable to engage the vMHb. Further, lesions of the zebrafish dorsal habenula (analogous to the mammalian MHb) cause increased freezing to conditioned stressors, increased anxiety-like behaviors, and prevent the induction of avoidance behaviors^{177,198,199}. The cholinergic vMHb population seem to be responsible for these adaptive responses, as functional inhibition of vMHb cholinergic neurons blocks the acquisition of fear extinction, whereas optogenetic stimulation of this same region accelerates extinction²⁰⁰. Lastly, chronic stress causes a decrease

in various markers critical to vMHb cholinergic signaling, including *Chat*, *vAcht*, *Cht*, *Chrna3*, *Chrn3*, and *Chrn4*¹⁶⁷. Loss of cholinergic signaling from the vMHb has been linked to anhedonia-like behaviors; knockdown of vMHb *Chat* induces a decrease in sucrose consumption that is resistant to the anti-depressant effects of fluoxetine. This hypocholinergic phenotype is reflected in suicide victims with comorbid MDD, as MHb samples collected post-mortem show decreased expression of various genes associated with cholinergic signaling, including significant decreases to *CHAT* and *CHRN3* and trending decreases in *CHAT*, *CHRN4*, *CHRNA3* expression¹⁶⁷. In light of this body of work, it seems less likely that the MHb is causal to a learned helplessness/depressive phenotype than responsible for generating an adaptive response to it.

While activity in the MHb has a clear role in generating adaptive behaviors, the upstream regulation of the MHb and the downstream effects of Hb activity are less understood. Ablation of the triangular septal cholinergic input to the vMHb and optogenetic activation of the glutamatergic posterior septal input to the vMHb both have been shown to be anxiolytic^{201,202} (the role of nicotine, acetylcholine, and nAChRs in habenula-mediated anxiety will be further discussed below). Although both inputs presumably lead to increased MHb activity, the cholinergic inputs from the triangular septal nucleus appear to be anxiogenic, while the glutamatergic inputs from the posterior septum anxiolytic. With regard to the downstream targets of MHb, there is conflicting evidence of the impact MHb activity may have; changes in activity in the LHb-RMTg-VTA and vMHb-IPN pathways often correlate as predicted, yet the downstream effects of activity in Hb pathways is unclear. More specifically, aside from the feedforward inhibition of VTA DA neurons by the LHb, what other neural circuitry does the Hb complex affect to generate these behavioral outcomes? Given the work implicating serotonin in anxiety and depressive phenotypes^{203–206} and the recent circuit tracing linking the vMHb to the DRN and MRN^{164,166}, the Hb likely functions

through regulation of DRN and MRN serotonin. Indeed, in animals with Hb lesions, there is a loss of stress induced serotonin signaling in the DRN²⁰⁷ and, when activated, vMHb cholinergic neurons have been shown to inhibit DRN serotonin turn over¹⁶⁷. Furthermore, LHb activity has been shown to both negatively^{190,208} and positively²⁰⁷ regulate serotonergic outputs of the DRN. This contradictory effect of the LHb is likely mediated by the LHb direct inputs to the DRN and indirect inputs to the DRN through the GABAergic RMTg. Yet, a causal link between the MHb regulation of DRN/MRN and adaptive responses to stress and aversion remain missing.

The conflicting behavioral and pharmacological evidence would suggest that the role of the MHb is more complex than the characterization as an aversive brain region. Both gain and loss of function studies in the vMHb often overlook the importance of the tonic firing of the MHb, the transmitter systems engaged and, subsequently, being employed by the MHb; preventing induction of MHb activity (maintaining tonic firing) is likely to have unique behavioral outcomes than a total loss of MHb activity. As such, complete functional characterization and an understanding of the endogenous function of the MHb will likely rely on subcircuit specific, real-time, reversible manipulations. Nevertheless, due to its position in regulating serotonergic and dopaminergic circuitry in addition to its unique transcriptome, researchers have looked to the MHb as a target for drugs of abuse.

In Substance Use Disorder: Nicotine

The unique transcriptome of the MHb can provide incredible insight into its role in SUD. The MHb-IPN pathway has the densest expression of nAChRs and of note are the uncommon $\alpha 5$ and $\beta 4$ ^{209,210}. As such, nicotine researchers have targeted the MHb-IPN circuit and demonstrated that it as a significant regulator of nicotine-associated behaviors. Pharmacological antagonists of the $\beta 4$ -containing nAChRs within the MHb blocks nicotine-induced CPP, self-administration, and

nicotine-induced dopamine release in the VTA^{209,211–213}. $\beta 4$ KO animals show similar deficits in nicotine self-administration and nicotine-induced dopamine release that is partially restored with viral-mediated restoration of MHb- $\beta 4$ expression²¹⁴. However, this is not to say that the MHb solely regulates the reinforcing properties of nicotine. Studies focusing on the role of the $\alpha 5$ subunit provide contrasting evidence for how the MHb regulates nicotine-associated behaviors. Animals with $\alpha 5$ KO in the MHb show significant increases in nicotine self-administration, even at doses that are known to generate nicotine aversion²¹⁵. This effect is reversed when $\alpha 5$ expression is restored in the cholinergic neurons of the MHb, demonstrating that $\alpha 5$ -mediated signaling in the MHb facilitates nicotine aversion and functions as a clamp on nicotine consumption²¹⁵. The MHb, however, not only regulates the acute response to nicotine intake, but also modulates the adaptations to long-term nicotine treatment.

Chronic nicotine exposure generates long-lasting adaptations within the vMHb. For example, nicotine withdrawal sensitizes the cholinergic neurons of the vMHb to subsequent nicotine re-exposures²¹⁶. As with the acute response to nicotine, nicotine withdrawal is dependent on vMHb nAChR activity. Chronically nicotine treated $\alpha 5$ -KO animals are resistant to precipitated somatic withdrawal symptoms²¹⁰. Perplexingly, while nAChRs of the vMHb are clearly necessary for the somatic expression of nicotine withdrawal, experimentally, these symptoms are often precipitated with mecamylamine, a nonspecific antagonist to various nAChRs including $\alpha 3\beta 4$ in addition to $\alpha 4\beta 2$. This same pharmacological antagonists that induces somatic withdrawal symptoms, has also been shown to alleviate anxiety-like behaviors during withdrawal from chronic nicotine²¹⁷. This conflict suggests that the MHb's role in regulating nicotine, nicotine withdrawal, and nicotine-induced anxiety-like behaviors is more complex than up- or down-regulation of vMHb firing alone but involves not yet understood signaling cascades by either $\beta 4$ - or $\alpha 5$ -

expressing nAChRs (or other nAChR subunits contained in the MHb). It is the balance of expression between $\beta 4$ - and $\alpha 5$ -containing nAChR responses to acute nicotine that generates MHb-induced nicotine aversion²¹⁸. It has been recently demonstrated that the firing rate of the vMHb dictates the neurotransmitter released in the IPN; tonic firing appears to be glutamate dependent while long-lasting burst firing engages acetylcholine release²¹⁹. This switch to acetylcholine release in the vMHb-IPN pathway is solely dependent on activation of $\beta 4$ -containing nAChR, as individual KO of all other nAChR subunits (including the $\alpha 3$ and $\alpha 5$) has no effect on vMHb acetylcholine release²²⁰. $\alpha 5$ -containing nAChR mediated responses to nicotine, on the other hand, are dependent on concurrent neurokinin inputs²²¹, so it is possible (but remains untested) that activation of $\alpha 5$ -containing nAChRs is alone unable to alter nicotine sensitivity and MHb neurotransmitter release, but the combinatorial $\alpha 5$ /neurokinin activation can engage comparable signaling mechanisms as $\beta 4$ -containing nAChR activation. As $\alpha 5$ and $\beta 4$ subunits are often contained in function nAChR subtypes, it is likely the individual contributions of each subunit to the totality of nAChR function underlies these unique effects on nicotine response. Future studies will need to build upon this critical work to understand how MHb function is changed by each unique nAChR and ultimately regulate nicotine-associated behaviors.

In Substance Use Disorder: Morphine

Various studies have shown the MHb holds (as like the case of nAChRs) the densest expression of the MOR1^{222,223} and deletion of MHb MORs significantly disrupts MHb-IPN connectivity²²⁴. Indeed, the MHb is sensitive to the effects of chronic morphine. Chronic morphine enhances MHb cholinergic signaling (as measured by decreases in acetylcholinesterase in the MHb-IPN junction and increased nAChR expression in the MHb)^{225,226}. Disruption of MHb function subsequently disrupts behavioral and neural response to morphine. KO of RSK2 (a kinase

involved in CREB-regulated gene expression) in the vMHb blocks morphine-induced analgesia²²⁷. Although $\beta 4$ -KO decreases MHb activity during morphine withdrawal, it does not affect withdrawal behaviors²²⁶. However, $\beta 4$ antagonists does block morphine self-administration and morphine-induced dopamine sensitization in the NAc (with no effect on acute morphine response)^{225,228}, further iterating the role of the vMHb in behavioral and circuit adaptations. Despite the density of MOR in the MHb, it still remains unclear how altered MHb signaling during opioid exposure regulates behavioral responses.

In Substance Use Disorder: Psychostimulants

Early pharmacological studies identified a regulatory role for the MHb in the responses to psychostimulants such as methamphetamine and cocaine. Lesions to the habenula block cocaine mediated effects on raphe serotonergic activity²²⁹. Blockade of the MHb-IPN enriched $\alpha 3\beta 4$ nAChR prevents various psychostimulant-associated behaviors such as methamphetamine self-administration, cocaine self-administration, and cocaine-induced CPP^{211,230,231}. Although the bulk of the literature has focused on nicotine's effects on MHb function, there is growing evidence that the MHb responds to cocaine as well. Chronic cocaine leads to a desensitized response to future cocaine challenges in the MHb and a suppression of MHb activity that is only restored with a significantly increased dose of cocaine²³². This contrasts with the response to chronic nicotine in the MHb, as chronic nicotine does not change baseline activity of vMHb neurons and nicotine withdrawal sensitizes the MHb to further nicotine challenges^{216,233}, suggesting these two drugs of abuse have unique effects on habenula circuitry. Furthermore, the MHb shows increased *cFos* expression during cue-primed reinstatement of cocaine self-administration²³⁴, yet, presumptive VTA-projecting MHb neurons are not the engaged population²³⁵. Although it appears cocaine history alters MHb function, the underlying causes of long-term MHb changes remains elusive.

The MHb (enriched with GABA_B receptors²³⁶) is preserved from chronic cocaine-induced changes to GABA_B expression²³⁷. Additionally, DAT, the canonically studied site of cocaine antagonist function, is absent in the MHb. However, a dense non-raphe¹⁶³ sourced serotonergic input does innervate the MHb (likely from the IPN¹⁶⁵). The serotonin transporter is a known target of cocaine, radiolabeling studies have also shown cocaine binding sites in the MHb²³⁸, and, as previously mentioned, the MHb expresses a unique array of serotonin receptors sensitive to cocaine, including 5-HT_{3A} receptor^{170,239}. Therefore, it is possible that repeated cocaine treatment alters this serotonergic input in a way that leaves the MHb primed for reinstatement of cocaine-associated behaviors.

Thus, this dissertation explores the MHb as a complex region involved in various motivated and drug-associated behaviors. Even though it is enriched with various regulators of cocaine-associated behaviors (such as DARPP-32, HDAC3, and NR4A2), the molecular adaptations to cocaine within the MHb, as well as how the MHb may regulate cocaine associated behaviors have not been extensively studied. NR4A2 has been demonstrated to be necessary for vMHb development (as in VTA DA neurons)¹⁷³, yet its role in the adult habenula remains uncharacterized. Does HDAC3 regulate MHb function through NR4A2? Does NR4A2 provide a similar function in associative processes in MHb-mediated behaviors as it does in the NAc and hippocampus? To answer these questions, I first observed the response of the MHb to cocaine-primed reinstatement of cocaine-associated behaviors (Chapter 1). Then, I characterized a chemogenetic technique to manipulate memory formation and associative processes in behaving animals (Chapter 2) and investigated the role of cholinergic neurons within the vMHb in reinstatement of cocaine-associated behavior (Chapter 3). Lastly, I developed viral approaches to alter HDAC3 and NR4A2 function in the vMHb to study their influence on MHb-mediated

cocaine-associated behaviors (Chapter 4). Together, these experiments provide the first evidence for the role of HDAC3 and NR4A2 in the MHb in cocaine-associated behaviors. Furthermore, these studies contribute to the literature a function for the MHb in regulating cocaine response.

Chapter 1: Functional Adaptations of the Medial Habenula During Reinstatement of Conditioned Place Preference

Rationale

SUD is a chronic relapsing neuropsychiatric disorder that is underlied by long-lasting changes to neural circuit function. The relapsing nature of SUD is often modeled with stress-, drug-, or cue-primed reinstatement of drug-associated behavior models; much of the underlying circuitry regulating cue- and drug-primed reinstatement of cocaine-associated behaviors has been identified and is overlapping (although not necessarily identical). The MHb is one brain region whose function is altered by repeated cocaine exposures and has been linked to various cocaine-associated behaviors, such as acquisition of cocaine-induced CPP and cue-primed reinstatement of self-administration. Yet, the full extent of cocaine treatments that alter MHb function, the epigenetic changes within the MHb in response to cocaine, and how these cocaine-induced changes to MHb function may fit into the circuitry regulating relapse-like behaviors is unknown. Our laboratory and others have shown that various epigenetic adaptations occur in response to repeated cocaine exposure and cocaine-associated behaviors. Here, we investigated the molecular response of the MHb to various cocaine exposures, consolidation of cocaine-induced CPP, and cocaine-primed reinstatement of CPP.

Methods

Animals:

8-week old wild-type c57BL/6J male mice were purchased from Jackson Laboratory. All mice were maintained on a 12:12hr ON/OFF light-dark cycle and were given *ad libitum* access to food and water. All experiments were conducted according to the National Institutes of Health guidelines for animal care and use and approved by the University of California, Irvine Institutional Animal Care and Use Committee.

Cocaine Exposure and Cocaine CPP-Reinstatement Paradigm:

Chronic Cocaine Treatment: To test MHb activity during cocaine re-exposure, animals were handled for 2 min for 3 consecutive days. Following handling, animals received, in the homecage, cocaine-HCl (10mg/kg, I.P.) once/day for 7 consecutive days. Following 14d forced abstinence, animals received either saline or cocaine-HCl (5mg/kg, I.P.). 1 hr later, animals were sacrificed and brains flashfrozen on dry-ice chilled isopentane.

CPP-Reinstatement Paradigm: Cocaine-induced CPP was performed as previously described^{42,144,240,241}. Briefly, animals were handled for 2 min for 3 consecutive days. Following handling, mice were conditioned over 4 consecutive days, receiving either cocaine-HCl (10mg/kg, IP; Sigma) or 0.9% saline, in a context-dependent manner (counter-balanced, unbiased). Following conditioning, animals were allowed to freely explore, in a drug-free state, the complete chamber to assess preference, established as the difference between time spent in the cocaine-paired chamber and the saline-paired chamber, in seconds. To extinguish preference, animals were repeatedly reintroduced to the chamber, daily for 5 consecutive days. Once extinguished, animals were reinstated with either cocaine-HCl (5mg/kg, IP; Sigma) or 0.9% saline and allowed to freely explore the complete chamber for 15 minutes. 45 minutes following reinstatement session, animals were sacrificed and brains flash frozen on dry-ice chilled isopentane.

Whole cell recording:

Coronal slices (250-300 μ m) through the thalamus were cut on a vibratome) and transferred into ACSF containing (in mM): 124 NaCl, 3 KCl, 1.25 KH₂PO₄, 1.5 MgSO₄, 26 NaHCO₃, 2.5 CaCl₂, and 10 dextrose. Recordings were made in a submerged chamber superfused with carbogen-saturated ACSF at a speed of 2-3 ml / min., 32°C. Neurons of the medial habenular nuclei were identified using an upright fluorescence/brightfield microscope. Loose cell attached-recordings

(110-250 M Ω) were achieved from identified cells using infrared differential interference contrast¹⁶⁰. Recordings (Axopatch 200A amplifier) were made with 5–7 M Ω pipettes filled with 0.9% NaCl. Data were analyzed with pClamp (Molecular Device) and Minianalysis (Synaptosoft). *RT-qPCR, fluorescent in-situ hybridization, and fluorescent immunohistochemistry:*

For RT-qPCR experiments, flash frozen 20 μ m coronal sections and 500 μ m, 0.5mm² punches containing the Hb complex were collected using a Leica CM 1850 cryostat at -18°C. To examine *c-fos* expression, RNA was isolated from aforementioned punches using RNeasy Mini Kit (Qiagen, 74106) and total RNA was reverse-transcribed. cDNA was analyzed using Roche Light Cycler via Roche proprietary algorithms and REST 2009 software Pfaffl method^{242,243}. All values were normalized to *Gapdh* expression levels generated simultaneously. Both *cFos*, *Syt9*, and *gapdh* primers were generated from Roche Universal Probe Library; *c-fos*: left c-Fos primer, 5'-ggggcaaagtagagcagcta-3'; right c-Fos primer 5'-agctccctctccgattc-3'; c-Fos probe 46, atggctgc; *Syt9*: left Syt9 primer, 5' - ggagaactgtgccatgc - 3'; right Syt9 primer 5' – tgagctgtcttcggattgag – 3'; Syt9 probe 21; *gapdh*: right GAPDH primer, 5'-atggtgaaggctcgggtgta-3', left GAPDH primer, 5'-aatctccactttgccactgc-3', GAPDH probe, tggcggattgg¹³⁵. *Syt9* is enriched in the MHb²⁴⁴ and was used to initially validate flash frozen punches can be taken to enrich for the MHb (**Fig. 1.1A**).

For fluorescent in-situ hybridization, 20 μ m coronal sections were collected using a Leica CM 1850 cryostat at -18°C. For hybridization, a fluorescent oligodeoxynucleotide against *cFos* was used in an adapted hybridization protocol to quantitatively analyze gene expression²⁴⁵. Briefly, tissue was fixed in 4% PFA and blocked in 0.5% Triton X-100 in PBS. Tissue was then hybridized with a fluorescent *cFos*-specific probe [100nM] in hybridization buffer (4X SSC, 4% salmon sperm DNA, 0.5mM EDTA, 25% formamide in ddH₂O.). Following hybridization, tissue was

washed in 2X SSC, incubated in DAPI [1:15000] in 0.1M PBS, and subsequently coverslipped using VectaShield Mounting Medium (product #H-1000). For immunohistochemistry slices were fixed in 4% PFA for 10 min, washed in 0.1M PBS, and permeated in 0.1% Triton X-100 in 0.1M PBS. Slices were then incubated in blocking serum (8% NGS, 0.3% Triton X-100, in PBS; 1 hr) and incubated at 4°C overnight in primary solution (2% NGS, 0.3% Triton X-100; anti-AcH4K8 [1:1000], Cell Signaling #2594S). Slices were then incubated in secondary solution (2% NGS, 0.3% Triton X-100; AcH4K8, goat anti-rabbit Alexa Fluor 488 [1:1000] in PBS). Tissue was imaged using Olympus Slide Scanner VSBX61. Fluorescence was quantified using ImageJ. Briefly, background signal was collected from a soma-free region and subtracted from MHb signal. All values were normalized to saline-reinstated controls.

Data analysis:

All data was analyzed and graphed using Graphpad Prism 7.02.

Results

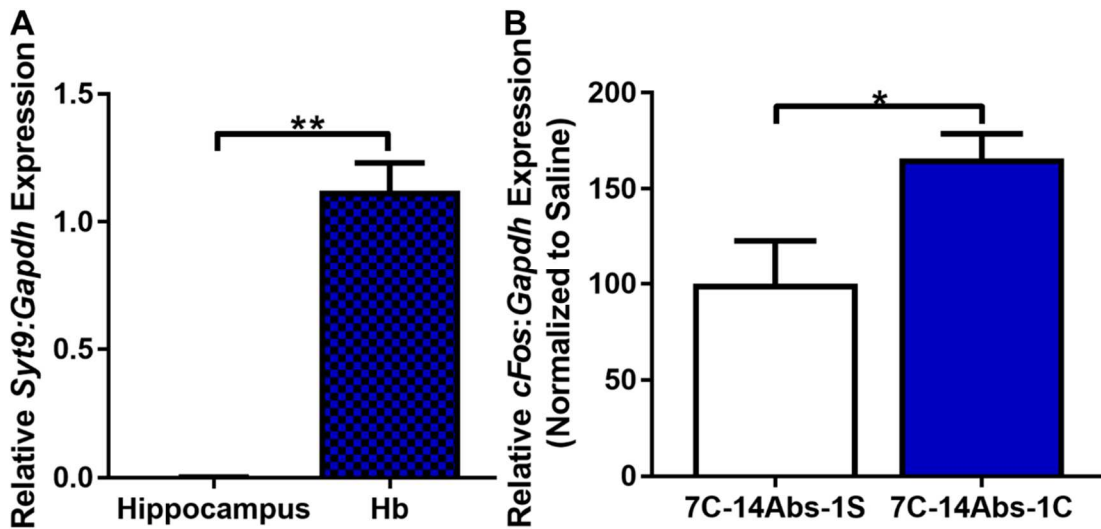


Figure 1.1: The MHb responds to cocaine re-exposure. (A) Epithalamic punches (n=4) are significantly enriched for *Syt9* (a marker for the MHb) compared to neighboring dorsal hippocampus (n=4; $t_3=10.39$, $p=0.0019$). (B) Cocaine re-exposure (n=6) significantly increases *cFos* expression in the Hb complex compared to saline controls (n=5; $t_9=2.602$, $p=0.0286$). (* indicates $p \leq 0.05$, ** indicates ≤ 0.01)

The Hb complex responds to cocaine re-exposure following a period of forced abstinence

Following 7 days of repeated cocaine administration (10 mg/kg, I.P.) and 14 days of forced abstinence in the home cage, animals received a cocaine re-exposure (5 mg/kg, I.P.) or saline. Cocaine re-exposed animals showed a significant increase in *cFos* expression in the Hb complex compared to saline injected controls (**Fig. 1.1B**).

The MHb is functionally engaged during cocaine-primed reinstatement of CPP

To determine if the MHb is engaged during cocaine-primed reinstatement of cocaine-induced CPP, wild-type C57BL/6J mice were conditioned, extinguished, and reinstated with either saline or cocaine using a previously described counter-balanced protocol (**Fig. 1.2A**)^{132,144}. Both saline-reinstated and cocaine-reinstated animals equally acquired and extinguished a conditioned preference (**Fig. 1.2B** and **Fig. 1.2C**). 24 hours following final extinction session, animals were primed with either saline or cocaine-HCl immediately prior to the reinstatement test. As predicted, cocaine-primed animals exhibited a significant increase in preference score compared to saline-primed animals during the cocaine-primed reinstatement test. To limit analysis to the MHb, fluorescent in-situ hybridization was used to measure changes in *cFos* expression. In cocaine-reinstated animals, we found a significant increase in *cFos* expression (**Fig. 1.2E** and **1.2F**) and (using immunohistochemistry) an increase in acetylated H4K8 (**Fig. 1.2G** and **1.2H**) in the MHb. We have observed that increased H4K8Ac associated with increased expression of *c-Fos* and *Nr4a2* in a previous study^{132,240}. The alterations in *cFos* expression within the MHb are not induced acutely following a single acquisition of cocaine-paired CPP (**Fig. 1.2I, 1.2K**) or a single injection of cocaine in the home cage (**Fig. 1.2J, 1.2L**). These data suggest that the MHb is engaged during cocaine-primed reinstatement of a cocaine-induced conditioned place preference.

To understand the direct effects of cocaine on MHb activity, we recorded from vMHb neurons of naïve or CPP extinguished animals. Bath application of cocaine (20 μ M) had no effect on the firing rate of vMHb neurons in naïve (**Fig. 1.3A**) or CPP extinguished animals. (**Fig. 1.3B**).

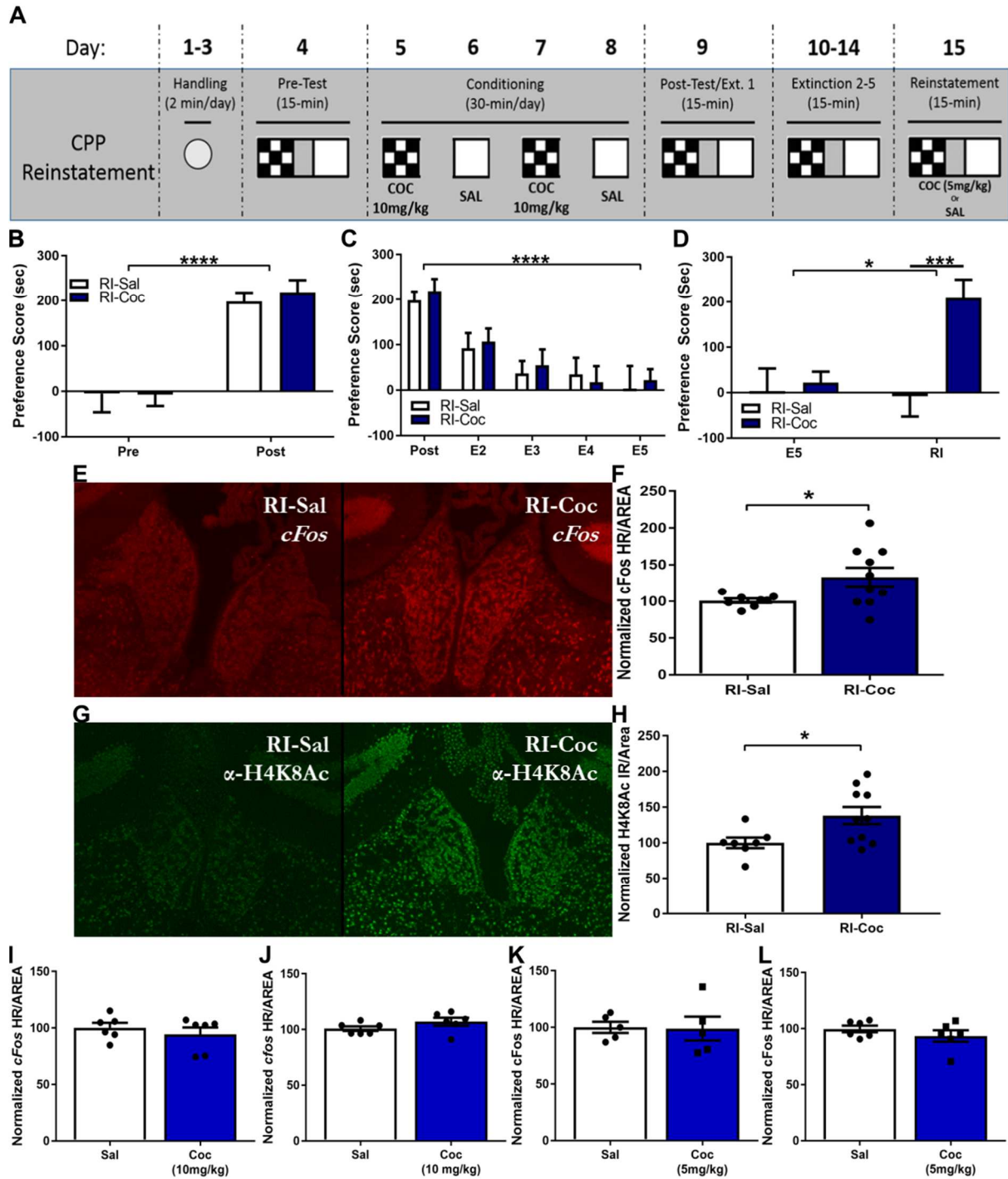


Figure 1.2: The MHb is engaged by cocaine-primed reinstatement of CPP. (A) Cocaine-induced CPP cocaine-primed reinstatement paradigm. (B) Wild-type mice acquire cocaine-induced CPP (Two-way ANOVA, main effect of Conditioning: $F_{(1,18)}=56.15$, $p<0.0001$), with no differences between saline-primed ($n=9$) and cocaine-primed animals ($n=11$) (Two-way ANOVA, No main effect of Reinstatement-Priming: $F_{(1,18)}=0.0958$, $p=0.7604$). (C) CPP can be extinguished with repeated drug-free exposures to conditioning apparatus (Two-way ANOVA, main effect of Extinction: $F_{(4,72)}=17.99$, $p<0.0001$); saline-primed and cocaine-primed animals extinguish equally (No main effect of Reinstatement-priming, $F_{(1,18)}=0.1222$, $p=0.7308$). (D) Cocaine-primed animals significantly reinstate previously extinguished cocaine-induced CPP compared to saline-primed controls (Two-way ANOVA, main effect of Cocaine-Priming: $F_{(1,18)}=7.359$, $p=0.0143$; Main effect of Reinstatement Session: $F_{(1,15)}=5.814$, $p=0.0268$; effect of Interaction $F_{(1,15)}=7.431$, $p=0.0139$). Sidak's post-hoc analysis indicates cocaine-primed animals have a significantly increased preference during reinstatement test compared to final extinction session ($t_{(15)}=4.204$, $p=0.0015$) and reinstatement of saline-primed controls ($t_{(30)}=3.829$, $p=0.0025$). (E) Representative images of FISH against *cFos* in the MHb of animal reinstated with (*left*) saline and reinstated with (*right*) 5mg/kg cocaine-HCl. (F) Cocaine-reinstated animals ($n=10$) show a significant increase in *cFos* hybridization reactivity in the MHb compared to saline-primed ($n=8$) controls (Welch's corrected two-tailed t-test $t_{(9,922)}=2.467$, $p=0.0334$) (G) Representative images of IHC against H4K8Ac in the MHb of (*left*) saline-reinstated animal and (*right*) cocaine-HCl reinstated animal. (H) Cocaine-reinstated animals ($n=10$) show a significant increase in H4K8Ac immunoreactivity in the MHb compared to saline-primed ($n=7$) controls (Two-tailed t-test $t_{(15)}=2.407$, $p=0.0294$). (I) A single cocaine ($n=6$, 10mg/kg) CPP conditioning session does not alter *cFos* expression in the MHb compared to saline-paired controls ($n=6$, equal w/v) ($t_{(10)}=0.7891$, $p=0.4484$). (J) An acute dose of cocaine ($n=6$, 10mg/kg) alone does not alter *cFos* expression in the MHb compared to saline-injected controls ($n=6$, equal w/v) ($t_{(10)}=1.5$, $p=0.1645$). (K) A single cocaine ($n=5$, 5mg/kg) CPP conditioning session does not alter *cFos* expression in the MHb compared to saline-paired controls ($n=5$, equal w/v) ($t_{(8)}=0.09397$, $p=0.9274$). (L) An acute dose of cocaine ($n=6$, 5mg/kg) alone does not alter *cFos* expression in the MHb compared to saline-injected controls ($n=6$, equal w/v) ($t_{(10)}=1.061$, $p=0.3137$). (* indicates $p \leq 0.05$, *** indicates $p \leq 0.001$, **** indicates $p \leq 0.0001$)

Moreover, we observed no differences baseline firing rate in the vMHb of naïve or CPP extinguished animals (**Fig. 1.3C**).

Discussion

Previous work has shown that chronic cocaine suppresses MHb activity that is restored by a subsequent increased dose of cocaine²³². Yet, no studies have characterized the MHb response to cocaine following a period of forced abstinence. Here, we demonstrate that the Hb is activated (as measured by increase in *cFos* expression) by a cocaine re-exposure following abstinence from chronic cocaine treatment. From a technical perspective, even though punches are enriched with MHb tissue, it is more than likely collected tissue also contains LHb and paraventricular thalamus, two neighboring structures known to be altered by cocaine experience. Also, from a theoretical perspective, it is unclear if this increased activity during cocaine re-exposure is potentially linked to behaviors associated with repeated cocaine administration, such as cocaine-primed reinstatement. To address this, we adapted a fluorescent in-situ hybridization protocol that would

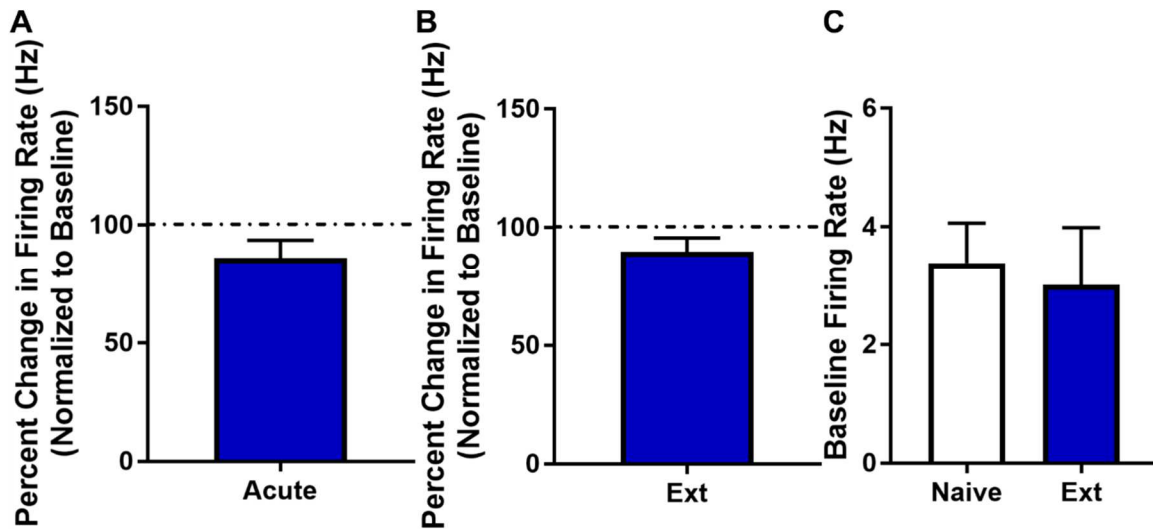


Figure 1.3: Cocaine does not directly alter vMHB activity. Bath application of cocaine-HCl (20 μ M) does not alter firing rate of vMHB neurons from (A) naïve ($t_{(3)}=1.857$, $p=0.1603$) or (B) CPP extinguished ($t_{(7)}=1.743$, $p=0.1248$) animals. (C) Baseline firing rates between naïve and extinguished animals show no significant difference ($t_{(15)}=0.7577$, $p=0.4604$).

allow for the quantification of *cFos* expression explicitly in the MHb following cocaine-primed reinstatement of CPP. Using this approach, we demonstrate that the MHb is activated during cocaine-primed reinstatement of extinguished CPP, but not during acute cocaine and cocaine-associated memory formation. Also, we demonstrate that in response to cocaine-primed reinstatement, the MHb is in an epigenetically permissive state linked to the increased expression of IEGs, such as *cFos* and *Nr4a2*. This aligns with previous work demonstrating increased *cFos* in the MHb during cue-primed reinstatement of cocaine self-administration. However, in our electrophysiological experiments, cocaine alone was unable to induce stimulation of vMHB neurons from naïve or animals extinguished in CPP. This data suggests that the increases in MHb activity during cocaine re-exposure and cocaine-primed reinstatement are not mediated by cocaine's direct influence on the MHb, but cocaine is acting upon inputs to the MHb to recruit MHb activity. Nevertheless, these observed changes do not *causally* link MHb function to the reinstatement of cocaine-associated behaviors, nor do they demonstrate an epigenetic regulation of MHb function.

Chapter 2: Controlling Neuronal Function Through Chemogenetics

Rationale

We demonstrate various functional adaptations of the MHb to cocaine-associated behaviors, specifically, reinstatement of cocaine-primed CPP. However, these changes in function do not causally link the MHb to reinstatement behaviors. More so, due to the small size of the MHb and its proximity to the LHb and PVT, it does not easily lend itself to acute pharmacological manipulations. To address this, chemogenetics provides a novel method of controlling and studying neural function in behaving animals. Specifically, Designer Receptors Exclusively* Activated by Designer Drug (DREADDs) allow for a unique approach to investigate circuit activity of specific brain regions, circuits, and their role in driving behavior. DREADDs are a family of mutated muscarinic acetylcholine receptors that provide reversible activation of G-protein coupled receptor (GPCR) signaling cascades that can induce depolarization (G_q , G_s) or hyperpolarization (G_i) upon application of clozapine-n-oxide (CNO). Although originally reported as an inert ligand, work from several groups has identified off-target effects of CNO and, in rodents, its back metabolism to clozapine^{246–248}. Still, the use of DREADD-free controls combined with appropriate CNO concentrations make DREADDs a powerful method for providing gain-of- and loss-of-function manipulations in the CNS.

Previous work has shown that these designer receptors can be effectively employed to bidirectionally modulate neuronal activity in a spatially and temporally specific manner^{249–255}. To demonstrate feasibility of this technique in our hands, we utilized a DREADD approach to investigate their ability to regulate hippocampal LTP and hippocampus-dependent long-term memory. The novel object recognition (NOR) series of tasks have been widely used to assess memory formation²⁵⁶. These tasks exploit rodents' inherent preference for novelty and can be used to study long-term memory formation in an incidental, noninvasive fashion. Recent work by our

lab and others, has shown that in rodents the object location memory (OLM) task is a hippocampus-dependent task. Specifically, OLM requires the dorsal region of the CA1 subfield for long-term memory retrieval^{102,112,113,257-262}. Conversely, retrieval of memory in the object recognition memory (ORM) task, in rodents, has been shown to be hippocampus-independent, relying on cortical structures^{112,113,122,263}. Here, we show DREADDs in the dorsal hippocampus can be used to bidirectionally modulate formation in the OLM task, but not ORM task. Surprisingly, however, we discovered promoter-specific effects of expressing DREADDs in the hippocampus on hippocampal LTP.

Methods

Animals:

8-week old male c57BL/6J mice were purchased from Jackson Laboratory. Animals were maintained in 12:12 light/dark cycle with food and water provided *ad libitum*. All experiments were conducted according to the National Institutes of Health guidelines for animal care and use. Furthermore, experiments were approved by the Institutional Animal Care and Use Committee of the University of California, Irvine.

Stereotaxic surgeries:

For hSyn-HM3D experiments, animals received 1uL bilateral infusions to the dorsal hippocampus (ML: +/-1.5, AP: -2.0, DV: -1.5) of either *AAV2.8-hSyn-GFP* (n=10-12; viral titer 3.7×10^{12}) control or *AAV2.8-hSyn-HA-HM3D-IRES-mCitrine* (n=10-12; 2.3×10^{12}). For hSyn-HM4D experiments, animals received similar infusions of either *AAV2.8-hSyn-GFP* (n=10-12; 3.7×10^{12}) control or *AAV2.8-hSyn-HA-HM4D-IRES-mCitrine* (n=10-12; 4.2×10^{12}). For CaMKII α -HM3D experiments, animals received 1uL bilateral infusions to the dorsal hippocampus of either *AAV2.8-CaMKII α -GFP* (n=10-12; 5.6×10^{12}) or *AAV2.8-CaMKII α -HA-HM3D-IRES-mCitrine*

(n=10-12; 3.1×10^{12}). For CaMKII α -HM4D experiments, animals received similar infusions of either *AAV2.8-CaMKII α -GFP* (n=10-12; 5.6×10^{12}) or *AAV2.8-CaMKII α -HA-HM4D-IRES-mCitrine* (n=10-12; 3.3×10^{12}). Viruses were infused at a rate of 100nl/min using a 30 gauge Neuros Hamilton syringe (Product #: 65459-01) mounted to either Harvard Apparatus Nanomite Syringe Pump (Product #: MA1 70-2217) or Leica Biosystems Nanoinjector Motorized f/Stereotaxics (Product #: 39462901). All infusions used the Leica Microsystems Angle Two Stereotaxic system. Animals were allowed to recover for 7 days prior to handling. Behavioral testing and electrophysiological recordings began at post-surgery day 21, to allow for full expression of DREADD receptors.

Novel Object Recognition Tasks:

NOR Tasks were carried out as previously described^{122,256}. Briefly, animals were handled for 2 minutes over 5 consecutive days. Beginning on Day 4 of handling, animals were habituated for 5 min to the OLM chamber for 6 consecutive days in the absence of the test objects. Animals then underwent a task training session. For HM3D experiments, animals were presented with two identical 100mL beakers for 3 mins. For HM4D experiments, animals were presented with these OLM training objects for 10 mins. Animals were systemically injected 40 minutes prior to the training session with 3mg/kg of CNO (I.P, 0.3mg/ml, 0.5% DMSO, 0.9% saline; made fresh daily). Both GFP and DREADD-expressing animals were injected 40 minutes prior to behavior to allow for peak activation of DREADD receptors by CNO. After 24 hours, long-term memory formation was tested for 5 minutes, where the OLM training objects were presented, one of which in a novel location. Following OLM testing, animals were allowed to recover for 5 days. Animals were then habituated to the ORM chamber for 6 consecutive days in the absence of the test objects. For HM3D experiments, animals were presented with two identical objects (either metal tins or glass

candle holders) for 3 mins. For HM4D, animals were presented with these ORM training objects for 10 minutes. Both GFP and DREADD-expressing animals were systemically injected 40 minutes prior to training session with 3mg/kg of CNO (I.P, 0.3mg/ml, 0.5% DMSO, 0.9% saline; made fresh daily). 24 hours later, animals' retention was tested for 5 minutes, where one of the ORM training objects was replaced with a novel, previously unexplored object. Both the Training and Testing sessions were video recorded and hand scored by individuals blind to animal treatments. Videos were analyzed for total exploration of objects in addition to the discrimination index ($[(\text{time spent exploring novel object} - \text{time spent exploring familiar object}) / (\text{total time exploring both objects})]$).

Tissue harvesting for Immunohistochemistry and PCR:

For HM3D experiments, at least 72 hours following testing, both HM3D and GFP animals received a subsequent dose of CNO, returned to their home cage, and sacrificed after 70 minutes. For HM4D experiments, at least 72 hours following testing, animals received a subsequent dose of CNO, returned to their home cage for 40 minutes, introduced to a novel context for 10 minutes, and sacrificed 30 minutes later. Because the HM4D virus was predicted to inhibit hippocampal activity, it would be difficult to interpret this by simply giving a subsequent CNO injection and returning to home cage. This would lead to a floor effect as there would be very limited basal hippocampal activity and would be difficult to parse out differences between GFP and HM4D animals. The introduction to the novel context was an attempt to induce hippocampal activity, which presumably the HM4D virus would have inhibited. For immunohistological and c-fos expression experiments, animals were cervically dislocated and brains flash frozen in chilled isopentane. Flash frozen 20um coronal sections and 500µm, 1.0mm² punches of CA1 subfield of dorsal hippocampus were collected using a Leica CM 1850 cryostat at -18°C. To examine c-fos

expression, RNA was isolated using RNeasy Mini Kit (Qiagen, 74106) and total RNA (50ng) was reverse-transcribed. cDNA was analyzed using Roche Light Cycler via Roche proprietary algorithms and REST 2009 software Pfaffl method^{242,243}. All values were normalized to *Gapdh* expression levels generated simultaneously. Both *c-fos* and *gapdh* primers were generated from Roche Universal Probe Library; *c-fos*: left c-Fos primer, 5'-ggggcaaagtagagcagcta-3'; right c-fos primer 5'-agctccctctccgattc-3'; c-fos probe 46, atggetgc; *gapdh*: right GAPDH primer, 5'-atggtgaaggctcggtgtga-3', left GAPDH primer, 5'-aatctccacttggccactgc-3', GAPDH probe, tggcggattgg¹³⁵. For verification of viral expression in electrophysiological experiments, RNA was isolated using RNeasy Mini Kit (Qiagen, 74106) and total RNA was reverse-transcribed. cDNA was analyzed using Bio-Rad MJ Mini-Personal Thermal Cycler for expression of either HM3D or HM4D viruses. Both HM3D and HM4D primers were generated from Roche Universal Probe Library; *hm3d*: left HM3D primer, 5'-agtacaacctcgcctttgtttc-3'; right HM3D primer, 5'-atcggaggggctgtgtatc-3'; *hm4d*: left primer, 5'-tgaagcagagcgtcaagaag-3'; right HM4D primer, 5'-tctccagcttggcattg-3'.

Immunohistochemistry:

To confirm expression of DREADD, flash frozen sections were mounted to glass slides and stained for HA tag. Briefly, slices were fixed in 4% PFA for 10 minutes, washed twice in 0.1M PBS for 5 minutes, and quenched in 1.5% H₂O₂ for 20 minutes. Tissue was permeated with a single 5 min wash in 0.1% Triton X-100 in PBS solution, PBS-washed three times for 5 minutes, and blocked for an hour in 8% Normal Goat Serum, 0.3% TX-100 in 0.1M PBS. Following 3, 5-min PBS washes, slices were incubated overnight in an HA primary antibody solution containing anti-HA ([1:1000], Roche Diagnostics, Rat monoclonal, Product #: 11867423001), 2% NGS, 0.3% TX-100 in PBS at 4°C. Slices were washed three times for 5 minutes in PBS. Slices were then

incubated in secondary solution (Alexa Fluor Goat anti-Rat 555 [1:1000], 2% NGS, 0.3% TX-100, in PBS) for 2 hours at RT. Following secondary incubation slices were washed 3 times for 5 minutes in PBS, incubated in DAPI [1:15000] in PBS, and washed in PBS 3 times. Slides were air dried and coverslipped with VectaShield Mounting Medium (Product #: H-1000). Tissue was imaged using Olympus Scanner VSBX61 to confirm expression of either HA-tagged DREADD receptor or GFP control.

Slice preparation and electrophysiological recording:

Hippocampal slices were prepared as previously described¹⁰². Briefly, following isoflurane anesthesia, mice were decapitated and the brain was quickly removed and submerged in ice-cold, oxygenated dissection medium containing (in mM): 124 NaCl, 3 KCl, 1.25 KH₂PO₄, 5 MgSO₄, 26 NaHCO₃, and 10 glucose. Transverse hippocampal slices (375 μ m) through the mid-third of the septotemporal axis of the hippocampus were prepared using a FHC vibrating tissue slicer (Model:OTS-5000) before being transferred to an interface recording containing preheated artificial cerebrospinal fluid (aCSF) of the following composition (in mM): 124 NaCl, 3 KCl, 1.25 KH₂PO₄, 1.5 MgSO₄, 2.5 CaCl₂, 26 NaHCO₃, and 10 glucose and maintained at 31°C. Slices were continuously perfused with this solution at a rate of 1-1.5 ml/min while the surface of the slices were exposed to warm, humidified 95% O₂/ 5% CO₂. Recordings began following at least 1.5 hr of incubation.

Field excitatory postsynaptic potentials (fEPSPs) were recorded from CA1b stratum radiatum using a single glass pipette (2-3 M Ω). Stimulation pulses (0.05Hz) were delivered to Schaffer collateral-commissural projections using a bipolar stimulating electrode (twisted nichrome wire, 65 μ m) positioned in CA1c. Current intensity was adjusted to obtain 50% of the maximal fEPSP response. In a separate set of experiments, antagonists of the AMPA and NMDA

receptors were infused to block the negative-going fEPSP that is characteristic of excitatory transmission leaving a positive-going evoked response that is blocked by picrotoxin, a GABA_A receptor antagonist (field inhibitory postsynaptic potential; fIPSP)^{264,265}. Input/output curves were established before testing began to adjust current intensity that produced near maximal responses.

After establishing a 10-20 min stable baseline, compounds were introduced into the infusion line by switching from control aCSF to drug-containing aCSF. To determine whether CNO treatment affects the threshold level of LTP in slices from hSyn-GFP control, hSyn-HM3D, and hSyn-HM4D infused mice, LTP was induced by delivering 3 theta bursts, with each burst consisting of four pulses at 100 Hz and the bursts themselves separated by 200 msec (theta burst stimulation; TBS). The stimulation intensity was not increased during TBS. Data were collected and digitized by NAC 2.0 Neurodata Acquisition System (Theta Burst Corp., Irvine, CA).

Reagents:

For behavioral experiments, CNO was provided by the National Institute of Mental Health Chemical Synthesis and Drug Supply Program. For electrophysiological experiments, DNQX (Tocris Biosciences), D-(-)APV (Tocris Biosciences), and picrotoxin (Sigma) were prepared fresh in aCSF, while a 10mM stock solution of CNO (abcam# 141704) was dissolved in water and subsequently diluted to a working concentration (5 μ M) in aCSF.

Data analysis:

All statistical tests were performed using GraphPad Prism 5. Habituation data (distance traveled during individual habituation sessions), training, and testing videos were collected using ANY-maze behavioral analysis software. Habituation was analyzed using a 2-way ANOVA comparing total distance travelled across the habituation sessions. Training and testing data was analyzed using a Student's t-test comparing either exploration or discrimination index between

control and test animals. Slice physiology data in the text are presented as means \pm SD and fEPSP slope was measured at 10–90% fall of the slope. Data in figures on LTP were normalized to the last 10 min of baseline and presented as mean \pm S.E. CNO-induced changes on baseline measures were analyzed using a *paired*-Student's t-test comparing pre-CNO with post-CNO infusion period and assessed as significant if $p < 0.05$. Baseline measures on paired-pulse facilitation and LTP were analyzed using a 2-way ANOVA.

Results

hSyn-HM3D-dependent activation of the dorsal hippocampus can transform subthreshold training into LTM in OLM, but not ORM

To test if activation of the dorsal hippocampus during a subthreshold training event can lead to LTM, hSyn-HM3D and hSyn-GFP infused animals received CNO 40 min prior to a 3 min training session. Human synapsin-1 is ubiquitously expressed throughout neurons and viruses employing the *hSyn* promoter have been shown to have high neuron-specific expression²⁶⁶. We have previously shown that a 3 min training period is insufficient to generate long-term memory tested at 24 hours^{112–114,263}. Following CNO-primed training, animals were tested for LTM in the OLM task (**Fig. 2.1A**). hSyn-HM3D animals showed a significant increase in DI compared to hSyn-GFP controls during the test session ($t_{(19)}=3.387$, $p=.0031$), demonstrating that HM3D-mediated activation in the hippocampus transforms a subthreshold training period into robust LTM for object location (**Fig. 2.1Bii**). There were no differences between groups in training DI (**Figure 2.1Bi**; $t_{19}=0.6511$, $p=0.5228$), habituation ($F_{1,5}=0.02544$, $p=0.8749$), training exploration ($t_{19}=1.083$, $p=0.2924$), or test exploration ($t_{19}=0.2446$, $p=0.8094$) in the OLM experiment (data not shown).

Following testing in the OLM task, animals underwent a similar training and testing paradigm in the ORM task (**Fig. 2.1A**). hSyn-HM3D animals tested for LTM in the ORM task following CNO-primed training showed no difference in DI compared to hSyn-GFP controls ($t_{(19)}=0.05526$, $p=0.9565$), demonstrating that HM3D-mediated activation in the hippocampus does not affect LTM for object recognition (**Fig. 2.1Biv**). There were no measurable differences between groups in training DI (**Figure 2.1Biii**; $t_{19}=1.240$, $p=0.23$), habituation ($F_{1,5}=0.4782$, $p=0.4976$), training exploration ($t_{19}=0.9064$, $p=0.3761$), or test exploration ($t_{19}=0.5898$, $p=0.5623$) in the ORM experiment (data not shown). Immunohistochemistry was used to verify expression of both hSyn-GFP and hSyn-HM3D viruses (**Fig 2.1C**). To confirm *in-vivo* hSyn-HM3D function, animals received a subsequent dose of CNO before being sacrificed. RT-qPCR was used to measure *cfos* expression in tissue collected from the dorsal hippocampus. Tissue expressing hSyn-HM3D showed a dramatic increase in normalized *cfos:GAPDH* expression compared to hSyn-GFP control following a subsequent dose of CNO (**Fig. 2.1D**; $t_{(12.46)}=8.637$, $p<0.0001$). These results suggest that chemogenetic activation of the during training can transform a subthreshold learning event into LTM for OLM, a hippocampus specific task, but not for ORM.

hSyn-HM4D-dependent inactivation can block LTM formation in OLM, but not ORM

To test if dorsal hippocampus inactivation can block LTM formation during a training event that normally generates LTM, we administered CNO 40 min prior to 10 min training of hSyn-HM4D and hSyn-GFP infused animals. We have previously shown that a 10 min training period is sufficient for generating reliable LTM tested at 24 hours^{112,114,122,256}. 24 hours following CNO-primed training, animals were tested for LTM in the OLM task (**Fig. 2.1E**). hSyn-HM4D animals showed a significant decrease in DI compared to hSyn-GFP controls during the test session ($t_{(22)}=2.177$, $p=0.0405$), demonstrating that HM4D-mediated inhibition of the dorsal

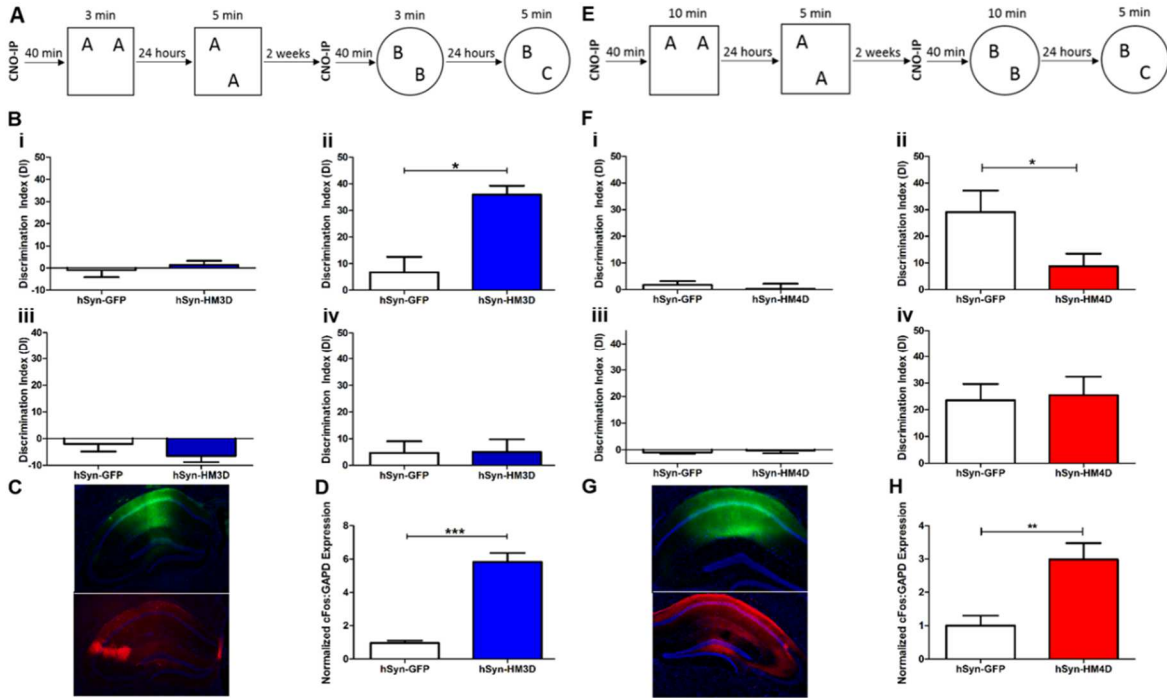


Figure 2.1: Bidirectional modulation of dorsal hippocampus via hSyn-DREADDs affects long-term memory processes. (A) Subthreshold training and testing paradigm for Novel Object Recognition tasks. (B) Training and testing discrimination indices of hSyn-GFP (white) and hSyn-HM3D (blue), shown as mean \pm S.E.M. (i) Mean discrimination index for OLM training, (ii) Mean discrimination index for OLM testing, (iii) Mean discrimination index for ORM training (iv) mean discrimination index for ORM testing. (C) Immunohistochemistry against DAPI (blue), GFP (green), and HA (red) in hSyn-GFP or hSyn-HM3D infused dorsal hippocampus. (D) Normalized RT-qPCR measuring relative *c-fos:GAPD* expression in hSyn-GFP (white) and hSyn-HM3D (blue). (E) Threshold training and testing paradigm for Novel Object Recognition tasks. (F) Training and testing discrimination indices of hSyn-GFP (white) and hSyn-HM4D (red), shown as mean \pm S.E.M. (i) Mean discrimination index for OLM training, (ii) Mean discrimination index for OLM testing, (iii) Mean discrimination index for ORM training (iv) mean discrimination index for ORM testing. (G) Immunohistochemistry against DAPI (blue), GFP (green), and HA (red) in hSyn-GFP or hSyn-HM4D infused dorsal hippocampus. (H) Normalized RT-qPCR measuring relative *c-fos:GAPD* expression in hSyn-GFP (white) and hSyn-HM4D (red). For HM3D OLM and ORM experiments, hSyn-GFP n=10 and hSyn-HM3D n=11. For HM4D OLM experiments, hSyn-GFP n=11, hSyn-HM4D n=12. For HM4D ORM experiments, hSyn-GFP n=12, hSyn-HM4D n=12. (* indicates $p \leq 0.05$, ** indicates $p \leq 0.01$, *** indicates $p \leq 0.001$)

hippocampus disrupts LTM for object location (**Fig. 2.1Fii**). There were no measurable differences between groups with regard to training DI (**Figure 2.1Fi**; $t_{22}=0.6071$, $p=0.55$), habituation ($F_{1,5}=0.3796$, $p=0.5441$), training exploration ($t_{22}=0.4126$, $p=0.6839$), or test exploration ($t_{22}=1.934$, $p>0.05$) in the OLM experiment (data not shown). hSyn-HM4D animals were subsequently tested for LTM in the ORM task following CNO-primed training and showed no difference in DI compared to hSyn-GFP controls ($t_{21}=0.2171$, $p=0.8302$), demonstrating that HM4D-mediated inhibition of the dorsal hippocampus does not affect LTM for object recognition

(**Fig. 2.1Fiv**). There were no measurable differences between groups in training DI (**Figure 2.1Fiii**; $t_{21}=0.5423$, $p=0.5933$), habituation ($F_{1,5}=0.3923$, $p=0.5379$), training exploration ($t_{21}=1.034$, $p=.3127$), or test exploration ($t_{21}=0.9842$, $p=.3362$) in the ORM experiment (data not shown).

Together, these results indicate that inhibition of dorsal hippocampal activity during training sufficient for LTM can block the formation of LTM for OLM, but not for ORM. Expression of hSyn-GFP and hSyn-HM4D viruses was confirmed immunohistologically (**Fig. 2.1G**). To confirm in-vivo hSyn-HM4D function, animals received a subsequent dose of CNO and RT-qPCR was used to measure *cfos* expression in tissue collected from the dorsal hippocampus. Surprisingly, tissue expressing hSyn-HM4D also showed a dramatic increase in normalized *cfos:GAPDH* expression compared to hSyn-GFP control following a subsequent dose of CNO (**Fig. 2.1H**; $t_{22}=3.483$, $p=0.021$). The cause of this *cfos* induction is unknown and could be attributed to several factors, including interneuron function throughout the dorsal hippocampus. To more accurately characterize the hSyn-mediated effects on hippocampal function, we evaluated DREADD modulation electrophysiologically.

hSyn-dependent expression of DREADD receptors differentially affects synaptic transmission and LTP in hippocampal field CA1

We predicted that chemogenetic activation (HM3D-G_q) would increase synaptic transmission and LTP, whereas chemogenetic inhibition (HM4D-G_i) would block synaptic transmission and LTP in the dorsal hippocampus. We tested these predictions in acute hippocampal slices prepared from hSyn-GFP-control, hSyn-HM3D, and hSyn-HM4D infused mice. CNO infusions had no detectable influence on fEPSP slope and amplitude in slices from hSyn-GFP animals (**Fig. 2.2A and 2.2B**). However, unexpectedly, CNO application to hSyn-

HM3D expressing slices caused a substantial decrease in the slope and amplitude of the fEPSP relative to pre-CNO infusion (**Fig. 2.2A, 2.2B, and 2.2D**). Field responses in slices from hSyn-HM4D mice also produced surprising results. CNO-application to hSyn-HM4D expressing slices caused a transient increase in slope, while the amplitude of the field response remained significantly elevated 20 min into the washout period relative to pre-CNO baseline values. Strangely, engagement of hSyn-HM3D *inhibits* glutamatergic signaling in the dorsal hippocampus, while engagement of hSyn-HM4D appears to *enhance* glutamatergic signaling (aligning with the enhanced *cFos* expression seen in **Fig. 2.1H**). It is important to note that while the hSyn-promoter does provide neuronal specificity, it does not provide neuronal cell-type specificity. It is possible that both the unexpected *cFos* induction in hSyn-HM4D expressing animals and the counter-intuitive electrophysiological effects are mediated by DREADD-mediated changes in local GABA neuron activity.

To test the role of hippocampal GABA-interneurons in CNO-induced changes, we pharmacologically isolated the fIPSP. In the dorsal hippocampus, fIPSPs can be isolated using combined AMPA and NMDA receptor antagonists; this fIPSP is picrotoxin (PTX)-sensitive, demonstrating it is mediated by GABA_A receptor activation (**Fig. 2.2Ei**). Following a stable baseline recording, the fIPSP remained unchanged during a 20 min CNO infusion period in hSyn-GFP expressing slices (**Fig. 2Ei**). However, CNO application on hSyn-HM4D expressing slices blocked the fIPSP in the dorsal hippocampus, while CNO application on hSyn-HM3D expressing slices enhanced the fIPSP (**Fig. 2Eii**). Collectively, these results suggest that, hSyn-HM4D increases excitatory drive in the dorsal hippocampus through inhibition of local GABA neurons, while hSyn-HM3D inhibits the fEPSP by activating local GABA neurons.

We subsequently tested how these DREADD-mediated changes would effect changes in LTP. TBS in CNO-treated slices from hSyn-GFP injected mice produced strong short-term potentiation that gradually stabilized over a 20 min period to a level that was $+27\pm 12\%$ above pre-TBS baseline 60 min post-induction (**Fig. 2.3**). CNO-pretreatment in hSyn-HM4D expressing slices enhanced TBS-induced LTP, while in hSyn-HM3D expressing animals, CNO-pretreatment impaired TBS-induced LTP (**Fig. 2.3**). The enhancement in LTP in hSyn-HM4D slices is consistent with previous studies showing that blocking GABA_A receptor activation enhances LTP in area

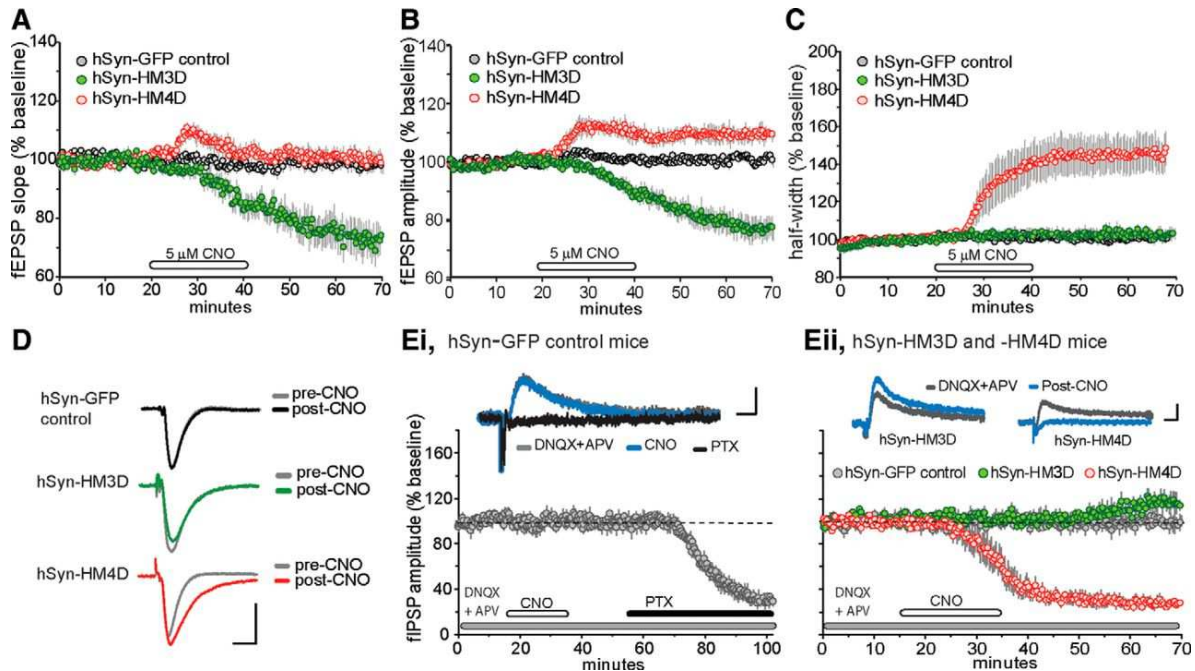


Figure 2.2: Characterization of baseline synaptic transmission in hippocampal slices expressing hSyn-driven excitatory and inhibitory DREADD receptors. (A-C) Hippocampal slices were prepared from adult GFP-control (grey circle, $n=6$), hSyn-HM3D (green circle, $n=7$), and hSyn-HM4D (red circle, $n=6$) mice. The graphs show the mean \pm S.E.M. fEPSP (A) slope, (HM3D; $t_{(6)}=5.3$, $p=0.0018$; HM4D; ($t_{(5)}=4.5$, $p=0.006$) (B) amplitude, ($t_{(6)}=4.4$, $p=0.004$) and (C) half-width plotted as a percent change of baseline in hippocampal slices treated for 20 min with 5 μ M CNO followed by a washout. (D) representative field responses collected from GFP-control, hSyn-HM3D, and hSyn-HM4D slices during the baseline recording period (Pre-CNO) and 30 min after the end of CNO infusion (Post-CNO). Calibration: 1 mV, 5 ms. (E) (i) Pharmacologically isolated field IPSP amplitudes (responses recorded in the presence of 20 μ M DNQX and 100 μ M APV, antagonists for AMPA and NMDA receptors, respectively) were evoked by stimulation of the Schaffer-commissural projections (Pre-CNO, grey line, upper trace) in slices prepared from GFP-control animals ($n=5$ slices). Graph shows the mean \pm S.E.M. change in field IPSP amplitude as a percent change of baseline. These responses were completely blocked by the GABA_A receptor antagonist picrotoxin (PTX, black line, upper traces) and were unaffected by infusions of 5 μ M CNO (blue line, upper traces). Calibration: 0.1 mV, 10 ms. (ii) In slices prepared from hSyn-HM3D mice ($n=7$ slices), CNO infusions produced a delayed but significant increase in the fIPSP; $t_{(5)}=3.0$, $p=0.03$. In contrast, CNO infusions mimicked the effects of PTX by causing a dramatic decrease in the fIPSP and completely eliminating the field response 30 min after the end of the infusion period in slices ($n=5$) from hSyn-HM4D mice. Field IPSP were unaffected by infusions of CNO in slices from GFP-controls ($n=5$) during the recording session. Calibration: 0.1 mV, 10 ms.

CA1^{267,268}. To confirm viral infusions in hSyn-HM3D and hSyn-HM4D slices, PCR on collected tissue was used with primers specific to either HM3D or HM4D receptors to rule out the possibility of crossed viral infusion; i.e. to validate that the inhibitory effect of the hSyn-HM3D virus is not due to being accidentally injected with hSyn-HM4D, but is truly a characteristic of the hSyn-HM3D virus and vice-versa. PCR with primers specific to the HM3D virus yielded bands only in tissue isolated from HM3D animals. Moreover, PCR with primers specific to the HM4D virus yielded bands only in tissue isolated from HM4D animals, thus, precluding the possibility of virus cross-contamination (data not shown). Taken together, these studies strongly suggest that the hSyn-mediated DREADD expression transduces a global population of neurons in hippocampal region CA1 that regulate both excitatory and inhibitory synaptic inputs.

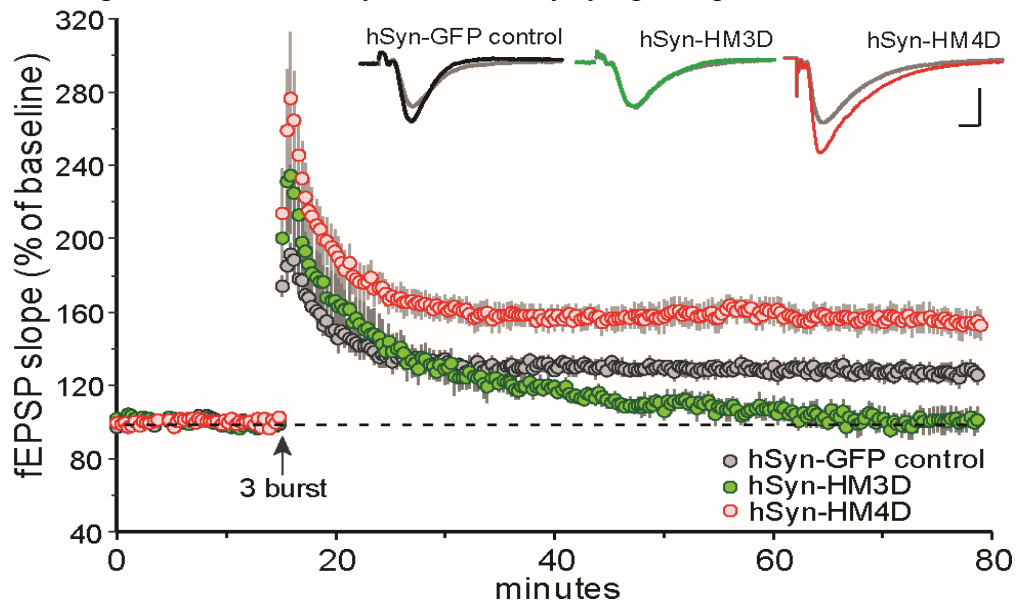


Figure 2.3: Long-term plasticity changes associated with hSyn-driven DREADD receptor expression in adult hippocampal slices. The slope of the fEPSP was normalized to the mean of the last 60 responses (10 min) collected in the presence of 5 μ M CNO before application of theta burst stimulation (upward arrow). A single train of 3 theta bursts was effective in inducing stable potentiation in slices from GFP-control mice ($n=6$), but produced a supranormal amount of potentiation in slices from hSyn-HM4D mice ($n=6$). In contrast, theta burst-induced LTP decayed toward baseline values in slices from hSyn-HM3D ($n=6$) mice. main effect of DREADD $F_{(2,15)}=73$, $p=0.001$ Inset: Traces collected during the last 5 min of CNO treatment (grey line) and 60 min post-TBS (black, green, and red lines). Calibration: 1 mV, 5 ms

Targeting the excitatory cell-population via promoter specificity corrects for predicted outcome on synaptic transmission and long-term plasticity.

To limit DREADD-mediated effects to the glutamatergic population of the dorsal hippocampus, we use *CamkII α* driven viral vectors. Use of the *CamkII α* promoter has been shown to restrict viral expression to forebrain excitatory neurons^{269–272}. Thus, we predicted animals infused with the CaMKII α -regulated HM3D and -HM4D DREADD receptors would alter excitatory transmission in a positive and negative manner, respectively. In agreement with our hypotheses, bath applied CNO (5 μ M) caused a rapid increase in glutamatergic transmission beginning 5-10 min after the start of infusion in slices prepared from animals treated with CaMKII α -HM3D (Fig. 2.4A). In CaMKII α -HM4D expressing slices, CNO caused a significant drop, in fEPSP slope that was 15% below baseline values, while the synaptic responses collected from CaMKII α -GFP-control slices remained unchanged during the infusion and recording session. (Fig. 2.4A). We then tested CNO's effects on theta burst-induced LTP in CaMKII α -HM3D and –HM4D infused mice. Consistent with our previous predictions, TBS in CaMKII α -GFP expressing

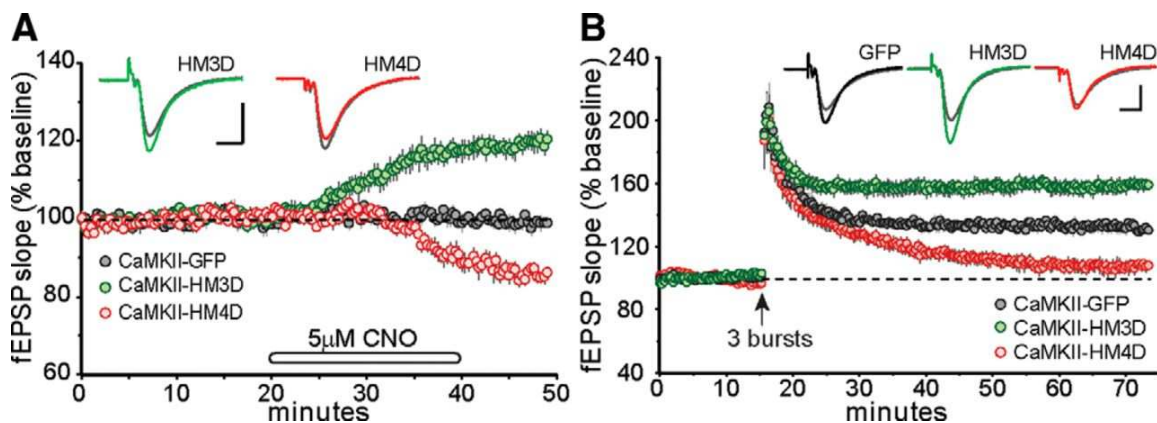


Figure 2.4: Promotor-specific effects of CaMKII α DREADD receptors on synaptic transmission and long-term plasticity. (A) Following stable baseline recordings, infusions of CNO (5 μ M) produced a rapid increase in field responses collected from CaMKII α -HM3D (n=8) slices. In contrast, CNO infusions caused a marked decrease in fEPSP slope in slices from CaMKII α -HM4D (n=6) mice. Field responses from CaMKII α -GFP (n=6) slices were unaffected by CNO infusion. Inset: Representative traces collected during baseline recording (grey line) and 10 min after the end of CNO infusion (colored lines). Calibration: 1mV, 5 ms. (B) The slope of the fEPSP was normalized to the mean of the last 60 responses (10 min) collected in the presence of 5 μ M CNO before application of theta burst stimulation (upward arrow). A single train of 3 theta bursts delivered at the end of CNO infusion period was sufficient to induce short-term potentiation that then stabilized for the remainder of the recording period in control slices (CaMKII α -GFP, n=6), but not in slices from CaMKII α -HM4D (n=6). The same train applied at the end of the CNO infusion generated robust and stable LTP that was greater in magnitude in slices from CaMKII α -HM3D (n=8) mice than controls. Inset: Traces collected during the last 5 min of CNO treatment (grey line) and 60 min post-TBS (black, green, and red lines). Calibration: 1 mV, 5 ms

slices pretreated with CNO (+32±7%). CNO-pretreatment on CaMKII α -HM3D expressing slices generated a significantly enhanced TBS- (+59±11%) that was suppressed in CaMKII α -HM4D expressing slices.

CaMKII α -HM3D-dependent activation of dorsal hippocampus can transform subthreshold training into LTM in OLM, but not ORM

Although the effects of CaMKII α -HM3D excitation of the dorsal hippocampus on LTP were as predicted, it was necessary to compare these hippocampal synaptic plasticity results to those of hippocampal learning. To test if CaMKII α -HM3D mediated excitation of the dorsal hippocampus can transform a subthreshold training event into LTM, CaMKII α -HM3D and CaMKII α -GFP infused animals received CNO 40 min prior to a 3 min training session (**Fig. 2.5A**). 24 hours following CNO-primed training, animals were tested for LTM in the OLM task. CaMKII α -HM3D animals showed a significant increase in DI compared to CaMKII α -GFP controls ($t_{(21)}=4.774$, $p=0.0001$), demonstrating that HM3D-mediated excitation in the hippocampus transforms a subthreshold training period into robust LTM for object location (**Fig. 2.5Bii**). There were no significant differences between groups in training DI (**Figure 2.5Bi**; $t_{(21)}=0.01476$, $p=0.9884$) or test exploration ($t_{(21)}=1.298$, $p=0.2082$) (data not shown). However, there was a modest, yet statistically significant, increase in CaMKII α -HM3D animals' training exploration (7.891 +/-0.3704 sec) compared to CaMKII α -GFP (6.394 +/-0.4156 sec) ($t_{(21)}=2.698$, $p=0.0135$). Furthermore, there was a significant difference in habituation ($F_{(1,5)}=4.821$, $p=0.0395$). However, a Bonferroni post-test revealed the difference was only significant during Day 1 of habituation and was no longer significant throughout Days 2-6, suggesting that both groups of animals equally habituated to the OLM training context prior to training (data not shown).

Following OLM testing, animals were subsequently trained and tested in the ORM task (**Fig. 2.5A**). CaMKII α -HM3D and CaMKII α -GFP animals tested for LTM in the ORM task 24 hours following CNO-primed training showed no difference in DI compared to CaMKII α -GFP controls ($t_{(21)}=0.1542$, $p=0.8789$), with no measurable differences in habituation ($F_{(1,5)}=3.276$, $p=0.0846$), training DI (**Figure 2.5Bii**; $t_{(21)}=0.1478$, $p=0.8839$), training exploration ($t_{21}=1.079$, $p=0.2928$), or test exploration ($t_{(21)}=1.079$, $p=0.2928$) (data not shown). Expression of either CaMKII α -GFP or CaMKII α -HM3D in the dorsal hippocampus was confirmed immunohistologically (**Fig. 2.5C**). These results indicate that CaMKII α -HM3D mediated excitation of the dorsal hippocampus parallels the electrophysiological effects on LTP and transforms the subthreshold training event into LTM for the OLM task, but not the ORM task.

CaMKII α -HM4D-dependent inactivation of the dorsal hippocampus can block LTM formation in OLM, but not ORM

To test if CaMKII α -HM4D mediated inhibition of dorsal hippocampal neurons can disrupt LTM formation, we primed 10-min training of CaMKII α -HM4D or CaMKII α -GFP infused animals with CNO administration. 24 hours following CNO-coupled training, animals were tested for LTM in the OLM task (**Fig. 2.5D**). CaMKII α -HM4D animals showed a significant decrease in DI compared to CaMKII α -GFP controls (**Fig. 2.5Eii**; $t_{(21)}=5.490$, $p<0.0001$), with no significant differences in training DI (**Figure 5Ei**; $t_{(21)}=1.296$, $p=0.2090$), habituation ($F_{(1,5)}=0.0569$, $p=0.8136$), training exploration ($t_{(21)}=0.4539$, $p=0.6545$), or test exploration ($t_{(21)}=0.5871$, $p=0.5634$) (data not shown). Animals were subsequently tested for LTM in the ORM task 24 hours following CNO-primed training (**Fig. 2.5D**). CaMKII α -HM4D animals showed no differences in testing DI compared to CaMKII α -GFP controls (**Fig. 2.5Eiv**; $t_{(22)}=0.1125$, $p=0.9114$). Moreover, there were no measurable differences in training DI (**Figure 5Eiii**;

$t_{22}=0.07847$, $p=0.9382$), habituation ($F_1=0.2521$, $p=0.6206$), training exploration ($t_{22}=0.6564$, $p=0.5184$), or test exploration ($t_{22}=0.8065$, $p=0.4286$) (data not shown). Immunohistochemistry was used to confirm expression of CaMKII α -GFP or CaMKII α -HM4D (**Fig. 2.5F**). These results suggest that CaMKII α -HM4D mediated inhibition of the dorsal hippocampus parallels the electrophysiological effects on LTP and is able to prevent the formation of LTM for the OLM task, but not the ORM task.

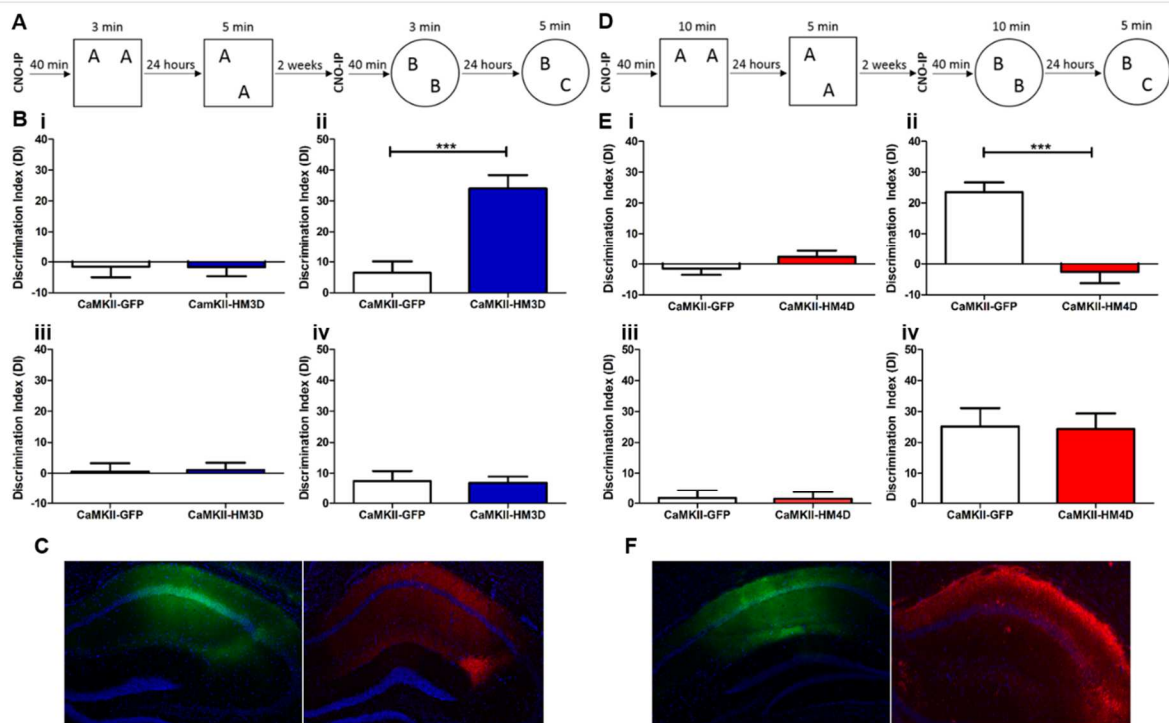


Figure 2.5: Modulation of dorsal hippocampus via CaMKII α -DREADDs leads to bidirectional changes in long-term memory processes. (A) Subthreshold training and testing paradigm for Novel Object Recognition task. (B) Training and testing discrimination index of CaMKII α -GFP (*white*) and CaMKII α -HM3D (*blue*), shown as mean \pm S.E.M. (i) Mean discrimination index for OLM training, (ii) Mean discrimination index for OLM testing, (iii) Mean discrimination index for ORM training (iv) mean discrimination index for ORM testing. (C) Immunohistochemistry against DAPI (*blue*), GFP (*green*), and HA (*red*) in CaMKII α -GFP or CaMKII α -HM3D infused dorsal hippocampus. (D) Threshold training and testing paradigm for Novel Object Recognition task. (E) Training and testing discrimination index of CaMKII α -GFP (*white*) and CaMKII α -HM4D (*red*), shown as mean \pm S.E.M. (i) Mean discrimination index for OLM training, (ii) Mean discrimination index for OLM testing, (iii) Mean discrimination index for ORM training (iv) mean discrimination index for ORM testing. (F) Immunohistochemistry against DAPI (*blue*), GFP (*green*), and HA (*red*) in CaMKII α -GFP or CaMKII α -HM4D infused dorsal hippocampus. For HM3D OLM and ORM experiments, CaMKII α -GFP $n=11$, CaMKII α -HM3D $n=12$. For HM4D OLM experiments, CaMKII α -GFP $n=12$, CaMKII α -HM3D $n=11$. For HM4D ORM experiments, CaMKII α -GFP $n=12$, CaMKII α -HM3D $n=12$. (***) indicates $p \leq 0.001$)

Discussion

We implemented DREADDs to bidirectionally modulate the dorsal hippocampus to validate the use of DREADDs in a well characterized behavioral paradigm. Both hSyn-HM3D- and CaMKII α -HM3D-mediated activation of the dorsal hippocampus were able to transform a subthreshold learning event into LTM for object location, but not object recognition. Additionally, hSyn-HM4D- and CaMKII α -HM4D-mediated inactivation of the same region was able to block LTM formation for object location, but not object recognition. These behavioral results support previous findings in mice that the dorsal hippocampus appears to be particularly involved in object location memory, but not object recognition^{102,113,122,256,258,259}. Memory for object recognition appears to be more dependent on the perirhinal cortex^{273–275} and the insular cortex^{275,276}. However, the role of the hippocampus in memory for object recognition is more controversial^{257,260}, as results tend to be dependent on various parameters including species and stime between training and testing^{113,275,277}.

Most importantly in this study, we discovered promoter-specific effects of expressing DREADDs in the hippocampus on hippocampal LTP. The function of DREADDs on hippocampal LTP induced by TBS, a neuronal firing pattern occurring during exploratory behavior in rodents²⁷⁸, had not previously been investigated. The hSyn-HM3D and hSyn-HM4D behavioral experiments led us to predict that hSyn-HM3D expression in the hippocampus would produce an enhancement in LTP, while an impairment in LTP was expected in slices from hSyn-HM4D expressing mice. Surprisingly, application of CNO to slices expressing hSyn-HM3D in the dorsal hippocampus, led to a significant decrease in amplitude of fEPSP and blocked TBS-induced LTP. In contrast, application of CNO to slices expressing hSyn-HM4D led to a significant increase in fEPSP amplitude and an enhancement of TBS-induced LTP. Our electrophysiological data suggest that CNO-induced depression of field responses in hSyn-HM3D mice may be driven by activation of

local GABA interneurons^{279,280}, while hSyn-HM4D mediated increase of fEPSP appears to be driven by GABA interneuron suppression. These results suggest that data obtained with hSyn promoter driven DREADDs should be carefully interpreted, particularly when used in adult *ex vivo* tissue with diverse local subpopulations.

The contrast between electrophysiological and behavioral results via hSyn-mediated altered signaling remains poorly understood. The disparate results may largely be due to non-specific viral infected cells within local interneuron population which are known to tightly regulate activity of CA1 pyramidal cells in this region^{263,281,282}. hSyn viral expression in local interneurons would explain the increase in *cfos* expression following CNO exposure in hSyn-HM4D infused mice (See **Fig. 2.1H**). Interestingly, numerous reports have shown a dissociation between hippocampal LTP and hippocampus-dependent LTM using genetically modified mice^{283–289}. It is important to note (and it is often overlooked in studies implementing the DREADD technique) that that changes in neuronal firing are nothing more than a convenient artifact of the GPCR signaling cascades engaged by CNO-DREADD interaction. While it is convenient to catalog HM3D as an excitatory DREADD and HM4D as an inhibitory DREADD, this subtle lack of accuracy has the potential to cause inconsistencies in interpreting chemogenetic results. In this study, we demonstrate that hSyn-HM3D suppresses fEPSP in the dorsal hippocampus. Yet, *in vivo*, hSyn-HM3D significantly induced *cFos* expression, to an extent that is unlikely mediated by increased firing of GABA neurons responsible for the fEPSP suppression. This suggests that while there was electrophysiological inhibition, intracellularly, the Gq signaling cascade was still being engaged, leading to the curious results on gene expression and may underlie the enhancement in hippocampus-dependent learning despite fEPSP inhibition. Nevertheless, DREADDs still provide

an avenue of cell-type specific manipulations that can be *relatively* easily adapted to study the role of the MHb in relapse-like behaviors.

Chapter 3: Medial Habenula Cholinergic Neurons Regulate Cocaine-primed Reinstatement

Rationale

Propensity to relapse, even following long periods of abstinence, is a key feature in SUD. Relapse and relapse-like behaviors are known to be induced, in part, by re-exposure to drugs of abuse and/or drug-associated cues. Yet, while many critical nodes in the neural circuitry contributing to relapse have been identified and studied, a full description of the networks driving reinstatement of drug-seeking behaviors is lacking. One area that may provide further insight to the mechanisms of relapse is the MHb. Due to the density of cholinergic neurons and the expression of unique nicotinic acetylcholine receptors (including the $\beta 4$ and $\alpha 5$ subunits) in the vMHb, much of the addiction field has focused on nicotine-associated behaviors^{179,210,215,290,291}. The cholinergic population of the vMHb has been shown to be necessary for nicotine self-administration, withdrawal, and the aversive properties of nicotine^{215,218,292}. While it is clear the vMHb has a key role in regulating nicotine response and behavior, few studies have extensively evaluated how the vMHb regulates the response to other drugs of abuse^{223,224,227}. Recent work, however, implicates the cholinergic population of the MHb in regulating self-administration and reinstatement behavior of other psychostimulants, including cocaine and methamphetamine^{209,225,228}. Yet, the mechanisms by which the MHb may modulate the behaviors associated with cocaine are unknown. We have previously demonstrated (See **Chapter 1**) that the MHb is activated during cocaine-primed reinstatement of CPP. The goal of this study is to investigate how the MHb may regulate relapse-like behavior and adaptive response to cocaine. Here, we use a cell-type specific chemogenetic approach to causally link vMHb activity to changes in cocaine-associated behaviors.

Methods

Animals:

ChAT-IRES-CreCre/Cre mice were purchased from the Jackson Laboratory (Stock No. 006410). Male and female heterozygous ChAT-IRES-Cre mice (ChAT-Cre) were bred and maintained in 12 h light/dark cycle with food and water provided *ad libitum*. All experiments were conducted according to the National Institutes of Health guideline for animal care and use. Experiments were approved by the Institutional Animal Care and Use Committee of the University of California, Irvine.

Stereotaxic Surgeries:

2-5-month-old heterozygous ChAT-Cre mice received 0.5 μ L bilateral infusions to the medial habenula (M/L, +/-0.35mm; A/P, -1.5 mm; D/V; -3.0) of *AAV2.8-hSyn-DIO-HM3D-Gq-mCherry* (2.2×10^{12} vg/ml) or *AAV2.8-hSyn-DIO-mCherry* (5.3×10^{12} vg/ml). Viruses were infused at a rate of 100nl/min using a 30 gauge Neuros Hamilton syringe (product #65459-01) mounted to either a Harvard Apparatus Nanomite Syringe Pump (product #MA1 70-2217) or Leica Biosystems Nanoinjector Motorized f/Stereotaxics (product #39462901)²⁹³. All infusions used the Leica Microsystems Angle Two Stereotaxic System. For behavioral experiments, animals were allowed to recover for a minimum of 7 d before handling. For electrophysiological recordings, animals were allowed to recover for a minimum of 4 w before recording.

Chemogenetic Viruses:

All viruses were purchased from UNC Vector Core (HM3D Lot: AV4979bc, 2013, mCherry Lot: AV4981CD, 2014) or AddGene (HM3D Lot: v4330, 2016). Viral cDNA was extracted with Proteinase K in 1%SDS/10mM Tris-HCl in water and viral purity of chemogenetic constructs was confirmed via Sanger Sequencing (Genewiz) and Endpoint PCR. Universal Amplification Forward Primer: 5' - gccacccttggtcaccttcag - 3', Universal Amplification Reverse

Primer: 5' - gccatacgggaagcaatagca - 3'. Universal Sequencing Primer: 5' -cgatctcgaactcgtggccgt - 3'

Whole cell recording:

Coronal slices (250-300 μm) through the thalamus were cut on a vibratome) and transferred into ASCF containing (in mM): 124 NaCl, 3 KCl, 1.25 KH_2PO_4 , 1.5 MgSO_4 , 26 NaHCO_3 , 2.5 CaCl_2 , and 10 dextrose. Recordings were made in a submerged chamber superfused with carbogen-saturated ACSF at a speed of 2-3 ml / min, 32°C. Labeled neurons of the medial habenular nuclei were identified using an upright fluorescence microscope. Loose cell attached-recordings (110-250 $\text{M}\Omega$) were achieved from identified fluorescent cells using infrared differential interference contrast¹⁶⁰. Recordings (Axopatch 200A amplifier) were made with 5–7 $\text{M}\Omega$ pipettes filled with 0.9% NaCl. Data were analyzed with pClamp (Molecular Device) and Minianalysis (Synaptosoft).

CPP-Reinstatement Paradigm:

Cocaine-induced CPP was performed as previously described^{42,144,240,241}. Briefly, animals were handled for 2 min for 3 consecutive days. Following handling, mice were conditioned over 4 consecutive days, receiving either cocaine-HCl (10mg/kg, IP; Sigma) or 0.9% saline, in a context-dependent manner (counter-balanced, unbiased). Following conditioning, animals were allowed to freely explore, in a drug-free state, the complete chamber to assess preference, established as the difference between time spent in the cocaine-paired chamber and the saline-paired chamber, in seconds. To extinguish preference, animals were repeatedly reintroduced to the chamber, daily for 6 consecutive days. Once extinguished, animals received either 3mg/kg CNO (0.3mg/ml CNO, 0.5% DMSO, 0.9% saline, IP) or vehicle (0.5% DMSO, 0.9% saline) 40 minutes prior to being reinstated with 0.9% saline. Animals were sorted post-hoc into reinstatement groups following extinction to ensure reinstatement groups equally acquired and extinguished preference.

For CNO Acquisition experiments, animals received on alternating days either 3mg/kg CNO (0.3mg/ml CNO, 0.5% DMSO, 0.9% saline, IP) or vehicle (0.5% DMSO, 0.9% saline) 40 minutes prior to 30-minute conditioning sessions. Behavior was assessed and analyzed using Ethovision XT 11.5.

Immunohistochemistry:

Animals were euthanized and brains flash frozen in dry ice-chilled isopentane. 20 μ M coronal sections were collected using a Leica CM 1850 cryostat at -18°C. For immunohistochemical confirmation of HM3D or mCherry expression, MHb containing slices were fixed in 4% PFA for 10 min, washed in 0.1M PBS, and permeated in 0.1% Triton X-100 in 0.1M PBS. Slices were then incubated in blocking serum (8% NGS, 0.3% Triton X-100, in PBS; 1 hr) and incubated at 4°C overnight in primary solution (2% NGS, 0.3% Triton X-100; anti-DsRed [1:1000], Clontech #1408015). Slices were then incubated in secondary solution (2% NGS, 0.3% Triton X-100; DsRed, Alexa Fluor goat anti-rabbit 555; in PBS). Tissue was imaged using Olympus Slide Scanner VSBX61.

Data analysis:

All data was analyzed and graphed using Graphpad Prism 7.02.

Results

Chemogenetic activation of the cholinergic MHb population reinstates place preference

To establish a causal link between MHb activity and reinstatement of cocaine-induced CPP, we employed a chemogenetic approach to selectively activate the vMHb during reinstatement. DIO-HM3D(Gq)-mCherry was infused bilaterally in the MHb of ChAT-IRES-Cre^{Cre/+} knockin mice (called ChAT-Cre mice). ChAT-Cre animals have been shown to effectively limit expression of Cre-dependent (DIO) constructs within cholinergic cell populations,

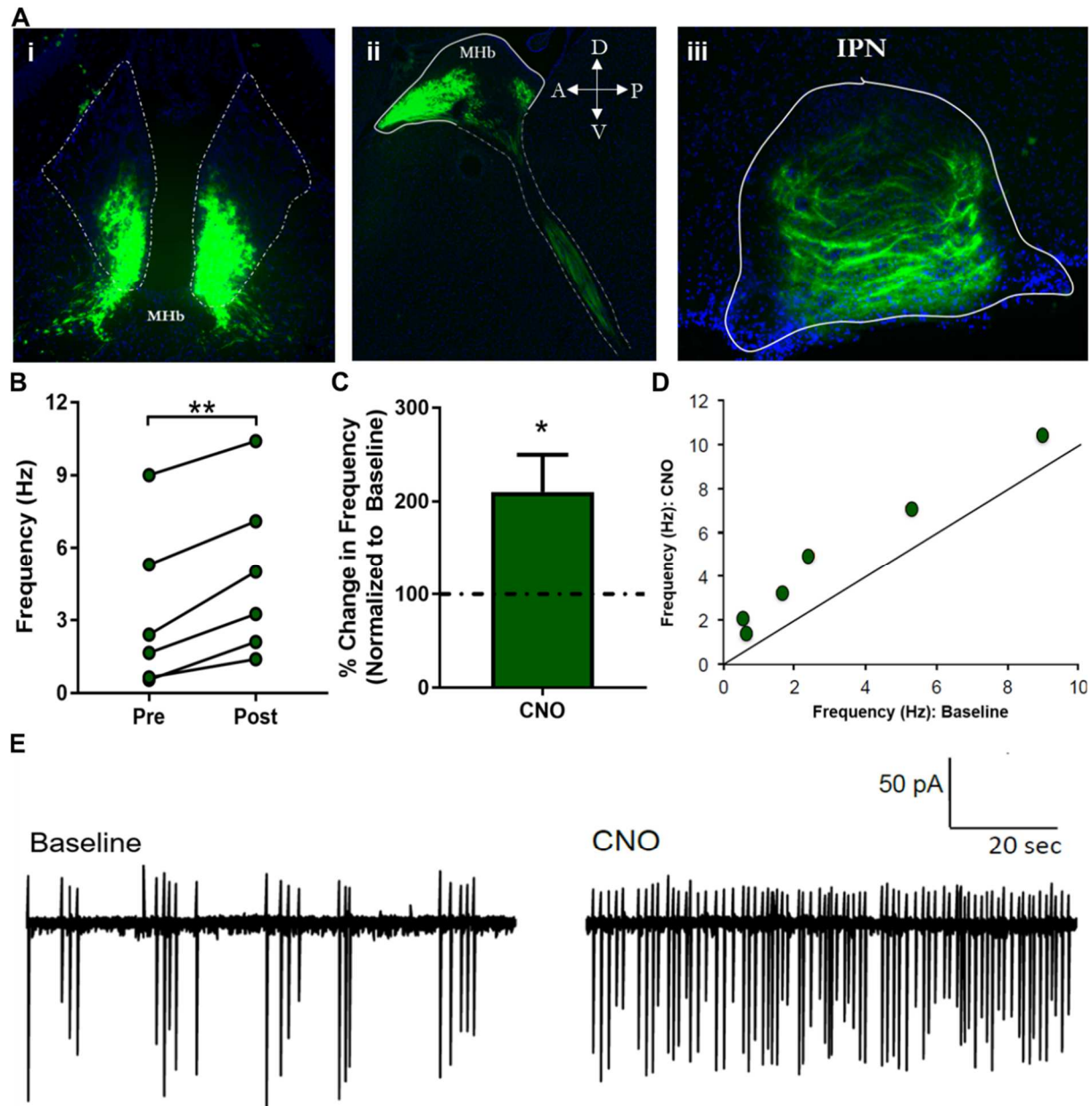


Figure 3.1: Combinatorial approach using Cre-dependent DREADD in Cre-drive line. (A) Immunohistochemistry against DIO-HM3D(Gq)-mCherry; (i) coronal and (ii) sagittal sections show limited expression of mCherry-tagged HM3D DREADD to MHb^{CHAT} population. (iii) Coronal section of IPN shows expression of HM3D DREADD in axon terminals in the IPN, known to receive dense innervation from the cholinergic population of the vMHb. (B) Mean firing rate during baseline and following CNO (10 μ M) infusion. HM3D-mCherry expressing MHb neurons (n=6) showed a $110.2 \pm 39.5\%$ increase in firing rate following CNO application (Paired t-test, $t_{(5)}=6.574$, $p=0.0012$) (C) When normalized to baseline, HM3D-mCherry expressing MHb neurons showed a significant increase in percent change in firing rate ($t_{(5)}=2.787$, $p=0.0386$). (D) Frequency of spiking for HM3D-mCherry expressing MHb cells during infusion, as a function of baseline values (E) Loose seal recordings from representative fluorescent MHb neuron prior to Baseline and two minutes following CNO (10 μ M) infusion. (* indicates $p \leq 0.05$, ** indicates $p \leq 0.01$).

particularly in the MHb (Fig. 3.1A)²⁹⁴. First, we examined whether engagement of Gq-coupled

signaling increases firing of MHb ChAT expressing neurons. DIO-HM3D was injected bilaterally in the MHb of ChAT-Cre mice and recordings made with loose seal (110 – 250 M Ω) clamps from labeled neurons in coronal slices through the medial habenula prepared from mice injected at least 4 weeks previously¹⁶⁰. Recording was continued until a stable, ten-minute baseline rate (0.5 to 9.0 Hz) of spontaneous spiking was collected. CNO (10 μ M) was then infused for an additional ten minutes. The agonist increased firing frequency within 1-2 minutes of application in all cells examined (**Fig. 3.1B-D**, representative trace **Fig. 3.1E**). The mean increase in rate was $110.2 \pm 39.5\%$ (**Fig. 3.1B** and **3.1C**), with the largest percent effects occurring in cells with an initially low spiking rate (**Fig. 3.1D**), demonstrating that HM3D-mCherry expressing MHb ChAT neurons can be activated chemogenetically, in a CNO-dependent manner.

To determine if chemogenetic activation of MHb ChAT expressing neurons is sufficient for reinstatement of cocaine-induced CPP, we infused DIO-HM3D bilaterally into the MHb of ChAT-Cre mice. HM3D-infused ChAT-Cre animals underwent CPP conditioning and extinction as previously described (**Fig. 3.2A**). HM3D-infused animals both acquired (**Fig. 3.2B**) and extinguished (**Fig. 3.2C**) a cocaine-induced CPP, with no differences between CNO-reinstated and Veh-reinstated animals. To test whether activity within MHb ChAT expressing neurons is sufficient to drive reinstatement of a cocaine-induced CPP, we administered CNO or vehicle 40 min prior to a saline-primed reinstatement session. We found CNO-primed animals had a significantly increased preference score compared to Veh-primed controls during the reinstatement test (**Fig. 3.2D**). Additionally, we did not find sex-dependent effects on CPP acquisition between males (n=8) and females (n=9) (Two-way ANOVA, no main effect of Sex, $F_{(1,15)}=0.5065$, $p=0.4876$; no Sex-Conditioning interaction, $F_{(1,15)}=1.172$, $p=0.2961$) nor sex-dependent effects on extinction (No main effect of Sex, $F_{(1,15)}=0.01755$, $p=0.8964$). Although there was a Sex-

Extinction Interaction ($F_{(5,75)}=2.734$, $p=0.0253$), Sidak's post-hoc analysis does not indicate any significant differences between sexes across extinction trials. Lastly, our initial analyses did not find a Sex-dependent effect on CNO-induced reinstatement between males ($n=6$) and females ($n=3$) (No Sex-Reinstatement Interaction, $F_{(1,7)}=3.242$, $p=0.1148$; no main effect of Sex, $F_{(1,7)}=0.5496$, $p=0.4836$) (**data not shown**). Thus, chemogenetic activation of MHb ChAT

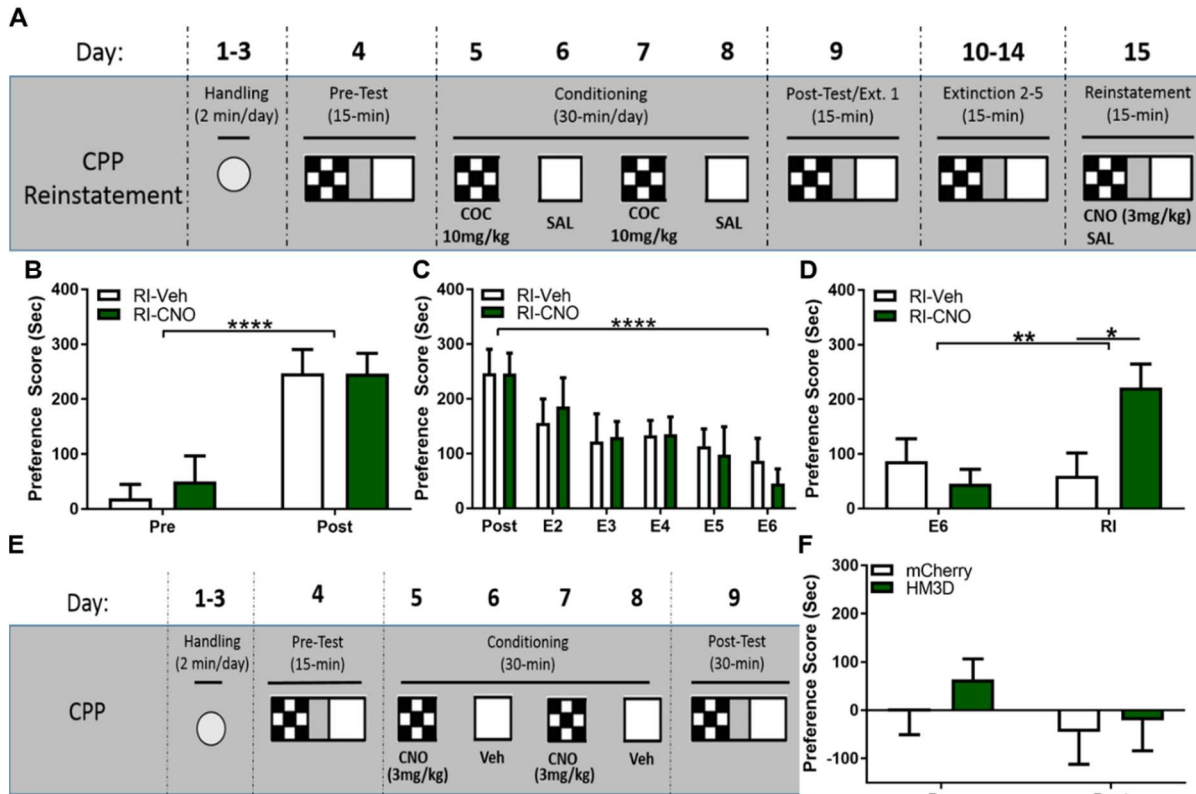


Figure 3.2: Chemogenetic activation of MHb^{ChAT} artificially induces reinstatement of CPP. (A) Cocaine-induced CPP CNO-primed reinstatement paradigm. (B) ChAT-Cre HM3D infused mice acquire cocaine-induced CPP (Two-way ANOVA, main effect of Conditioning, $F_{(1,15)}=37.52$, $p<0.0001$), with no differences between CNO-primed ($n=9$) and Veh-primed ($n=8$) animals (No main effect of CNO-Priming $F_{(1,15)}=0.1159$, $p=0.7383$). (C) CPP in HM3D-infused animals is subsequently extinguished with repeated drug-free exposures to chamber (Two-way ANOVA, main effect of Extinction, $F_{(5,75)}=9.002$, $p<0.0001$). Both CNO-primed and Veh-primed animals extinguish CPP equally (No main effect of CNO-Priming, $F_{(1,15)}=0.0055152$, $p=0.9437$). (D) CNO-primed animals significantly reinstate previously extinguished cocaine-induced CPP (Two-way ANOVA, Interaction between CNO-Priming and Reinstatement Session, $F_{(1,15)}=16.02$, $p=0.0012$; main effect of CNO-Priming, $F_{(1,15)}=8.721$, $p=0.0099$). Sidak's post-hoc analysis reveals a significant increase in preference score during reinstatement session in CNO-primed animals compared to final extinction session ($t_{(15)}=5.07$, $p=0.0003$) and compared to reinstatement of Veh-primed animals ($t_{(30)}=2.988$, $p=0.0111$). (E) CNO-induced CPP paradigm. (F) CNO alone is unable to establish a conditioned place preference or aversion in either mCherry-infused ($n=6$) or HM3D-infused ($n=6$) animals (No main effect of CNO Conditioning, $F_{(1,10)}=3.749$, $p=0.0816$; No main effect of DREADD, $F_{(1,10)}=0.3974$, $p=0.5426$; No Interaction, $F_{(1,10)}=0.431$, $p=0.5263$). Although there may be a trend of CNO Conditioning, Sidak's post-hoc analysis shows no significant difference in change in preference score of mCherry-infused animals ($t_{(10)}=0.9049$, $p=0.6240$) or HM3D-infused animals ($t_{(10)}=1.833$, $p=0.1839$). (* indicates $p \leq 0.05$, ** indicates $p \leq 0.01$, **** indicates $p \leq 0.0001$)

expressing neurons artificially induces reinstatement behavior in previously cocaine-conditioned animals, even in the absence of cocaine, demonstrating that the cholinergic signaling in the MHb mediates behavioral effects of cocaine-primed reinstatement.

Activation of cholinergic MHb neurons does not induce CPP or CPA

We have demonstrated that MHb cholinergic neurons are sufficient for inducing reinstatement of cocaine-induced CPP, mimicking the drug-primed phenotype. However, how activity in the vMHb, specifically the cholinergic population, affects reward processing and associative learning remains unclear. Thus, we tested if chemogenetic activation of the MHb ChAT expressing neurons alone induces a conditioned preference or aversion. ChAT-Cre animals were infused bilaterally with either DIO-mCherry or DIO-HM3D in the MHb. Animals were subsequently handled and underwent an adapted CNO-primed CPP paradigm where animals received alternating conditioned pairings of Veh (0.5% DMSO, 0.9% saline; I.P.) or CNO (3 mg/kg, 0.5% CNO, 0.9% saline; I.P) 40 minutes prior to exposure to conditioning chambers (**Fig. 3.2E**). 24 hours following final conditioning session, animals were tested for preference for or aversion to CNO-paired chamber, in a CNO-free state. We found no effect of CNO-conditioning in either DIO-mCherry or DIO-HM3D animals during post-test (**Fig. 3.2F**). These data suggest that activation of the MHb is unable to induce a conditioned preference or aversion.

CNO administration does not induce reinstatement behavior in DREADD-free mice

Recent work has further characterized the pharmacological mechanism by which chemogenetic manipulations, specifically DREADDs, function. Others have demonstrated that CNO alone has no effect on reinstatement behaviors or psychostimulant self-administration^{295–299}. However, Gomez et al. implicates clozapine as the specific ligand to DREADDs and its back metabolism from CNO to engage DREADD-mediated changes in cell function (2017). Due to the

potential psychoactive effects of clozapine, we next tested if the chemogenetic-induced reinstatement (see Fig. 3.2D) and changes to MHB^{ACh} firing rate (see Fig. 3.1B-D) were due to engagement of the expressed DREADD-receptor or an off-target effect of CNO exposure. We infused DIO-mCherry in the MHB of ChAT-Cre mice. DIO-mCherry infused animals subsequently underwent CPP acquisition and extinction as previously described (Fig. 3.3A). mCherry-infused animals both acquired (Fig. 3.3B) and extinguished (Fig. 3.3C) a cocaine-

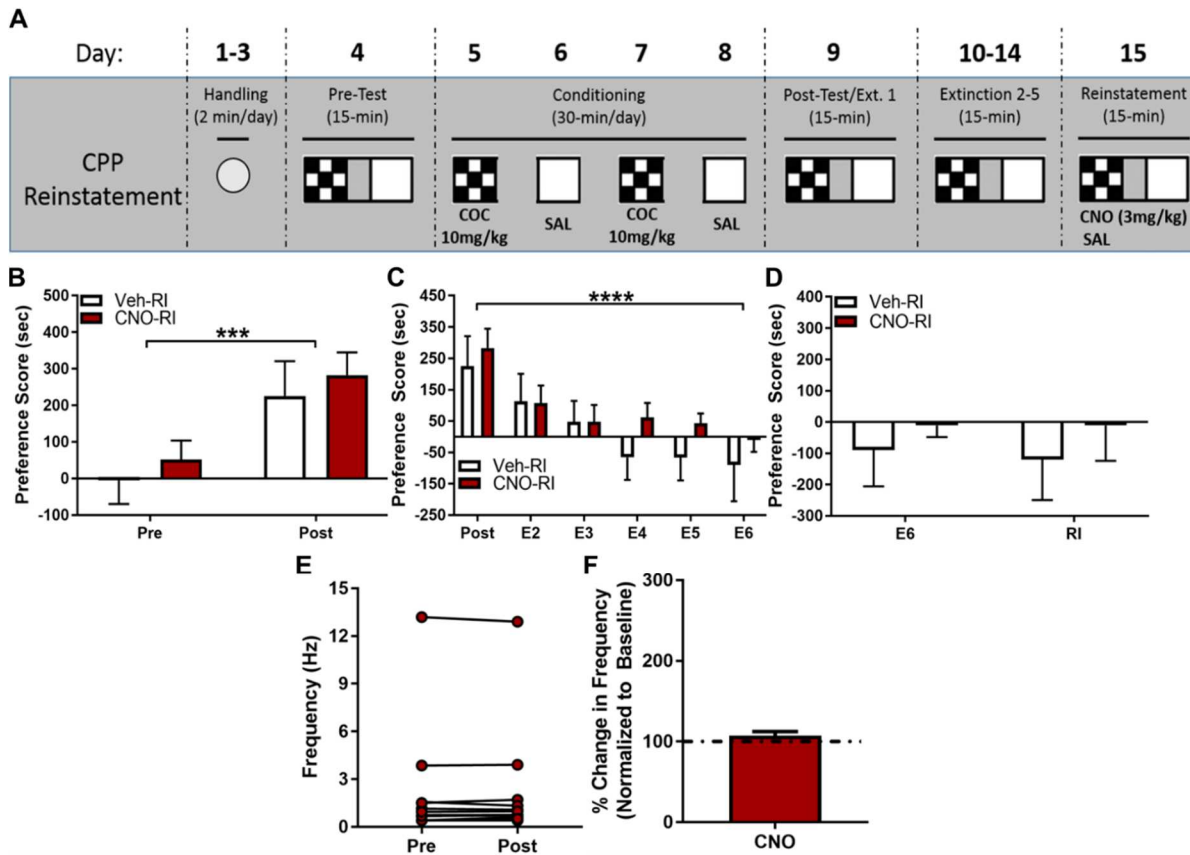


Figure 3.3: CNO-priming does not induce reinstatement of CPP in DREADD-free animals. (A) Cocaine-induced CPP CNO-primed reinstatement paradigm. (B) ChAT-Cre DIO-mCherry infused mice acquire cocaine-induced CPP (Two-way ANOVA, main effect of Conditioning, $F_{(1,9)}=30.56$, $p=0.0004$), with no differences between CNO-primed ($n=6$) and Veh-primed ($n=5$) animals (No effect main effect of CNO-priming ($F_{(1,9)}=0.4273$, $p=0.5297$)). (C) CPP in mCherry-infused animals is subsequently extinguished with repeated drug-free exposures to chamber (Two-way ANOVA, main effect of Extinction, $F_{(5,45)}=10.77$, $p<0.0001$). Both CNO-primed and Veh-primed animals extinguish CPP equally (No main effect of CNO-priming, $F_{(1,9)}=0.7064$, $p=0.4224$). (D) CNO-primed animals show no significant reinstatement of previously extinguished cocaine-induced CPP compared to Veh-primed controls (Two-way ANOVA, no main effect of Reinstatement, $F_{(1,9)}=0.06347$, $p=0.8068$; no main effect of CNO-priming, $F_{(1,9)}=0.5076$, $p=0.4942$). (E) Mean firing rate during baseline and following CNO ($10\mu\text{M}$) infusion. mCherry expressing MHB neurons ($n=11$) show no significant change in firing rate following CNO application (Paired t-test, $t_{(10)}=0.1149$, $p=0.9108$). (F) When normalized to baseline, mCherry expressing MHB neurons show no significant increase in percent change in firing rate ($t_{(10)}=1.382$, $p=0.1971$). (***) indicates $p \leq 0.001$, **** indicates $p \leq 0.0001$).

induced CPP, with no differences between CNO-reinstated and Veh-reinstated animals. To test whether CNO is sufficient to drive reinstatement of a cocaine-induced CPP in DREADD-free animals, we administered CNO or vehicle 40 min prior to a saline-primed reinstatement session. We found no difference between CNO-primed or Veh-primed controls during reinstatement test (**Fig. 3.3D**). We further demonstrate that CNO alone has no effect on firing rate of DREADD-free MHb-ChAT neurons. CNO (10 μ M) was infused in MHb containing slices of DIO-mCherry infused animals with no effect on firing rate in mCherry-expressing MHb-ChAT neurons (**Fig. 3.3E & 3.3F**), demonstrating that effects on firing and reinstatement behavior occur in a CNO/DREADD combinatorial fashion.

Discussion

In this study, using chemogenetics, we more causally linked activity within the MHb with changes in reinstatement behavior. DREADD-mediated activation of MHb ChAT expressing neurons artificially induces reinstatement for a previous cocaine-induced CPP, demonstrating that vMHb activity is sufficient for inducing reinstatement, even in the absence of cocaine. We further demonstrate that chemogenetic activation of the vMHb is unable to induce a preference or aversion alone. Others found that modulating cholinergic signaling in nicotine-naïve animals has no effect in mediating anxiety-like behaviors, supporting the notion that neuroplastic adaptations within the vMHb pathway are altered and recruited by repeated exposure to drugs of abuse to drive reward-associated and reward-seeking behaviors²¹⁷. Conversely, previous work has shown that artificial activation of the dMHb is reinforcing and is able to induce intracranial self-stimulation; meanwhile, optogenetic inhibition of the dMHb elicits a conditioned place aversion³⁰⁰. Together, these results highlight the unique roles of MHb subcircuits within the MHb-IPN axis that should be further studied.

Although we selectively modulate cholinergic neurons of the MHb, this cell population has been previously shown to release glutamate and/or acetylcholine^{169,219,301}. Therefore, it remains unclear which neurotransmitter system is responsible for driving the reinstatement phenotype. Recently, it has been demonstrated that MHb firing rate alters the neurotransmitter system used by the vMHb; tonic firing appears to engage glutamatergic transmission, while high-rate phasic firing drives acetylcholine release²¹⁹. Given the significant increase in firing induced by CNO exposure in HM3D-expressing MHb cells (see **Fig. 3.1D**), it is likely that acetylcholine is being utilized *in vivo* to induce reinstatement behavior. Studies have linked vMHb-IPN circuit activity with changes in median raphe nuclei and ventral tegmental function; downregulation of cholinergic signaling in the vMHb leads to a depressive-like phenotype correlated with increase in serotonergic function from the median raphe, whereas increases in MHb signaling activates ventral tegmental dopaminergic neurons and suppresses raphe serotonin¹⁶⁷. It is possible that similar changes to cholinergic signaling within these pathways occur during cocaine-primed reinstatement.

Previous work in the field has implicated the ChAT-expressing MHb population in processing the aversive properties of nicotine and the negative affect throughout nicotine withdrawal^{179,210}. Work from Fowler and Kenny demonstrated that $\alpha 5$ -KO ($\alpha 5$ -expressing nAChRs are enriched in the vMHb-IPN pathway) mice show escalations of nicotine self-administration through a blunting of the aversive properties of nicotine and not an increase in the rewarding aspects of the drug^{215,302}. Conversely, pharmacological antagonists of $\beta 4$ -expressing nAChR (also enriched in the vMHb-IPN pathway) inhibit the self-administration of morphine, cocaine and blocks the formation of cocaine CPP^{228,230,231}. It is likely that a balance between $\alpha 5$ - and $\beta 4$ -containing nAChRs is more influential in regulating drug response than a single subunit^{214,218}. Yet, how cocaine and nicotine exposure differentially affect MHb activity remains

a key open question. MHb activity may regulate the rewarding properties of other drugs of abuse, while encoding for the aversive properties of nicotine. Conversely, due to the population of nAChR in the MHb, but absence of known cocaine targets (dopamine transporter, serotonin transporter, and norepinephrine transporter), it is possible that nicotine can directly modulate MHb activity, while other drugs of abuse, such as cocaine, engage the adaptive behaviors with which MHb function has been associated.

Recent work has brought into question the exclusivity of CNO as the ligand for DREADDs and demonstrated that rodents are capable of CNO to clozapine back-metabolism²⁴⁶. While it has been shown that CNO is not significantly back metabolized to clozapine in mice, it is possible that the limited clozapine produced is sufficient to induce DREADD activity reported in Gomez et al., while being subthreshold for off-target effects³⁰³. Moreover, while it has been demonstrated that systemic clozapine is able to induce changes in neural activity, these changes occur in response to significantly higher doses (35 mg/kg) than what could be back metabolized from our doses of CNO (3 mg/kg)^{247,248,304}. Within this current study, the inability of CNO alone to induce a conditioned preference/aversion (see **Fig. 3.2E**), induce reinstatement (see **Fig. 3.3D**), or induce changes in MHb firing rate (see **Fig. 3.3E & 3.3F**) support the idea that it is not CNO alone, or potential back metabolism to clozapine, that is mediating the observed effects during reinstatement.

How the MHb is recruited to regulate cocaine-reinstatement behaviors remains unclear, especially considering that the main targets of cocaine action (dopamine transporter, norepinephrine transporter, and serotonin transporter) are largely absent within the MHb. Recent work characterized the downstream targets of the MHb-IPN pathway and show that serotonergic raphe nuclei receive dense innervation from vMHb-innervated IPN neurons¹⁶⁴. The MHb also densely expresses the 5-HT_{3A}, -4, -5A, and -5B receptors, suggesting it receives serotonergic

inputs, potentially from the same raphe-serotonergic population receiving innervation from the IPN^{170,175,305}. It is possible that these inputs may be directly, but differentially, modulated by cocaine and nicotine.

The above study demonstrates a specific function of the vMHb in the reinstatement of cocaine-induced CPP and adds to the growing body of work implicating the MHb in substance use disorders. The most relevant study with regard to cocaine is from James et al. (2011), which demonstrated changes in MHb activity during cue-primed reinstatement of cocaine self-administration²³⁴. MHb activity was indirectly measured using Fos protein expression (as in our studies in **Chapter 1**) from rats following reinstatement. In support of this approach (measuring Fos expression), James et al. (2011) found high-reinstating animals exhibited higher Fos expression in the medial habenula as compared to low-reinstating animals. There remain numerous key open questions regarding the role of the MHb in reinstatement. How are specific molecular mechanisms engaged within the MHb (such as the increases in H4K8Ac shown in **Chapter 1**), and how do they contribute to drug-associated behaviors? As the MHb is a key regulator of withdrawal and relapse-like behaviors, do long-lasting molecular adaptations (such as epigenetic modifications) within the MHb confer the persistence and resilience of drug-associated memories and drug-seeking behavior?

Chapter 4: Epigenetic Control of Habenula-mediated Cocaine-associated Behaviors

Rationale

We have shown that the MHb is engaged during cocaine-primed reinstatement of cocaine-induced CPP. Moreover, using chemogenetics, we demonstrate that activity in the cholinergic neurons of the MHb is sufficient to induce reinstatement, providing a causal link between MHb function and relapse-like behaviors. We have also observed increases in H4K8Ac (apermissive epigenetic mark) in the MHb during cocaine-primed reinstatement. H4K8Ac has been associated with disengagement of HDAC3 deacetylase activity and increased *Nr4a2* expression^{135,240,306}. NR4A2 is a powerful regulator of associative learning that is enriched in the vMHb and is induced in the MHb by conditioned learning¹⁹⁷. However, it remains unclear if this reinstatement-induced H4K8Ac in the MHb is linked to HDAC3 disengagement, if these changes occur at *Nr4a2*, and if NR4A2 in the MHb is necessary for reinstatement behaviors. In the following studies, we assay HDAC3 at the promoters of various plasticity genes in the cholinergic neurons of the MHb and, using a viral approach, examine the role of HDAC3 enzymatic activity in cocaine-associated behaviors. Lastly, we use a recently discovered dominant-negative variant of NR4A2 (NURR2C) to determine if NR4A2 in the MHb is necessary for reinstatement of CPP.

Methods

Animals:

ChAT-IRES-Cre^{Cre/Cre} (ChAT-Cre; Stock No. 006410) and Lox-STOP-Lox-TdTomato mice (TdTomato; Stock No. 007909) were purchased from the Jackson Laboratory. Male and female ChAT-Cre were bred and maintained as heterozygous. Male and female LSL-TdTomato::ChAT-Cre (TdChAT) were bred as heterozygous for TdTomato and ChAT-Cre genes and genotype confirmed via end-point PCR. All mouse lines were maintained on a c57BL/6J

background. Mice were given *ad libitum* access to food and water while housed under a 12-h light cycle in a climate-controlled room. All experiments were conducted during the light portion of this cycle. Genotyping primers used are as follow: *Chat-IRES-Cre WT* Forward: 5' – gtttgagaagcgggtggg– 3', *Chat-IRES-Cre Shared* Reverse: 5' – agatagataatgagaggctc – 3', *Chat-IRES-Cre Mutant* Forward: 5'- cttctatcgccttcttgacg – 3'; *Cre recombinase* Forward: 5' – ggtcgtgcaacgagtga – 3', *Cre recombinase* Reverse: 5' – ccctgatcctggcaattt – 3'; *TdTomato WT* Forward: 5' – aaggagctgcagtggagtat – 3', *TdTomato WT* Reverse: 5' – ccgaaaatctgtgggaagtc – 3', *TdTomato Mutant* Forward: 5' – ctgttctgtacggcatgg – 3', *TdTomato Mutant* Reverse: 5' – ggcattaaagcagcgtatcc – 3'.

Cloning and Viral packaging:

Wild-type HDAC3 (HDAC3^{W.T.}), loss of function HDAC3 (HDAC3^{Y298H}), and NURR2C were PCR amplified from mouse cDNA. HDAC^{Y298H} was generated via a single nucleotide substitution of Tyrosine 298 with a histidine. NURR2C was generated through deletion of *Nr4a2* Exons 3 and 7, as previously identified³⁰⁷.

For Cre-independent vectors, NURR2C-V5 or untagged NR4A2 was cloned under the *Camkiiα* promoter with the addition of β-globin intron to generate pAAV-CaMKIIα-βGlobin-NURR2C-V5 or pAAV-CaMKIIα-βGlobin-NR4A2 (untagged). For Cre-dependent vectors, products were subsequently cloned into a modified pAAV-hSyn-DIO-eGFP (Addgene #50457, a generous gift from Dr. Bryan Roth) with the addition of β-globin intron. GFP element was removed from the original vector and replaced with a V5-tag, generating a fusion to HDAC3^{W.T.}, HDAC3^{Y298H}, and NURR2C.

Determining NR4A2/NURR2C Interaction

HT22 cells (Salk Institute, La Jolla, CA) were Lipofectamine LTX with Plus Reagent (ThermoFisher, Waltham, MA) transfected with 1 μ g of CamKII α - β Globin-NURR2C-V5 with or without 1 μ g CamKII α - β Globin-NR4A2 (untagged). 48 hours later, cells were harvested, lysed in tissue lysis buffer (T-PER, ThermoFisher; 1X HALT protease inhibitor) and pelleted. Samples were centrifuged (13,000RPM, 10 min, 4°C) and supernatant aliquoted for immunoprecipitation. 5ul of total was set aside for Input positive control while 500ul of sample were incubated overnight at 4°C with 20ul Protein G (Invitrogen) beads, 5.25ul 100X HALT protease inhibitor, and 5ul of Mouse anti-V5 (Invitrogen #:46-0705). The following day samples were precipitated on a chilled magnet and washed for 5 minutes in 500ul of the following wash series: Low Salt Immune Complex, High Salt Immune Complex, LiCl Immune Complex Wash Buffer, and TE Buffer. Immediately following the final wash, samples were magnet precipitated, resuspended in 20uL of T-PER, heated to 75°C for 10min, and eluted from magnetic beads in 10.5ul NuPAGE LDS Sample Buffer/Sample Reducing Agent. Samples were immunoblotted using the Invitrogen XCell SureLock Mini-Cell and XCellIII Blot Module. Western blot was blocked in blocking buffer (5% powdered milk, 0.1% Tween-20, 1X TBS) for 1 hr at room temperature. NR4A2 immunoreactivity was assayed using mouse anti-NR4A2 (abcam#: ab41917, [1:1000]) or V5-selectivity using mouse anti-V5 (Invitrogen) in primary buffer (3% BSA, 0.1% Tween-20, 1X TBS) overnight at 4°C, triple washed in 0.1% Tween-20, 1X TBS for five minutes, and incubated with goat anti-mouse secondary (light-chain specific, HRP-conjugated [1:5000]) in secondary buffer (5% powdered milk, 0.1% Tween-20, 1X TBS) for 1 hr at room temperature. Blot was subsequently triple washed in 0.1% Tween-20, 1X TBS for five minutes and incubated in SuperSignal West Pico PLUS for protein detection.

Determining Cre-dependent expression

To confirm Cre-dependent expression of cloned plasmids, HT22 cells (Salk Institute, La Jolla, CA) were Lipofectamine LTX with Plus Reagent (ThermoFisher, Waltham, MA) transfected with 1 μ g of either DIO-V5-HDAC3^{W.T.} or DIO-NURR2C-V5, with and without 1 μ g of CMV-Cre-GFP. 48 hours later, cells were harvested, lysed in tissue lysis buffer (T-PER, ThermoFisher; 1X HALT protease inhibitor), and probed for expression of V5-tag via western blot (mouse anti-V5, Invitrogen; 1:1000).

Viral Packaging:

AAV constructs were packaged as previously described³⁰⁸. Briefly, HEK293 cells were transfected via by standard calcium phosphate precipitation and grown in high-glucose-containing (4.5 g/liter) DMEM (Invitrogen) supplemented with 10% fetal bovine serum (Life Technologies/Invitrogen, Carlsbad, CA), 100 units/ml penicillin and 100 μ g/ml streptomycin at 37°C in a 5% humidified. 2 hours prior to transfection, HEK293 cells were bathed in 5% fetal bovine serum in 25mL IMDM (Invitrogen). Cells were transfected with: 12ml H₂O, 1.65ml of 2.5M CaCl₂, plus AAV1 (30 μ g), AAV2 (31.25 μ g) and helper plasmid (125 μ g), combined with target plasmid (62.5 μ g) either rAAV-hSyn-DIO-GFP, rAAV-hSyn-DIO-HDAC3^{W.T.}, rAAV-hSyn-DIO-HDAC3^{Y298H}, or rAAV-hSyn-DIO-NURR2C. 13mL of 2x HEBS was vortexed into transfection buffer. 24 hours following transfection, cells were bathed in fresh DMEM. Following 60-65 hours, transfected HEK293 were harvested into PBS, pelleted, and resuspended in 150mM NaCl/20mM Tris. Cells were subsequently lysed in 10% NaDeoxycholate and 50U/ml benzonase. Cells were frozen at -20°C for at least 24 hours and virus was purified using Heparin columns. AAVs were concentrated using Amicon Ultra-4 concentrators. Viral titer was verified using qPCR. Briefly, AAVs were heat inactivated and nucleotide extracted with Proteinase K in ABI buffer (500mM KCL, 100mM Tris pH 8.0, 50 mM MgCl), incubated at 50°C for 1 hour and 95°C for 20 min.

Extracted nucleotides were serially diluted and underwent qPCR amplification to measure DNA concentration with primers designed to AAV ITRs. AAV titers are as follow: AAV-hSyn-DIO-GFP, 5.34×10^{10} ; AAV-hSyn-DIO-HDAC3^{W.T.}, 1.15×10^9 ; AAV-hSyn-DIO-HDAC3^{Y298H}, 1.71×10^9 ; AAV-hSyn-DIO-NURR2C, 6.58×10^{10} .

Stereotaxic Surgeries:

2-5-month-old heterozygous ChAT-Cre mice received 0.5 μ L bilateral infusions to the medial habenula (M/L, +/-0.35mm; A/P, -1.5 mm; D/V; -3.0) of *AAV-hSyn-DIO-GFP* (5.34×10^{10}); *AAV-hSyn-DIO-HDAC3^{W.T.}* (1.15×10^9); *AAV-hSyn-DIO-HDAC3^{Y298H}* (1.71×10^9); or *AAV-hSyn-DIO-NURR2C*, (6.58×10^{10}). Viruses were infused at a rate of 100nl/min using a 30 gauge Neuros Hamilton syringe (product #65459-01) mounted to either a Harvard Apparatus Nanomite Syringe Pump (product #MA1 70-2217) or Leica Biosystems Nanoinjector Motorized f/Stereotaxics (product #39462901)²⁹³. All infusions used the Leica Microsystems Angle Two Stereotaxic System. For behavioral experiments, animals were allowed to recover for a minimum of 7 d before handling.

CPP Reinstatement Paradigm:

Cocaine-induced CPP was performed as previously described^{42,144,240,241}. Briefly, animals were handled for 2 min for 3 consecutive days. Following handling, mice were conditioned over 4 consecutive days, receiving either cocaine-HCl (10mg/kg, IP; Sigma) or 0.9% saline, in a context-dependent manner (counter-balanced, unbiased). Following conditioning, animals were allowed to freely explore, in a drug-free state, the complete chamber to assess preference, established as the difference between time spent in the cocaine-paired chamber and the saline-paired chamber, in seconds. To extinguish preference, animals were repeatedly reintroduced to the chamber, daily for 6 consecutive days. Once extinguished, animals received a priming dose of

cocaine-HCl (5mg/kg, I.P.; Sigma) and immediately tested for reinstatement. Behavior was assessed and analyzed using Ethovision XT 11.5.

Fluorescence Activated Cell Sorting (FACS):

45 minutes following the completion of cocaine-primed reinstatement, animals (2-3/sample) were euthanized and Hb tissue was harvested into 1mL ice-chilled HABG (200 μ l 50X B27; 25 μ l 100X Glutamax; in 9.8 ml of Hibernate A cell media. Single cell lysates were generated as previously described³⁰⁹. Briefly, tissue was aspirated into 2mL papain buffer (14 μ l 100X Glutamax; 110U papain; 200U DNase; in 5.5ml Hibernate E cell media) and incubated at 32°C for 15 min with gentle rotation. Tissue was transferred into ice-chilled HABG + 1X protease inhibitor and gently triturated until larger pieces no longer visible. The 2ml Cell suspension was passed through a 70 μ m cell filter and filter was washed with an additional 5ml, to generate a final 7ml suspension. Cells were then pelleted and magnetically demyelinated using Myelin Removal Beads II (MACS Miltenyi Biotec). MHb TdTomato⁺ neurons were sorted and collected using the BD FACS Aria II Cell Sorter in collaboration with the Sue and Bill Gross Stem Cell Research Center at the University of California, Irvine.

Chromatin Immunoprecipitation qPCR (ChIP-qPCR):

MHb TdTomato⁺ neurons were collected into 250 μ l 2X MNase buffer (100mM Tris pH 8.0, 2mM CaCl₂, 0.4% Triton X-100) and diluted to a final volume of 500 μ l with nuclease free water. 15 μ l of diluted MNase (2000U MNase into 500 μ l 1X MNase buffer) was added to isolated cells and incubated at 37°C for 5 min. MNase was inactivated with 50 μ l of 10X MNase stop buffer (110mM Tris pH 8.0, 55mM EDTA). To lyse neurons, 550 μ l of 2X RIPA buffer (280mM NaCl, 1.8% Triton X-100, 0.2%SDS, 0.2% Na Deoxycholate, 5mM EDTA) was added and cells were incubated on ice for 15 min. Samples were centrifuged (13,000RPM, 10 min, 4°C) and supernatant

aliquoted for immunoprecipitation using the Millipore ChIP Kit. 5ul of total was set aside for Input positive control while 500ul of sample were incubated overnight at 4°C with 20ul Protein A (Invitrogen) beads, 5.25uL 100X protease inhibitor, and 5uL of anti-HDAC3 (Millipore) or anti-mouse IgG negative control (Millipore). The following day samples were precipitated on a chilled magnet and washed for 5 minutes in 500ul of the following wash series: Low Salt Immune Complex, High Salt Immune Complex, LiCl Immune Complex Wash Buffer, lastly TE Buffer. Immediately following the final wash, samples were magnet-precipitated, eluted from magnetic beads 100ul Elution Buffer (containing 1ul 100X Proteinase K), and DNA column purified. Enrichment at *cFos*, *Nr4a2*, *Cebpb*, *Ppp1r1b* (gene coding for DARPP-32), and *Nr4a3* promoters was measured via qPCR using the Roche 480 LightCycler and SYBR green systems. Promoter specific primer sequences were designed using Primer3 and are as follows: *cFos*, Forward 5' – tacgacccttcaggcatac- 3', Reverse 5' – gtttaaaggacggcagcac – 3'; *Nr4a2*, Forward 5' – gcgagtgttctttccgttc – 3', Reverse 5' – tgaagtccgtggtgatgcta – 3'; *Cebpb*, Forward 5' – acctgggtgggaggacat – 3', Reverse 5' – atcgttctccagctacacg – 3'; *Ppp1r1b*, Forward 5' – ggctccctaaaagtccac – 3', Reverse 5' – ttaatgaagtccagcgggta – 3'; and *Nr4a3*, Forward 5'- gaggaggaggagggtgacgta – 3', Reverse 5' – catagagtgcctggaatgcgaga – 3'.

ChIP-qPCR data was normalized using the percent input method; Input sample was adjusted to 100% and IP samples were calculated as a percent of Input using the following: $100 * AE^{(adjusted\ input - Ct\ (IP))}$. Fold enrichment was calculated as a percentage of total Input. AE = in-plate standard curve determined amplification efficiency.

Quantitative RT-PCR

RT-qPCR was performed to confirm cell identity of FACS isolated MHb TdTomato:ChAT+ neurons. Single cell lysates collected from the MHb of TdChAT animals

were FACS isolated into RLT buffer. RNA was isolated using the RNeasy Minikit (Qiagen) and cDNA was generated using High-Capacity cDNA Reverse Transcription Kit (Applied Biosystems). The following primers were used, derived from the Roche Universal Probe Library: *Chat* Forward: 5' – tttgatggcatcgtcctg – 3', Reverse: 5' – acgagcttctgttgctgt – 3', used with Roche Probe #62; *Syt9* Forward: 5' – ggagaactgtgccatgc – 3', Reverse: 5' – tgagctgtcttcggattgag – 3', used with Roche Probe #21; *Hprt5* Forward: 5' – tgctcgagatgcatgaagg – 3', Reverse: 5' – cttttatgtcccccggtgac – 3', used with Probe 5'HEX-atcacattgtggcctctgt -3'.

Loose-cell patch clamp electrophysiology

Coronal slices (250–300µm) through the epithalamus were collected via vibratome and transferred into 1X ACSF containing the following (in mM): 124 NaCl, 3 KCl, 1.25 KH₂PO₄, 1.5 MgSO₄, 26 NaHCO₃, 2.5 CaCl₂, and 10 dextrose. Recordings were made in a submerged chamber superfused at 2-3 ml/min with carbogen-saturated 1X ACSF 32°C. Labeled neurons of the medial habenula were identified by using an upright fluorescence microscope. Loose cell attached recordings (110–250 MΩ) were achieved from identified fluorescent cells by using infrared differential interference contrast. Recordings (Axopatch 200A amplifier) were made with 5–7MΩ pipettes filled with 0.9 percent NaCl (saline). Data were analyzed with pClamp (Molecular Device) and Minianalysis (Synaptosoft)

Immunohistochemistry:

Animals were euthanized and brains flash frozen in dry ice-chilled isopentane. 20µM coronal sections were collected using a Leica CM 1850 cryostat at -18°C. For immunohistochemical confirmation of V5-tagged viruses, MHb containing slices were fixed in 4% PFA for 10 min, washed in 0.1M PBS, and permeated in 0.1% Triton X-100 in 0.1M PBS. Slices were then blocked in blocking serum (8% NGS, 0.3% Triton X-100, in PBS; 1 hr) and

incubated at 4°C overnight in primary solution (2% NGS, 0.3% Triton X-100; Rabbit anti-V5 [1:1000], abcam #9116). Slices were then incubated in secondary solution (2% NGS, 0.3% Triton X-100; V5, Alexa Fluor goat anti-rabbit 555; in PBS). Tissue was imaged using Olympus Slide Scanner VSBX61.

Results

FACS-ChIP-qPCR can be used to assess HDAC 3 occupancy in the vMHb

Cocaine-primed reinstatement increases H4K8Ac throughout the MHb (Chapter 1), suggesting a disengagement of HDAC3 activity. Although we have also linked changes in MHb cholinergic function to reinstatement behavior, it is unknown if HDAC3 function is altered in the same cholinergic population (Chapter 3). Thus, to measure HDAC3 enrichment in only the cholinergic neurons in the MHb, we crossed the LSL-TdTomato mouse line to the ChAT-Cre mouse line. This cross-bred TdChAT mouse line limits expression of the fluorescent TdTomato reporter to cholinergic neurons, especially in the vMHb (Fig. 4.1A). Using RT-qPCR, we confirmed that TdTomato:ChAT⁺ neurons can be sorted from the vMHb of TdChAT mice (Fig. 4.1B). Moreover, in home cage animals, we detected HDAC3 occupancy at the promoters of *Nr4a2*, *Darpp32*, and *cFos* (Fig 4.1C). These results demonstrate the ability to use TdChAT mice

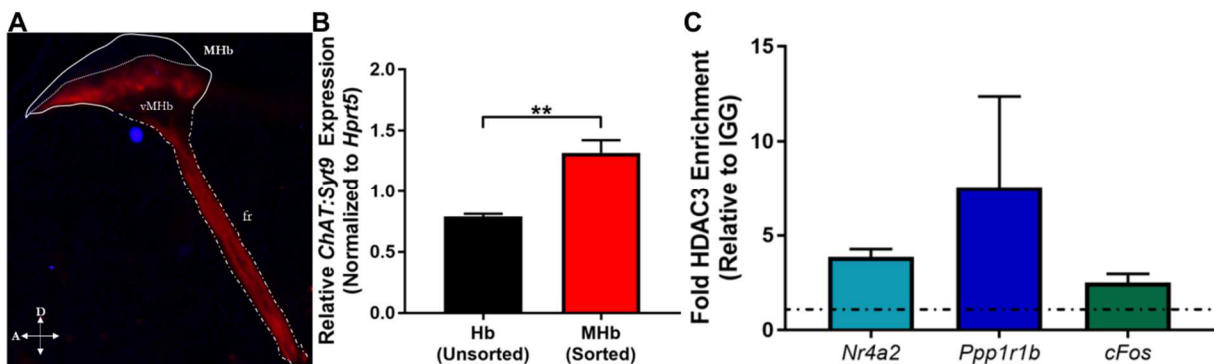


Figure 4.1: MHb ChAT neurons can be isolated via FACS. (A) TdChAT animals express TdTomato reporter in cholinergic neurons of the MHb. (B) FACS isolated TdTomato⁺ MHb neurons show increased enrichment for ChAT compared to unsorted habenula containing tissue. (C) At baseline, HDAC3 occupancy can be detected at the promoters of *Nr4a2*, *Ppp1r1b* (*Darpp32*), and *cFos* in FACS sorted TdTomato⁺ MHb neurons. (** indicates $p \leq 0.01$)

combined with FACS-ChIP-qPCR to examine HDAC3 occupancy in the cholinergic neurons of the MHB in a gene-specific manner.

HDAC3 occupancy is altered in the vMHB during cocaine-primed reinstatement of CPP

To determine if HDAC3 occupancy is altered during cocaine-primed reinstatement, TdChAT animals underwent cocaine-primed reinstatement. TdChAT animals acquire (Fig. 4.2A) and extinguish (Fig. 4.2B) cocaine-induced CPP. 24 hours following the final extinction session, animals were primed with either saline or cocaine-HCl (5mg/kg, I.P.) and immediately tested. Cocaine-primed animals show a significant reinstatement of preference score compared to saline-primed controls (Fig. 4.2C). 45 minutes following reinstatement session, animals were sacrificed, Hb tissue was harvested, and single-cell lysates were FACS sorted. Cocaine-primed animals show a significantly decreased HDAC3 occupancy at the promoter of *Nr4a2* (Fig. 4.2D) compared to

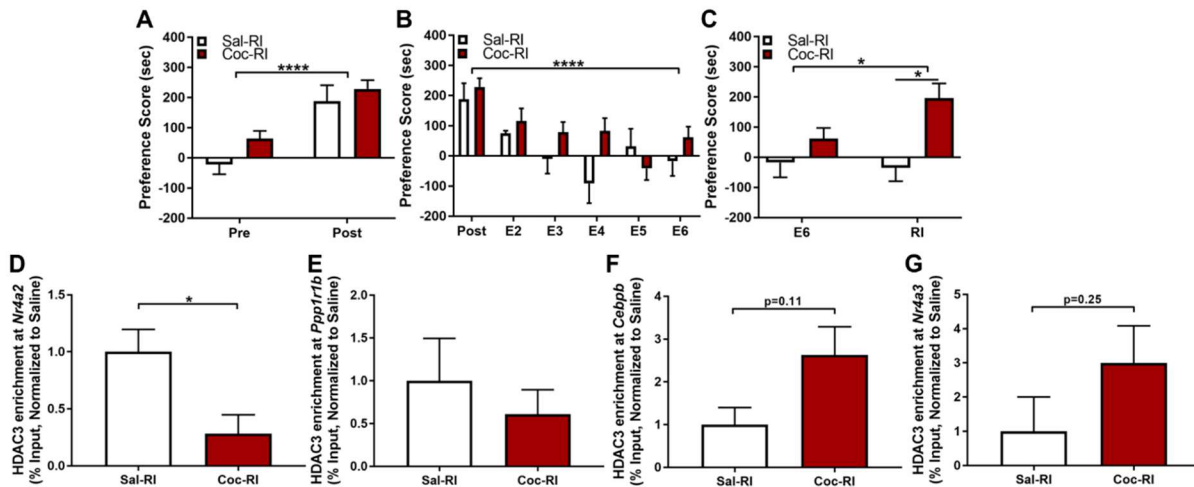


Figure 4.2: HDAC3 occupancy is altered in the MHB in response to cocaine-primed reinstatement. TdChAT mice (A) acquire cocaine-induced CPP (Two-way ANOVA, main effect of Conditioning: $F_{(1,16)}=29.33$, $p<0.0001$), with no differences between saline-primed ($n=7$) and cocaine-primed animals ($n=11$) (Two-way ANOVA, No main effect of Reinstatement-Priming: $F_{(1,16)}=3.347$, $p=0.0860$; although there is a trend, there is no Interaction between effects, $F_{(1,16)}=0.4218$, $p=0.5253$ and the trend is likely being driven by variability in Pre-Test score). (B) CPP can be extinguished with repeated drug-free exposures to conditioning apparatus (Two-way ANOVA, main effect of Extinction $F_{(5,80)}=8.023$, $p<0.0001$). (C) Cocaine-primed animals significantly reinstate previously extinguished cocaine-induced CPP compared to saline-primed controls (Two-way ANOVA, main effect of Cocaine-Priming: $F_{(1,16)}=8.389$, $p=0.0105$; trending Interaction $F_{(1,16)}=4.173$, $p=0.0579$; Sidak's Post-hoc analysis shows a significant difference between saline-primed animals and cocaine-primed animals during reinstatement session $t_{(32)}=3.544$, $p=0.0025$ but not during E6 $t_{(32)}=1.215$, $p=0.4120$). ChIP-qPCR shows HDAC3 occupancy is significantly lower in cocaine-primed animals at the (D) *Nr4a2* promoter ($t_{(5)}=2.802$, $p=0.0379$), with no differences at the promoters of (E) *Ppp1r1b* ($t_{(5)}=0.737$, $p=0.4961$), (F) *Cebpb* ($t_{(5)}=1.919$, $p=0.1131$), and (G) *Nr4a3* ($t_{(5)}=1.298$, $p=0.2508$). (* indicates $p \leq 0.05$, **** indicates $p \leq 0.0001$)

saline-primed controls. No significant change was observed at other HDAC3 target genes known to be critical in associative plasticity including *Ppp1r1b* (DARPP-32; **Fig. 4.2E**), *Cebpb* (NR4A2-target gene; **Fig. 4.2F**), and *Nr4a3* (Nr4a family member; **Fig. 4.2G**). Thus, HDAC3 disengages from the promoter of *Nr4a2* and leaves *Nr4a2* in a transcriptionally-permissive state in the MHb during cocaine-primed reinstatement. However, whether this change in MHb HDAC3 function is necessary for reinstatement behaviors remains unclear.

Loss of HDAC deacetylase activity in the MHb alters cocaine-associated memories

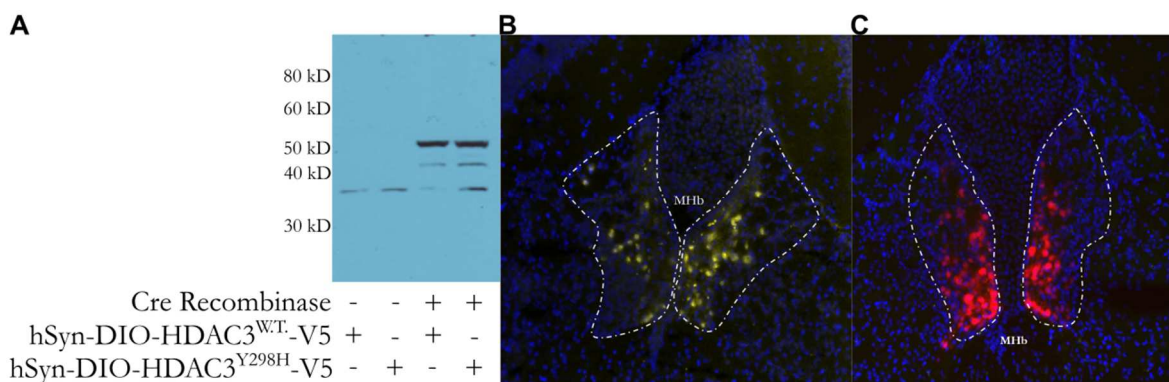


Figure 4.3: Expression of DIO-HDAC3^{W.T.} and -HDAC3^{Y298H} is limited to Cre-expressing cell populations. (A) Western blot probing for V5-tagged constructs expressed in HT22 cells. DIO Expression is limited to co-expression of Cre-recombinase and detected V5+ signal occurs at the predicted molecular weight of HDAC3 (50kD). (B) Representative image of DIO-HDAC3^{W.T.}-V5 expression (gold) in the MHb of ChAT-Cre mouse. (C) Representative image of DIO-HDAC3^{Y298H}-V5 expression (red) in the MHb of ChAT-Cre mouse. Note limited expression to the vMHb, where the cholinergic MHb population is enriched.

To determine if HDAC3 deacetylase activity is necessary for MHb-mediated reinstatement behavior, we developed a viral vector approach to overexpress either HDAC3^{W.T.} or a loss of function HDAC3 point-mutant, HDAC3^{Y298H}. The Y298H point mutation has been shown to generate a loss of HDAC3 deacetylase function¹¹⁷ and has been shown *in vivo* to affect histone acetylation and learning processes³⁰⁶. To limit expression to the cholinergic neurons of the MHb, HDAC3^{W.T.} and HDAC3^{Y298H} were cloned into Cre-dependent constructs (**Fig. 4.3A-C**). ChAT-Cre mice were subsequently injected in the MHb with either DIO-GFP or DIO-HDAC3^{Y298H} and underwent cocaine-primed reinstatement. Although both GFP and HDAC3^{Y298H} injected animals

equally acquired (**Fig. 4.4A**), animals injected with HDAC3^{Y298H} showed a significant impairment in extinction (**Fig. 4.4B**). Because these HDAC3^{Y298H} had a significant impact on extinction, interpretation of reinstatement behaviors is severely confounded.

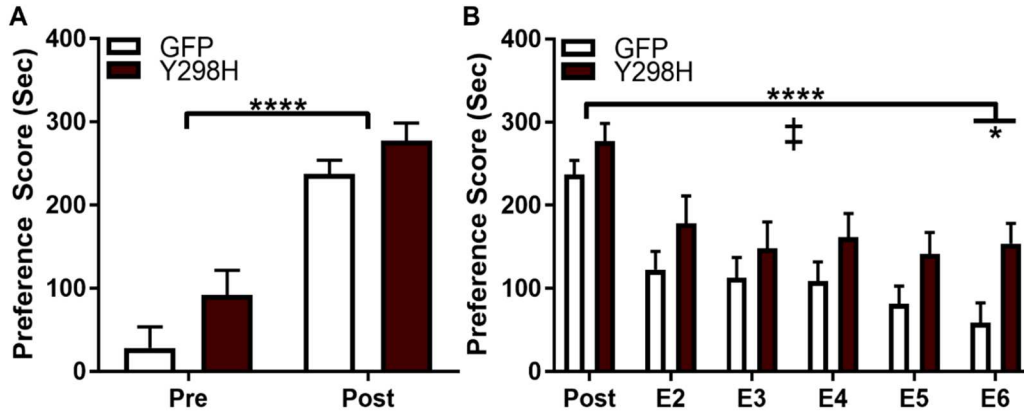


Figure. 4.4: Loss of HDAC3 deacetylase activity generates an extinction-resistant CPP. Animals infused with DIO-GFP (n=25) and DIO-HDAC3^{Y298H} (n=22) equally (**A**) acquire cocaine-induced CPP (main effect of Acquisition, $F_{(1,45)}=94.43$, $p<0.0001$, although trending effect of HDAC3^{Y298H} $F_{(1,45)}=3.84$, $p=0.0563$, no Interaction $F_{(1,45)}=0.347$, $p=0.5588$). Although both groups (**B**) extinguish conditioned preference (main effect of Extinction $F_{(5,225)}=21.48$, $p<0.0001$), animals expressing HDAC3^{Y298H} show blunted extinction of cocaine-induced CPP compared to GFP (main effect of Y298H $F_{(1,45)}=4.264$, $p=0.0447$; Sidak's posthoc analysis demonstrates a significant difference at E6 $t_{(270)}=2.711$, $p=0.0420$). (* indicates $p \leq 0.05$, **** indicates $p \leq 0.0001$, ‡ indicates $p \leq 0.05$ main effect of Y298H)

HDAC3 overexpression has no effect on MHb-mediated cocaine-associated behaviors.

To determine if disengagement of HDAC3 in the MHb is necessary for cocaine-primed reinstatement, we infused either DIO-GFP or DIO-HDAC3^{W.T.} into the MHb of ChAT-Cre mice. DIO-GFP and DIO-HDAC3^{W.T.} equally acquired (**Fig. 4.5A**) cocaine-induced CPP. However, unlike HDAC^{Y298H} (see **Fig. 4.4B**), overexpression of HDAC3^{W.T.} in the MHb had no effect on extinction of cocaine-induced CPP (**Fig. 4.5B**). 24 hours following the final extinction session, both GFP and HDAC3^{W.T.} expressing animals received a cocaine prime (5mg/kg, I.P.) and immediately tested for reinstatement. HDAC3^{W.T.} in the MHb had no effect on cocaine-primed

reinstatement of CPP (**Fig. 4.5C**), suggesting that HDAC3 activity in the MHb, alone, is insufficient to prevent relapse-like behaviors.

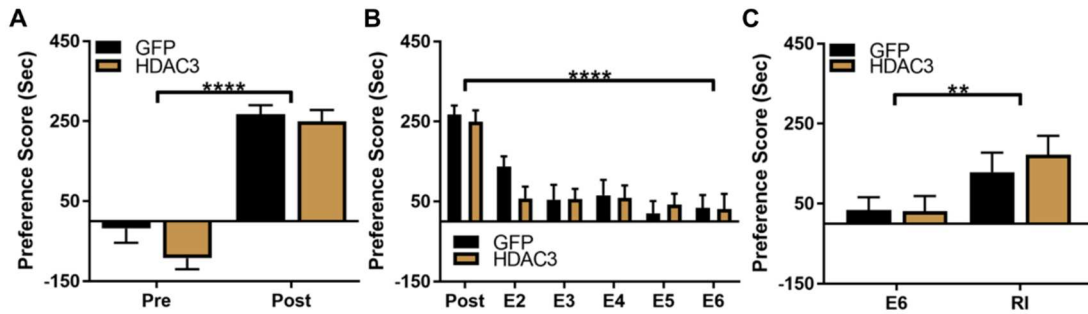


Figure 4.5: HDAC3^{W.T.} in the MHb does not affect cocaine-associated behaviors. Animals infused with DIO-GFP (n=15) and DIO-HDAC3^{W.T.}(n=13) equally (**A**) acquire cocaine-induced CPP (main effect of Acquisition, $F_{(1,26)}=134.9$, $p<0.0001$) and equally (**B**) extinguish (main effect of Extinction $F_{(5,130)}=28.8$, $p<0.0001$). Both GFP and HDAC3^{W.T.} equally reinstate preference following a cocaine-prime (main effect of Reinstatement $F_{(1,26)}=12.72$, $p=0.0014$). (** indicates $p \leq 0.01$, **** indicates $p \leq 0.0001$)

Loss of NR4A2 function in the MHb impairs cocaine-primed reinstatement of CPP

HDAC3 has been previously shown to be a powerful negative regulator of plasticity and associative processes, through negative regulation of *Nr4a2*. While *Nr4a2* is enriched in the vMHb, little is known about NR4A2 function in the adult habenula. Previous work has shown that an endogenously occurring *Nr4a2* splice-variant, NURR2C, blocks NR4A2-dependent transcription³⁰⁷. However, it is unknown if NURR2C functions as a direct dominant-negative to NR4A2 activity. First, to determine if NURR2C directly interacts with NR4A2, we expressed V5-NURR2C with or without untagged NR4A2 in HT22 cells. 48 hours following transfection, we immunoprecipitated V5-NURR2C using a V5-specific antibody and immunoblot analysis of V5-precipitates identified a ~65kD NR4A2-immunoreactive band (**Fig. 4.6A-B**), demonstrating a direct NURR2C/NR4A2 interaction.

To determine the role of NR4A2 in vMHb function, we cloned a Cre-dependent NURR2C expressing vector (**Fig. 4.6C**). NURR2C is an endogenously occurring splice-variant of NR4A2 that has been shown to block NR4A2 transcription factor activity³⁰⁷. This viral strategy allows limited overexpression of V5-NURR2C to the cholinergic neurons of the vMHb in ChAT-Cre

mice (**Fig. 4.6D**). To determine the effect of loss of NR4A2 function on MHb cholinergic function, we co-expressed DIO-mCherry + DIO-V5-NURR2C or DIO-mCherry alone in the vMHb of ChAT-Cre mice. 4 weeks following viral infusion, loose seal clamp recordings were taken from

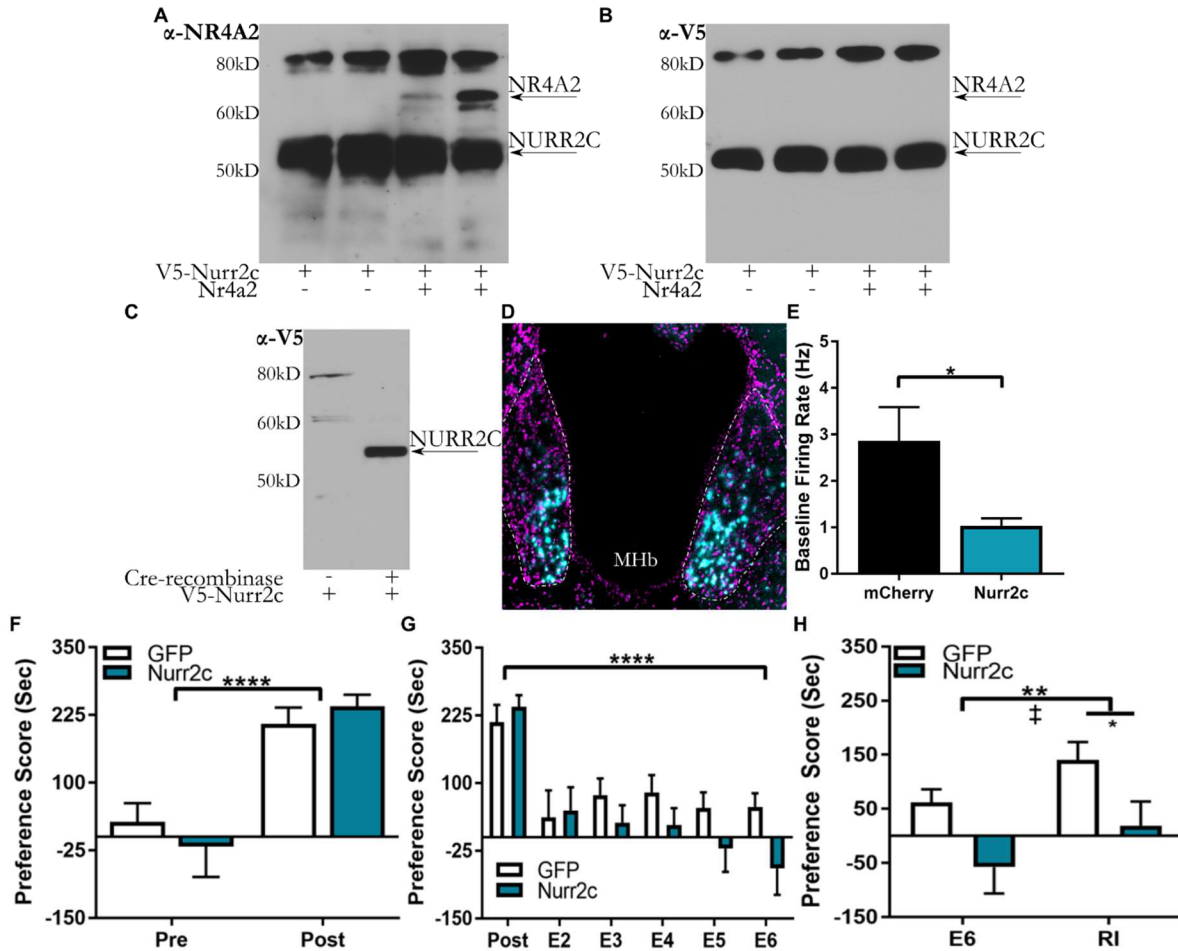


Figure 4.6: Expression of DIO-Nurr2c in the vMHb alters cocaine-primed reinstatement behavior. HT22 cells either expressing V5-NURR2C alone (*lane 1 and lane 2*) or co-expressing V5-NURR2C and untagged NR4A2 (*lane 3 and lane 4*). Cells underwent immunoprecipitation using anti-V5 and western blot probing for (A) NR4A2 (note NR4A2-immunoreactivity ~65kD) or (B) V5 (Note V5-NURR2C immunoreactivity ~55kD and absence of NR4A2-immunoreactivity ~65kD). (C). Western blot probing for V5-tagged constructs expressed in HT22 cells. DIO expression is limited to co-expression of Cre-recombinase and detected V5+ signal occurs at the predicted molecular weight of NURR2C (55kD). (D) Representative image of DIO-V5-NURR2C expression (*teal*) in the MHb of ChAT-Cre mouse. Note limited expression to the vMHb, where the cholinergic MHb population is enriched. (E) Overexpression of NURR2C blunts baseline firing rate of MHb cholinergic neurons ($t_{(14,25)}=2.473$, $p=0.0266$). Animals infused with DIO-GFP ($n=16$) and DIO-V5-NURR2C ($n=13$) equally (F) acquire cocaine-induced CPP (main effect of Acquisition, $F_{(1,27)}=61.98$, $p<0.0001$) and equally (G) extinguish (main effect of Extinction $F_{(5,130)}=21.95$, $p<0.0001$; although there is an Interaction $F_{(5,130)}=2.371$, $p=0.0427$, Sidak's posthoc analysis indicates there is no significant difference between GFP and NURR2C expressing animals on any extinction session). Following extinction, NURR2C expressing animals showed a (H) significantly blunted cocaine-primed reinstatement compared to GFP controls (main effect of Reinstatement $F_{(1,17)}=10.36$, $p=0.0033$; main effect of NURR2C $F_{(1,27)}=6.599$, $p=0.0160$; Sidak's posthoc analysis significant difference between GFP and NURR2C during reinstatement $t_{(54)}=2.3$, $p=0.05$). (* indicates $p \leq 0.05$, ** indicates $p \leq 0.01$, **** indicates $p \leq 0.0001$, ‡ indicates main effect of Nurr2c)

mCherry labeled neurons in coronal slices through the MHb. Cells co-expressing DIO-mCherry + DIO-V5-NURR2C had a significantly decreased baseline firing rate compared to cells expressing DIO-mCherry alone (**Fig. 4.6E**), suggesting NR4A2 function is necessary for maintenance of MHb firing.

To determine the role of NR4A2 in MHb-mediated relapse-like behaviors, we infused either DIO-GFP or DIO-NURR2C into the MHb of ChAT-Cre mice. NURR2C had no effect on the acquisition (**Fig. 4.6F**) or extinction (**Fig. 4.6G**) of cocaine-induced CPP. Following extinction, animals received a cocaine prime (5mg/kg, I.P.) and were immediately tested for reinstatement of conditioned preference. NURR2C expressing animals showed a blunted reinstatement compared to GFP expressing controls (**Fig. 4.6H**). This work demonstrates that NR4A2 transcription factor activity is necessary in the cholinergic neurons of the MHb for cocaine-primed reinstatement of CPP.

Discussion

Our previous work has demonstrated that the MHb is engaged during cocaine-primed reinstatement of CPP. Specifically, we show increases in H4K8Ac, an epigenetic mark negatively regulated by HDAC3 and positively correlating with increased *Nr4a2* expression. Previous work from the Wood lab and others have demonstrated that HDAC3 is a negative regulator of long-term memory in the hippocampus and amygdala and a regulator of cocaine-associated behaviors in the NAc, primarily through negative regulation of *Nr4a2*^{112,135,310}. Here, we demonstrate that during cocaine-primed reinstatement, HDAC3 disengages from *Nr4a2* in the cholinergic population of the MHb, aligning with the global increases in H4K8Ac. We detected no changes in other known HDAC3 target genes enriched in the MHb that are known players in cocaine response and plasticity (including *Cebpb* and *Ppp1r1b*), providing further evidence for HDAC3 functioning as

a molecular brake pad through negative regulation of *Nr4a2*. However, given the global changes in histone acetylation observed, it is unlikely that *Nr4a2* is the only gene with decreased HDAC3 occupancy. It is not completely surprising that we did not detect changes in *Ppp1r1b* transcriptional regulation, as various groups have shown the phosphorylation state of DARPP-32 is more relevant to its function than up or downregulation of its transcript. To fully characterize the array of HDAC3-regulated genes that are altered in the MHb during cocaine-primed reinstatement, future studies should employ a less hypothesis-drive approach, such as next generation ChIP-Sequencing.

We characterize the function of HDAC3 deacetylase activity in the MHb during cocaine-associated behaviors. Whereas loss of HDAC3 deacetylase activity in the vMHb (through overexpression of HDAC3^{Y298H}) had no effect on acquisition of cocaine-induced CPP, overexpression of HDAC^{Y298H} blunted extinction of CPP, thus preventing effective characterization of the role of HDAC3 in regulating reinstatement. As other gain of function manipulations in the vMHb (such as optogenetic stimulation) accelerate extinction memory²⁰⁰, it is surprising that loss of deacetylase activity would blunt extinction of CPP. Due to the experimental design (where viruses were delivered prior to CPP procedure), it is unclear if HDAC3^{Y298H} in the vMHb is affecting the extinction process (that is, the formation of extinction memory) or if it is generating a CPP that is stronger and therefore resistant to extinction. One may expect this effect to be parsed with differences in acquisition of CPP (that if HDAC^{Y298H} in the vMHb is strengthening acquisition, it should generate a higher preference score during the Posttest), yet it is likely that the conditioning dose used in these experiments (10mg/kg) is generating a ceiling effect preventing any super-induction in preference score during acquisition. Future studies can more fully characterize a role of HDAC3 in the MHb during acquisition using

subthreshold doses for cocaine-induced CPP (e.g. 2.5 and 5 mg/kg) Moreover, the mechanisms underlying this effect remain undetermined, but is likely to be mediated by other non-NR4A2 HDAC3 gene targets (as loss of NR4A2 does not appear to affect extinction). Endogenously, HDAC3 provides negative regulation to various genes in the vMHB, and specifically disengages from select genes (such as *Nr4a2*) when the MHB is engaged, such as during cocaine-primed reinstatement. Global loss of HDAC3 deacetylase activity possibly allows the expression of several genes negatively regulated by HDAC3 prematurely altering MHB function generating effects on extinction behavior.

Additionally, HDAC3^{W.T.} had no effect on the acquisition, extinction, or reinstatement of cocaine-induced CPP. While, again, it is possible the conditioning dose (10mg/kg) is too strong to detect subtle changes in acquisition, previous work has demonstrated that HDAC3 deacetylase activity is dependent on the formation of a complex with co-repressors NCoR and SMRT^{79,311}. Moreover, as HDAC3 does not in and of itself have a DNA binding domain for gene specific targeting, overexpression of HDAC3^{W.T.} without combinatorial overexpression of NCoR and SMRT is unlikely to have a significant effect on deacetylase activity. Future studies should more thoroughly evaluate what role HDAC3 in the MHB may have on the regulation of acquisition and extinction of CPP. With the advent of CRISPR/dCas9 technology, future studies will be able to specifically target either HDAC3^{W.T.} or HDAC3^{Y298H} to the *Nr4a2* locus to determine if HDAC3 negative regulation of *Nr4a2* is necessary and sufficient for cocaine-primed reinstatement.

Lastly, we evaluate what role NR4A2 may have on vMHB regulated behaviors. NR4A2 is an immediate early gene and transcription factor that has a versatile role throughout the CNS. It has been shown to be required for long-term memory formation in the hippocampus^{25,26,28}. Also, NR4A2 is necessary for proper development of dopaminergic neurons and has been shown to be

dysregulated throughout the ventral midbrain and ventral striatum following chronic cocaine administration^{16,32,312}. Whereas NR4A2 is known to also be required for proper MHb development¹⁷³, its role in the adult MHb remains unknown. Previous work demonstrates that *Nr4a2* is induced in the MHb following an associative learning paradigm, but does not provide a causal link between NR4A2 function and MHb-mediated behaviors¹⁹⁷. Here, we demonstrate for the first time that NURR2C directly interacts with endogenous NR4A2. Moreover, loss of NR4A2 function via NURR2C overexpression blunts the canonical baseline firing rate in MHb cholinergic neurons and, subsequently, overexpression of NURR2C in the cholinergic neurons of the MHb blocks cocaine-primed reinstatement. These results provide evidence that 1) NR4A2 is critical in endogenous MHb function and activity 2) NR4A2 function is required for MHb-mediated relapse-like behaviors. Yet, how NR4A2 affects MHb circuit function, what is NR4A2's contributions to MHb firing, and which gene targets of NR4A2 are subsequently engaged during cocaine-primed reinstatement remain key open questions. *Cebpb*, an NR4A2 target gene²², was one potential candidate gene for conferring changes in the epigenome to changes in circuit function. *Cebpb* expression is known to be activity dependent and it is required for plasticity and hippocampal long-term memory^{313,314}. Moreover, CEBP/β is a transactivator of genes associated with cholinergic signaling enriched in the vMHb (such as *Vacht* and *Chat*³¹⁵). However, as we detected no changes in HDAC3 occupancy during cocaine-primed reinstatement, these and other NR4A2 target genes may regulate vMHb function at a different time point, if at all. Also, it is possible our dominant-negative approach using NURR2C only affects a subset of NR4A2-dependent gene targets. The NR4A family of transcription factors are known to form homo- and heterodimers to regulate transcription²⁷; while NURR2C has been demonstrated to block known NR4A2-target genes³⁰⁷ it is unknown if NURR2C impact the function of NR4A2-containing heterodimers. Identifying the

full library of NR4A2 regulated genes and isolating those which contribute to adult MHb cholinergic function will be a critical step forward in understanding the MHb's contributions to relapse-like behaviors and SUD at large. Still, in the MHb, HDAC3 functions as a negative regulator of *Nr4a2* that is disengaged during cocaine-primed reinstatement.

The MHb has become a focus for addiction researchers over the past decade. The presented studies further link MHb function with relapse-like behaviors by identifying a key molecular mechanism, in HDAC3-dependent regulation of *Nr4a2*, underlying cocaine-primed reinstatement of conditioned place preference. Moving forward, identifying the downstream targets of HDAC3 and NR4A2 that may confer cocaine-induced changes to MHb circuit function will provide a novel avenue of studies regarding the molecular and circuit mechanisms regulating MHb activity during relapse and relapse-like behaviors.

Chapter 5: Conclusions and Moving Forward

While there are therapeutics of varying efficacy, SUD is a chronically relapsing disease with no current cure. Drugs of abuse establish long-lasting changes to various neural pathways and the underlying molecular mechanisms which control neural circuit function. These changes are believed to generate the resilience and persistence of drug-seeking behavior, even following long-periods of abstinence. Of note is the ability of drug-associated cues or even brief drug re-exposures to elicit powerful cravings and drive relapse. As such, researchers have continued to characterize the various adaptations in response to both acute and repeated drug exposures that provide the persistence of these drug associations.

Epigenetic mechanisms are powerful regulators of the molecular adaptations induced by drugs of abuse. Often, epigenetic modifiers themselves are recruited and can provide long-lasting changes in gene expression profiles throughout the CNS. Volumes of research in the mesolimbic pathway (including the VTA and NAc) demonstrate drug-induced epigenomic changes that may provide the persistence and resilience of drug-seeking behavior, including loci-specific changes to histone modifications (such as acetylation, methylation, and phosphoacetylation)^{32,133,134}. Of note is the altered HDAC3 function and the regulation of its target genes, such as *Nr4a2*, seen throughout various cocaine-associated behaviors^{135,240,316}. Recent work has begun to explore the epigenetic regulation of neural pathways that feed into the mesolimbic dopamine system and regulate drug-associated behaviors. The work in this dissertation focused on the epigenetic adaptations in the MHb that lead to cocaine relapse-like behaviors.

The MHb is a small, often ignored, epithalamic region. Canonically characterized as an aversion hub, more recent work has refined the function of the MHb as a region that responds to aversive associations to generate adaptive responses^{197,199,200}. Regarding SUD, the MHb has garnered significant attention from nicotine researchers, as the MHb-IPN pathway shows the

densest nAChR expression. Of note are the vMHb α 5- and β -4 subunit containing nAChRs, as these subunits are critical regulators of nicotine withdrawal, nicotine aversion, and nicotine mediated anxiety-like behaviors^{210,215,290,291,302}. While the endogenous function of the MHb remains elusive, the work presented above provides further evidence of the MHb's role in regulating drug-associated behaviors.

A clear role for the vMHb in regulating the responses to other drugs of abuse, such as cocaine, remains undefined, at best. The results presented in this dissertation broaden the known role of the vMHb in relapse-like behaviors by 1) confirming previous work demonstrating the MHb is engaged during reinstatement of cocaine associated behaviors²³⁴, 2) causally linking vMHb activity to reinstatement of cocaine-induced CPP, 3) demonstrating that epigenetic adaptations (via altered HDAC3 occupancy) regulate genes critical to MHb-function (*Nr4a2*) during relapse-like behaviors, and 4) causally linking NR4A2 function to MHb-mediated cocaine relapse-like behaviors. Although the results of this dissertation provide a significant advance in the knowledge of the neural circuitry and epigenetic adaptations regulating relapse behaviors, there remains several key open questions.

In **Chapter 1**, we assess the functional response of the MHb to various cocaine treatments. Whereas the MHb appeared insensitive to acute cocaine or the consolidation phase of cocaine-induced CPP, we demonstrate that the MHb responds to cocaine re-exposures. Specifically, we provide evidence that the MHb is engaged during cocaine-primed reinstatement of cocaine-induced CPP, recapitulating previous findings²³⁴ that the MHb is engaged during relapse-like behaviors. However, what adaptations that occur during repeated cocaine-exposure and/or forced abstinence/extinction that leave the vMHb primed for reinstatement? Although we demonstrate adaptations that occur in the MHb during reinstatement (such as increased *cFos* expression

(**Chapter 1**), increased histone acetylation (**Chapter 1**), and HDAC3 disengagement from *Nr4a2* (**Chapter 4**)), are these adaptations occurring as a direct response to cocaine re-exposure or is the vMHB responding to long-lasting circuit adaptations occurring elsewhere (such as changes to the serotonergic, setpal, or raphe inputs)? Our electrophysiological recordings from the vMHB show that bath application of cocaine is unable to induce vMHB firing, acutely or following extinction of cocaine-induced CPP, suggesting that the changes seen in vMHB activity during cocaine-primed reinstatement are likely caused by changes in upstream signaling that subsequently engage MHB activity. Various neurotransmitter systems feed into the MHB via the stria medullaris, including a dense serotonergic input. Future work should identify the source of altered signaling into the MHB as a potential mechanism for blocking relapse and relapse-like behaviors. Although others have shown repeated cocaine exposure can subsequently suppress MHB baseline activity, we did not see changes in baseline firing rates in the vMHB of animals with a cocaine treatment history (compared to naïve animals)²³². This difference suggests that either 1) our cocaine treatment was not sufficient to induce previously reported changes in MHB activity (Hammer et al. found changes following 7 consecutive days cocaine administration, while our CPP-based exposure paradigm only administers 2 days of cocaine), 2) the period of forced abstinence (or the extinction process) allows MHB activity to stabilize or 3) the MHB is sensitive to other differences in the schedules of cocaine treatment (such as dose). If vMHB activity were to stabilize during cocaine abstinence, there may be underlying epigenetic changes (that do not necessarily confer changes in neuronal activity) that prime the vMHB for cocaine-primed reinstatement.

In **Chapter 2**, we use chemogenetics to causally link changes in neuronal activity to changes in associative behavior. We demonstrate that chemogenetic activation of the dorsal hippocampus enhances long-term memory for the object location, but not object recognition task.

Further, chemogenetic inhibition of the dorsal hippocampus blocked long-term memory formation for the object location tasks but had no effect on object recognition memory. However, whereas the effects on hippocampal long-term memory were independent of viral promoter (i.e. hSyn-HM3D and CamKII α -HM3D both enhanced object location memory), the effects on synaptic plasticity diverged in a promoter-specific manner. Specifically, electrophysiological results were inverse of our prediction: chemogenetic activation using hSyn-HM3D lead to inhibition of local field potentials and theta-burst induced LTP, whereas hSyn-HM4D lead to enhancement of local field potentials and theta-burst induced LTP. Use of the non-cell-type specific *hSyn* promoter (although the author will note that the *hSyn* promoter provides specificity to neurons) allowed DREADD expression in both the glutamatergic and GABA-ergic neuronal populations in the dorsal hippocampus. Chemogenetic manipulations on the GABA-ergic neurons of the dorsal hippocampus likely underlie this unique electrophysiological effect. However, it remains unclear how electrophysiological inhibition caused by hSyn-HM3D led to the enhancements observed in hippocampal long-term memory. As synaptic plasticity and LTP are proposed mechanisms for long-term memory formation, future studies should explore this disconnect between chemogenetic induced synaptic plasticity and chemogenetic-mediated changes to long-term memory formation.

Our work (**Chapter 1**) has shown that the MHb is activated in response to cocaine-primed reinstatement of CPP. Moreover, the MHb has been previously shown to be engaged during cue-primed reinstatement of cocaine self-administration. However, these changes in MHb activity have not been causally linked to changes in cocaine-associated behaviors. In **Chapter 3**, we use chemogenetics to causally link vMHb activity to reinstatement of cocaine-induced CPP. Specifically, chemogenetic activation of the cholinergic neurons in the MHb (concentrated in the vMHb) induces reinstatement of a conditioned preference, even in the absence of cocaine.

However, chemogenetic activation of the vMHB alone is unable to induce a conditioned preference. This suggests that vMHB activity is critical in regulating previously formed associations, but does not acutely generate preference or aversion. However, because we failed to observe electrophysiological changes in MHB firing during bath application of cocaine (both acutely or during cocaine re-exposure, **Chapter 1**), it is unclear if the firing rate induced chemogenetically is comparable to the endogenous increase in activity during cocaine-primed reinstatement. Lastly, the downstream effects of the observed changes in vMHB activity on IPN circuitry and function remain unexplored. The GABA-ergic neurons of the IPN regulate various brain regions and neurotransmitter systems all linked to cocaine-associated behaviors (including the ventral hippocampus and serotonergic neurons of the raphe nuclei). A more thorough characterization of the MHB's circuitry during cocaine-primed reinstatement, including regulation of downstream IPN targets, will be necessary to form a more complete understanding of the vMHB's role in regulating relapse-like behaviors.

In **Chapter 4**, we characterize epigenetic gene regulation in the cholinergic neurons of the MHB during cocaine-primed reinstatement. Work from our lab has previously demonstrated changes in MHB histone acetylation in response to cocaine-primed reinstatement that has been previously correlated with changes in HDAC3 function and *Nr4a2* expression. We demonstrate that in response to cocaine-primed reinstatement in the cholinergic neurons of the MHB, HDAC3 disengages from the promoter of *Nr4a2*, but not other genes related to cocaine response and plasticity (e.g. *Cebpb*, *Ppp1r1b*, *Nr4a3*). To further elucidate the role of HDAC3 function in MHB-mediated reinstatement, we generated wild-type overexpression or deacetylase-dead variants of HDAC3. We demonstrate overexpression of HDAC3^{W.T.} had no effect on cocaine-associated behaviors, whereas loss of HDAC3 deacetylase activity (HDAC3^{Y298H}) in the cholinergic neurons

of the MHb disrupts extinction of cocaine-induced CPP. Yet, the underlying cause of this change remains unexplored. It is possible that endogenous HDAC3 prevents the recruitment of MHb circuitry during extinction of cocaine-associated CPP, but loss of HDAC3 activity allows the premature expression of various genes artificially altering MHb function during extinction. Previous studies have shown that the vMHb is critical in extinction of learned-fear²⁰⁰. Future studies should evaluate if the vMHb is similarly engaged during extinction of drug-associated behaviors, such as CPP. Also, while we demonstrate gene-specific changes in HDAC3 occupancy, the totality of HDAC3 regulated genes that are altered during cocaine-primed reinstatement is currently unknown. Identifying other downstream HDAC3 targets and how they impact MHb function will provide a more thorough understanding of the various cocaine-induced adaptations throughout the circuitry regulating drug-cravings, drug-seeking, and drug-relapse.

Lastly, *Nr4a2* is an immediate-early gene that has been previously linked to plasticity, associative memory, dopamine signaling, and is disrupted by various cocaine insults. However, whereas NR4A2 is known to be necessary for neuronal development in the MHb, the role of NR4A2 in the adult MHb is unknown. To further characterize NR4A2 function in the adult MHb, we used a dominant-negative variant of NR4A2, NURR2C, in a cell-type specific fashion. For the first time we demonstrate that NURR2C directly interacts with NR4A2, confirming its characterization as a dominant-negative. Furthermore, by overexpressing NURR2C in the cholinergic neurons of the MHb, we determine that loss of endogenous NR4A2 activity disrupts MHb function. Via overexpression of dominant-negative NURR2C, first we show that the endogenous baseline firing rate of cholinergic MHb neurons is blunted with loss of NR4A2 function. Secondly, we demonstrate that loss of endogenous NR4A2 activity prevents MHb-mediated reinstatement of cocaine-induced CPP. These results provide, for the first time, a

function of NR4A2 in the adult MHb and causally link NR4A2 activity to MHb-mediated behaviors.

Nevertheless, while it is convenient to rely on the changes to a known transcription factor (NR4A2), it is highly unlikely that *Nr4a2* is the one and only HDAC3 target critical to MHb function in response to cocaine. The goal of neuroepigenetics should not merely be to identify changes in nuclear acetylation states that regulate the expression of well-characterized transcription factors. But, as a field, we should strive to identify how these changes in the nucleus actually confer long-lasting changes in the neural circuits regulating behavior. Future studies should focus on identifying the cell-type specific gene targets of NR4A2 that contribute to MHb circuit function. Combinatorial Chip-Seq and RNA-seq studies provide researchers the ability to identify changes to both HDAC3 and NR4A2 transcriptional regulation, while simultaneously generating a MHb-specific transcriptome during cocaine-primed reinstatement. Identifying these downstream adaptations provide a currently unexplored avenue of therapeutics to reverse the drug-induced maladaptations leading to relapse.

References

1. [a Newmarket Films and Syncopy production] ; directed by Christopher Nolan ; screenplay by Jonathan Nolan and Christopher Nolan ; produced by Emma Thomas Christopher Nolan, A. R. The Prestige. (2006).
2. Justice, U. S. D. of. National Drug Intelligence Center. National Drug Threat Assessment. (2011).
3. U.S. Department of Health and Human Services, Centers for Disease Control and Prevention, National Center for Chronic Disease Prevention and Health Promotion, Office on Smoking and Health, National Center for Chronic Disease Prevention and Health Promot, O. on S. and H. The Health Consequences of Smoking—50 Years of Progress. A Report of the Surgeon General.o Title. (2014).
4. Prevention., C. for D. C. and. Excessive Drinking Costs U.S. \$223.5 Billion. (2014).
5. Association., A. P. *Diagnostic and statistical manual of mental disorders (5th ed.)*. (American Psychiatric Publishing, 2013).
6. Jalabert, M. *et al.* Neuronal circuits underlying acute morphine action on dopamine neurons. *Proc. Natl. Acad. Sci.* **108**, 16446–16450 (2011).
7. Hadfield, M. G., Mott, D. E. W. & Ismay, J. Cocaine: effect of in vivo administration on synaptosomal uptake of norepinephrine. *Biochem. Pharmacol.* **29**, 1861–1863 (1980).
8. Ross, S. B. & Renyi, A. L. Inhibition of the uptake of tritiated 5-hydroxytryptamine in brain tissue. *Eur. J. Pharmacol.* **7**, 270–277 (1969).
9. Kuhar, M. J., Ritz, M. C. & Boja, J. W. The dopamine hypothesis of the reinforcing properties of cocaine. *Trends in Neurosciences* **14**, 299–302 (1991).
10. Vrana, S. L., Vrana, K. E., Kovacs, T. R., Smith, J. E. & Dworkin, S. I. Chronic cocaine administration increases CNS tyrosine hydroxylase enzyme activity and mRNA levels and tryptophan hydroxylase enzyme activity levels. *J Neurochem* **61**, 2262–2268 (1993).
11. Beitner-Johnson, D. & Nestler, E. J. Morphine and cocaine exert common chronic actions on tyrosine hydroxylase in dopaminergic brain reward regions. *J. Neurochem.* **57**, 344–347 (1991).
12. Kumar, A. *et al.* Chromatin remodeling is a key mechanism underlying cocaine-induced plasticity in striatum. *Neuron* **48**, 303–314 (2005).
13. Robison, A. J. & Nestler, E. J. Transcriptional and epigenetic mechanisms of addiction. *Nat. Rev. Neurosci.* **12**, 623–637 (2011).
14. Ruffle, J. K. Molecular neurobiology of addiction: what’s all the (Δ)FosB about? *Am. J. Drug Alcohol Abuse* **2990**, 1–10 (2014).
15. Albertson, D. N. *et al.* Gene expression profile of the nucleus accumbens of human cocaine abusers: Evidence for dysregulation of myelin. *J. Neurochem.* **88**, 1211–1219 (2004).
16. Bannon, M. J., Pruetz, B., Barfield, E. & Schmidt, C. J. Transcription factors specifying dopamine phenotype are decreased in cocaine users. *Neuroreport* **15**, 401–404 (2004).
17. Bannon, M., Kapatos, G. & Albertson, D. Gene expression profiling in the brains of human cocaine abusers. *Addict. Biol.* **10**, 119–26 (2005).
18. Hermanson, E. *et al.* Nurr1 regulates dopamine synthesis and storage in MN9D dopamine cells. *Exp. Cell Res.* **288**, 324–334 (2003).
19. Saijo, K. *et al.* A Nurr1/CoREST pathway in microglia and astrocytes protects dopaminergic neurons from inflammation-induced death. *Cell* **137**, 47–59 (2009).
20. Blin, M., Norton, W., Bally-Cuif, L. & Vernier, P. NR4A2 controls the differentiation of selective dopaminergic nuclei in the zebrafish brain. *Mol. Cell. Neurosci.* **39**, 592–604 (2008).
21. Jankovic, J., Chen, S. & Le, W. D. The role of Nurr1 in the development of dopaminergic neurons and Parkinson’s disease. *Prog. Neurobiol.* **77**, 128–138 (2005).
22. Johnson, M. M., Michelhaugh, S. K., Bouhamdan, M., Schmidt, C. J. & Bannon, M. J. The transcription factor NURR1 exerts concentration-dependent effects on target genes mediating distinct biological processes. *Front. Neurosci.* **5**, 1–11 (2011).
23. Sacchetti, P., Mitchell, T. R., Granneman, J. G. & Bannon, M. J. Nurr1 enhances transcription of

- the human dopamine transporter gene through a novel mechanism. *J. Neurochem.* **76**, 1565–72 (2001).
24. Zhang, T. *et al.* Nurr1 is phosphorylated by ERK2 in vitro and its phosphorylation upregulates tyrosine hydroxylase expression in SH-SY5Y cells. *Neurosci. Lett.* **423**, 118–122 (2007).
 25. Peña de Ortiz, S., Maldonado-Vlaar, C. S. & Carrasquillo, Y. Hippocampal expression of the orphan nuclear receptor gene hzf-3/nurr1 during spatial discrimination learning. *Neurobiol. Learn. Mem.* **74**, 161–178 (2000).
 26. Colón-Cesario, W. I. *et al.* Knockdown of Nurr1 in the rat hippocampus: Implications to spatial discrimination learning and memory. *Learn. Mem.* **13**, 734–744 (2006).
 27. Hawk, J. D. & Abel, T. The role of NR4A transcription factors in memory formation. *Brain Res. Bull.* **85**, 21–9 (2011).
 28. McNulty, S. E. *et al.* Differential roles for Nr4a1 and Nr4a2 in object location vs. object recognition long-term memory. *Learn. Mem.* **19**, 588–92 (2012).
 29. Anderson, S. M. & Pierce, R. C. Cocaine-induced alterations in dopamine receptor signaling: Implications for reinforcement and reinstatement. *Pharmacol. Ther.* **106**, 389–403 (2005).
 30. Smith, R. J., Lobo, M. K., Spencer, S. & Kalivas, P. W. Cocaine-induced adaptations in D1 and D2 accumbens projection neurons (a dichotomy not necessarily synonymous with direct and indirect pathways). *Curr. Opin. Neurobiol.* **23**, 546–552 (2013).
 31. Brami-Cherrier, K. Parsing Molecular and Behavioral Effects of Cocaine in Mitogen- and Stress-Activated Protein Kinase-1-Deficient Mice. *J. Neurosci.* **25**, 11444–11454 (2005).
 32. Chandra, R. *et al.* Opposing role for Egr3 in nucleus accumbens cell subtypes in cocaine action. *J. Neurosci.* **35**, 7927–7937 (2015).
 33. Valjent, E. *et al.* Regulation of a protein phosphatase cascade allows convergent dopamine and glutamate signals to activate ERK in the striatum. *Proc. Natl. Acad. Sci. U. S. A.* **102**, 491–496 (2005).
 34. Bateup, H. S. *et al.* Cell type-specific regulation of DARPP-32 phosphorylation by psychostimulant and antipsychotic drugs. *Nat. Neurosci.* **11**, 932–939 (2008).
 35. Nairn, A. C. *et al.* The role of DARPP-32 in the actions of drugs of abuse. *Neuropharmacology* **47**, 14–23 (2004).
 36. Svenningsson, P. *et al.* DARPP-32: an integrator of neurotransmission. *Annu. Rev. Pharmacol. Toxicol.* **44**, 269–296 (2004).
 37. Zhang, Y. *et al.* Cocaine self-administration in mice is inversely related to phosphorylation at Thr34 (protein kinase A site) and Ser130 (kinase CK1 site) of DARPP-32. *J. Neurosci.* **26**, 2645–2651 (2006).
 38. Borgland, S. L. Acute and Chronic Cocaine-Induced Potentiation of Synaptic Strength in the Ventral Tegmental Area: Electrophysiological and Behavioral Correlates in Individual Rats. *J. Neurosci.* **24**, 7482–7490 (2004).
 39. Ungless, M. A., Whistler, J. L., Malenka, R. C. & Bonci, A. Single cocaine exposure in vivo induces long-term potentiation in dopamine neurons. *Nature* **411**, 583–7. (2001).
 40. Moussawi, K. *et al.* N-Acetylcysteine reverses cocaine-induced metaplasticity. *Nat. Neurosci.* **12**, 182–189 (2009).
 41. Levine, A. *et al.* Molecular mechanism for a gateway drug: epigenetic changes initiated by nicotine prime gene expression by cocaine. *Sci. Transl. Med.* **3**, 107ra109 (2011).
 42. Calipari, E. S. *et al.* In vivo imaging identifies temporal signature of D1 and D2 medium spiny neurons in cocaine reward. *Proc. Natl. Acad. Sci.* **113**, 2726–2731 (2016).
 43. Kourrich, S., Rothwell, P. E., Klug, J. R. & Thomas, M. J. Cocaine Experience Controls Bidirectional Synaptic Plasticity in the Nucleus Accumbens. *J. Neurosci.* **27**, 7921–7928 (2007).
 44. Grant, S. *et al.* Activation of memory circuits during cue-elicited cocaine craving. *Proc. Natl. Acad. Sci. U. S. A.* **93**, 12040–5 (1996).
 45. Hyman, S. E., Malenka, R. C. & Nestler, E. J. NEURAL MECHANISMS OF ADDICTION: The Role of Reward-Related Learning and Memory. *Annu. Rev. Neurosci.* **29**, 565–598 (2006).

46. Kufahl, P. R. *et al.* Neural responses to acute cocaine administration in the human brain detected by fMRI. *Neuroimage* **28**, 904–914 (2005).
47. Breiter, H. C. *et al.* Acute Effects of Cocaine on Human Brain Activity and Emotion. *Neuron* **19**, 591–611 (1997).
48. Childress, A. R. *et al.* Limbic activation during cue-induced cocaine craving. *Am. J. Psychiatry* **156**, 11–8 (1999).
49. Kilts, C. D. *et al.* Neural activity related to drug craving in cocaine addiction. *Arch. Gen. Psychiatry* **58**, 334–341 (2001).
50. Phillips, P. E. M., Stuber, G. D., Helen, M. L. A. V, Wightman, R. M. & Carelli, R. M. Subsecond dopamine release promotes cocaine seeking. *Nature* **422**, 614–618 (2003).
51. Sjulson, L., Peyrache, A., Cumpelik, A., Cassataro, D. & Buzsáki, G. Cocaine Place Conditioning Strengthens Location-Specific Hippocampal Coupling to the Nucleus Accumbens. *Neuron* 1–9 (2018). doi:10.1016/j.neuron.2018.04.015
52. Tropea, T. F., Kosofsky, B. E. & Rajadhyaksha, A. M. Enhanced CREB and DARPP-32 phosphorylation in the nucleus accumbens and CREB, ERK, and GluR1 phosphorylation in the dorsal hippocampus is associated with cocaine-conditioned place preference behavior. *J. Neurochem.* **106**, 1780–1790 (2008).
53. Shaham, Y., Shalev, U., Lu, L., De Wit, H. & Stewart, J. The reinstatement model of drug relapse: History, methodology and major findings. *Psychopharmacology (Berl)*. **168**, 3–20 (2003).
54. McFarland, K., Lapish, C. C. & Kalivas, P. W. Prefrontal glutamate release into the core of the nucleus accumbens mediates cocaine-induced reinstatement of drug-seeking behavior. *J. Neurosci.* **23**, 3531–3537 (2003).
55. Kumaresan, V. *et al.* Metabotropic glutamate receptor 5 (mGluR5) antagonists attenuate cocaine priming- and cue-induced reinstatement of cocaine seeking. *Behav. Brain Res.* **202**, 238–244 (2009).
56. Bäckström, P. & Hyttiä, P. Involvement of AMPA/kainate, NMDA, and mGlu5 receptors in the nucleus accumbens core in cue-induced reinstatement of cocaine seeking in rats. *Psychopharmacology (Berl)*. **192**, 571–580 (2007).
57. Wang, X., Moussawi, K., Knackstedt, L., Shen, H. & Kalivas, P. W. Role of mGluR5 neurotransmission in reinstated cocaine-seeking. *Addict. Biol.* **18**, 40–49 (2013).
58. WADDINGTON & H., C. The epigenotype. *Endeavour* **1**, 18–20 (1942).
59. FRANKLIN, R. E. & GOSLING, R. G. Molecular Configuration in Sodium Thymonucleate. *Nature* **171**, 740 (1953).
60. FRANKLIN, R. E. & GOSLING, R. G. Evidence for 2-Chain Helix in Crystalline Structure of Sodium Deoxyribonucleate. *Nature* **172**, 156 (1953).
61. Franklin, R. E. & Gosling, R. G. The structure of sodium thymonucleate fibres. I. The influence of water content. *Acta Crystallogr.* **6**, 673–677 (1953).
62. Hershey, A. D. & Chase, M. INDEPENDENT FUNCTIONS OF VIRAL PROTEIN AND NUCLEIC ACID IN GROWTH OF BACTERIOPHAGE. *J. Gen. Physiol.* **36**, 39–56 (1952).
63. Tjian, R. The binding site on SV40 DNA for a T antigen-related protein. *Cell* **13**, 165–179 (1978).
64. Kershner, 20th Century Fox ; Lucasfilm Ltd. ; directed by Irvin. Star wars. Episode V, Empire strikes back. (2006).
65. Kouzarides, T. Chromatin modifications and their function. *Cell* **128**, 693–705 (2007).
66. López, A. J. & Wood, M. a. Role of nucleosome remodeling in neurodevelopmental and intellectual disability disorders. *Front. Behav. Neurosci.* **9**, 1–10 (2015).
67. Krebs, J. E., Fry, C. J., Samuels, M. L. & Peterson, C. L. Global role for chromatin remodeling enzymes in mitotic gene expression. *Cell* **102**, 587–598 (2000).
68. Olave, I., Wang, W., Xue, Y., Kuo, A. & Crabtree, G. R. Identification of a polymorphic, neuron-specific chromatin remodeling complex. *Genes Dev.* **16**, 2509–17 (2002).
69. Alaghband, Y., Bredy, T. W. & Wood, M. A. The role of active DNA demethylation and Tet enzyme function in memory formation and cocaine action. *Neurosci. Lett.* (2016).

doi:10.1016/j.neulet.2016.01.023

70. Vogel-Ciernia, A. & Wood, M. a. Neuron-specific chromatin remodeling: A missing link in epigenetic mechanisms underlying synaptic plasticity, memory, and intellectual disability disorders. *Neuropharmacology* **80**, 18–27 (2014).
71. Li, X. *et al.* Neocortical Tet3-mediated accumulation of 5-hydroxymethylcytosine promotes rapid behavioral adaptation. *Proc. Natl. Acad. Sci. U. S. A.* **111**, 7120–5 (2014).
72. Baker-Andresen, D., Ratnu, V. S. & Bredy, T. W. Dynamic DNA methylation: a prime candidate for genomic metaplasticity and behavioral adaptation. *Trends Neurosci.* **36**, 3–13 (2013).
73. Bredy, T. W., Lin, Q., Wei, W., Baker-Andresen, D. & Mattick, J. S. MicroRNA regulation of neural plasticity and memory. *Neurobiol. Learn. Mem.* **96**, 89–94 (2011).
74. McQuown, S. C. & Wood, M. a. HDAC3 and the Molecular Brake Pad Hypothesis. *Neurobiol. Learn. Mem.* **96**, 27–34 (2012).
75. Barrett, R. M. & Wood, M. a. Beyond transcription factors: the role of chromatin modifying enzymes in regulating transcription required for memory. *Learn. Mem.* **15**, 460–7 (2008).
76. RUIJTER, A. J. M. de, GENNIP, A. H. van, CARON, H. N., KEMP, S. & KUILENBURG, A. B. P. van. Histone deacetylases (HDACs): characterization of the classical HDAC family. *Biochem. J.* **370**, 737–749 (2003).
77. Sharon Y. Roth, John M. Denu & Allis, C. D. HISTONE ACETYLTRANSFERASES. *Annu. Rev. Biochem.* 81–120 (2003).
78. Adachi, M. & Monteggia, L. M. Decoding transcriptional repressor complexes in the adult central nervous system. *Neuropharmacology* **80C**, 45–52 (2014).
79. Guenther, M. G., Barak, O. & Lazar, M. A. The SMRT and N-CoR Corepressors Are Activating Cofactors for Histone Deacetylase 3. *Mol. Cell. Biol.* **21**, 6091–6101 (2001).
80. Parker, D. *et al.* Phosphorylation of CREB at Ser-133 induces complex formation with CREB-binding protein via a direct mechanism. *Mol. Cell. Biol.* **16**, 694–703 (1996).
81. Renthal, W. & Nestler, E. J. Epigenetic mechanisms in drug addiction. *Trends Mol. Med.* **14**, 341–350 (2008).
82. Lo, W. S. *et al.* Phosphorylation of serine 10 in histone H3 is functionally linked in vitro and in vivo to Gcn5-mediated acetylation at lysine 14. *Mol. Cell* **5**, 917–926 (2000).
83. Jin, Q. *et al.* Distinct roles of GCN5/PCAF-mediated H3K9ac and CBP/p300-mediated H3K18/27ac in nuclear receptor transactivation. *EMBO J.* **30**, 249–262 (2011).
84. Kuo, Y. M. & Andrews, A. J. Quantitating the Specificity and Selectivity of Gcn5-Mediated Acetylation of Histone H3. *PLoS One* **8**, (2013).
85. Ciccarelli, A. & Giustetto, M. Role of ERK signaling in activity-dependent modifications of histone proteins. *Neuropharmacology* **80**, 34–44 (2014).
86. Sultan, F. A. & Day, J. J. Epigenetic mechanisms in memory and synaptic function. *Epigenomics* **3**, 157–181 (2011).
87. Schroeder, F. A. *et al.* Drug-induced activation of dopamine D1 receptor signaling and inhibition of class I/II histone deacetylase induces chromatin remodeling in reward circuitry and modulates cocaine-related behaviors. **33**, 2981–2992 (2008).
88. Bose, D. A. *et al.* RNA Binding to CBP Stimulates Histone Acetylation and Transcription. *Cell* **168**, 135–149.e22 (2017).
89. Agranoff, B. W., Davis, R. E., Casola, L. & Lim, R. Actinomycin D blocks formation of memory of shock-avoidance in goldfish. *Science (80-)*. **158**, 1600–1601 (1967).
90. Agranoff, B. W. Agents that block memory. 756–765 (1967).
91. Brink, J. J., Davis, R. E. & Agranoff, B. W. Effects of puromycin, acetoxycycloheximide and actinomycin D on protein synthesis in goldfish brain. *J. Neurochem.* **13**, 889–96 (1966).
92. Schmitt, M. & Matthies, H. [Biochemical studies on histones of the central nervous system. III. Incorporation of [¹⁴C]-acetate into the histones of different rat brain regions during a learning experiment]. *Acta Biol. Med. Ger.* **38**, 683–689 (1979).
93. Bousiges, O. *et al.* Spatial memory consolidation is associated with induction of several lysine-

- acetyltransferase (histone acetyltransferase) expression levels and H2B/H4 acetylation-dependent transcriptional events in the rat hippocampus. *Neuropsychopharmacology* **35**, 2521–2537 (2010).
94. Bredy, T. W. *et al.* Histone modifications around individual BDNF gene promoters in prefrontal cortex are associated with extinction of conditioned fear. *Learn. Mem.* 268–276 (2007). doi:10.1101/lm.500907.lation
 95. Guan, Z. *et al.* Integration of long-term-memory-related synaptic plasticity involves bidirectional regulation of gene expression and chromatin structure. *Cell* **111**, 483–493 (2002).
 96. Koshibu, K. *et al.* Protein Phosphatase 1 Regulates the Histone Code for Long-Term Memory. *J. Neurosci.* **29**, 13079–13089 (2009).
 97. Federman, N., Fustiñana, M. S. & Romano, A. Histone acetylation is recruited in consolidation as a molecular feature of stronger memories. *Learn. Mem.* **16**, 600–606 (2009).
 98. Morris, M. J., Karra, A. S. & Monteggia, L. M. Histone deacetylases govern cellular mechanisms underlying behavioral and synaptic plasticity in the developing and adult brain. *Behav. Pharmacol.* **21**, 409–19 (2010).
 99. Peixoto, L. & Abel, T. The Role of Histone Acetylation in Memory Formation and Cognitive Impairments. *Neuropsychopharmacology* **38**, 62–76 (2012).
 100. Stilling, R. M. *et al.* Klysine acetyltransferase 2a regulates a hippocampal gene expression network linked to memory formation. *EMBO J.* **33**, 19121927 (2014).
 101. Wood, M. a. *et al.* Transgenic mice expressing a truncated form of CREB-binding protein (CBP) exhibit deficits in hippocampal synaptic plasticity and memory storage. *Learn. Mem.* **12**, 111–119 (2005).
 102. Barrett, R. M. *et al.* Hippocampal focal knockout of CBP affects specific histone modifications, long-term potentiation, and long-term memory. *Neuropsychopharmacology* **36**, 1545–56 (2011).
 103. Alarcón, J. M. *et al.* Chromatin acetylation, memory, and LTP are impaired in CBP^{+/-} mice: A model for the cognitive deficit in Rubinstein-Taybi syndrome and its amelioration. *Neuron* **42**, 947–959 (2004).
 104. Bourtchuladze, R. *et al.* Deficient long-term memory in mice with a targeted mutation of the cAMP-responsive element-binding protein. *Cell* **79**, 59–68 (1994).
 105. Oike, Y. *et al.* Truncated CBP protein leads to classical Rubinstein-Taybi syndrome phenotypes in mice: implications for a dominant-negative mechanism. *Hum. Mol. Genet.* **8**, 387–396 (1999).
 106. Korzus, E., Rosenfeld, M. G. & Mayford, M. CBP histone acetyltransferase activity is a critical component of memory consolidation. *Neuron* **42**, 961–972 (2004).
 107. Oliveira, A. M. M., Abel, T., Brindle, P. K. & Wood, M. a. Differential role for CBP and p300 CREB-binding domain in motor skill learning. *Behav. Neurosci.* **120**, 724–729 (2006).
 108. Vecsey, C. G. *et al.* Histone deacetylase inhibitors enhance memory and synaptic plasticity via CREB:CBP-dependent transcriptional activation. *J. Neurosci.* **27**, 6128–40 (2007).
 109. Maurice, T. *et al.* Altered memory capacities and response to stress in p300/CBP-associated factor (PCAF) histone acetylase knockout mice. *Neuropsychopharmacology* **33**, 1584–1602 (2008).
 110. Oliveira, A. M. M., Wood, M. A., McDonough, C. B. & Abel, T. Transgenic mice expressing an inhibitory truncated form of p300 exhibit long-term memory deficits. *Learn. & Mem.* **14**, 564–572 (2007).
 111. Bredy, T. W. & Barad, M. The histone deacetylase inhibitor valproic acid enhances acquisition, extinction, and reconsolidation of conditioned fear. *Learn. Mem.* **15**, 39–45 (2008).
 112. McQuown, S. C. *et al.* HDAC3 is a critical negative regulator of long-term memory formation. *J. Neurosci.* **31**, 764–74 (2011).
 113. Haettig, J. *et al.* HDAC inhibition modulates hippocampus-dependent long-term memory for object location in a CBP-dependent manner. *Learn. Mem.* **18**, 71–9 (2011).
 114. Stefanko, D. P., Barrett, R. M., Ly, A. R., Reolon, G. K. & Wood, M. a. Modulation of long-term memory for object recognition via HDAC inhibition. *Proc. Natl. Acad. Sci. U. S. A.* **106**, 9447–52 (2009).
 115. Fischer, A., Sananbenesi, F., Wang, X., Dobbin, M. & Tsai, L.-H. Recovery of learning and

- memory is associated with chromatin remodelling. *Nature* **447**, 178–82 (2007).
116. Lattal, K. M., Barrett, R. M. & Wood, M. a. Systemic or intrahippocampal delivery of histone deacetylase inhibitors facilitates fear extinction. *Behav. Neurosci.* **121**, 1125–1131 (2007).
 117. Lahm, A. *et al.* Unraveling the hidden catalytic activity of vertebrate class IIa histone deacetylases. *Proc. Natl. Acad. Sci.* **104**, 17335–17340 (2007).
 118. Kwapis, J. L. *et al.* Context and Auditory Fear are Differentially Regulated by HDAC3 Activity in the Lateral and Basal Subnuclei of the Amygdale. *Neuropsychopharmacology* (2016). doi:10.1038/npp.2016.274
 119. Bridi, M. S., Hawk, J. D., Chatterjee, S., Safe, S. & Abel, T. Pharmacological Activators of the NR4A Nuclear Receptors Enhance LTP in a CREB/CBP-Dependent Manner. *Neuropsychopharmacology* **42**, 1243–1253 (2017).
 120. Wood, M. a, Attner, M. a, Oliveira, A. M. M., Brindle, P. K. & Abel, T. A transcription factor-binding domain of the coactivator CBP is essential for long-term memory and the expression of specific target genes. *Learn. Mem.* **13**, 609–17 (2006).
 121. Hawk, J. D. *et al.* NR4A nuclear receptors support memory enhancement by histone deacetylase inhibitors. *J. Clin. Invest.* **122**, 3593–3602 (2012).
 122. Vogel-Ciernia, A. *et al.* The neuron-specific chromatin regulatory subunit BAF53b is necessary for synaptic plasticity and memory. *Nat. Neurosci.* **16**, 552–61 (2013).
 123. Vogel Ciernia, A. *et al.* Mutation of neuron-specific chromatin remodeling subunit BAF53b: rescue of plasticity and memory by manipulating actin remodeling. *Learn. Mem.* **24**, 199–209 (2017).
 124. Shu, G. *et al.* Deleting HDAC3 rescues long-term memory impairments induced by disruption of the neuron- specific chromatin remodeling subunit BAF53b_AN022018. 109–115 (2018). doi:10.1101/lm.046920.117.25
 125. Pascual, M. *et al.* Changes in histone acetylation in the prefrontal cortex of ethanol-exposed adolescent rats are associated with ethanol-induced place conditioning. *Neuropharmacology* **62**, 2308–2318 (2012).
 126. Barbier, E. *et al.* DNA Methylation in the Medial Prefrontal Cortex Regulates Alcohol-Induced Behavior and Plasticity. *J. Neurosci.* **35**, 6153–6164 (2015).
 127. Koo, J. W. *et al.* Epigenetic basis of opiate suppression of Bdnf gene expression in the ventral tegmental area. *Nat. Neurosci.* **18**, 415–425 (2015).
 128. Renthal, W. & Nestler, E. J. Histone acetylation in drug addiction. *Semin. Cell Dev. Biol.* **20**, 387–394 (2009).
 129. Maze, I. & Nestler, E. The epigenetic landscape of addiction. *Ann N Y Acad Sci.* **1216**, 99–113 (2011).
 130. Mews, P. & Calipari, E. S. *Cross-talk between the epigenome and neural circuits in drug addiction. Progress in Brain Research* **235**, (Elsevier B.V., 2017).
 131. LaPlant, Q. & Nestler, E. J. CRACKing the histone code: Cocaine’s effects on chromatin structure and function. *Horm. Behav.* **59**, 321–330 (2011).
 132. Malvaez, M., Mhillaj, E., Matheos, D. P., Palmery, M. & Wood, M. a. CBP in the Nucleus Accumbens Regulates Cocaine-Induced Histone Acetylation and Is Critical for Cocaine-Associated Behaviors. *J. Neurosci.* **31**, 16941–16948 (2011).
 133. Jordi, E. *et al.* Differential effects of cocaine on histone posttranslational modifications in identified populations of striatal neurons. *Proc. Natl. Acad. Sci. U. S. A.* **110**, 9511–6 (2013).
 134. Bertran-Gonzalez, J. *et al.* Opposing Patterns of Signaling Activation in Dopamine D1 and D2 Receptor-Expressing Striatal Neurons in Response to Cocaine and Haloperidol. *J. Neurosci.* **28**, 5671–5685 (2008).
 135. Rogge, G. a, Singh, H., Dang, R. & Wood, M. a. HDAC3 is a negative regulator of cocaine-context-associated memory formation. *J. Neurosci.* **33**, 6623–32 (2013).
 136. Walker, D. M. *et al.* Cocaine self-administration alters transcriptome-wide responses in the brain’s reward circuitry. *Biol. Psychiatry* (2018). doi:10.1016/j.biopsych.2018.04.009

137. Maze, I. *et al.* Cocaine dynamically regulates heterochromatin and repetitive element unsilencing in nucleus accumbens. *Proc Natl Acad Sci U S A* **108**, 3035–3040 (2011).
138. Renthal, W. *et al.* Genome-wide Analysis of Chromatin Regulation by Cocaine Reveals a Role for Sirtuins. *Neuron* **62**, 335–348 (2009).
139. Feng, J. *et al.* Chronic cocaine-regulated epigenomic changes in mouse nucleus accumbens. *Genome Biol.* **15**, R65 (2014).
140. Stipanovich, A. *et al.* A phosphatase cascade by which rewarding stimuli control nucleosomal response. *Nature* **453**, 879–884 (2008).
141. Levine, A. A. *et al.* CREB-binding protein controls response to cocaine by acetylating histones at the fosB promoter in the mouse striatum. *Proc. Natl. Acad. Sci. U. S. A.* **102**, 19186–91 (2005).
142. Renthal, W. *et al.* Histone Deacetylase 5 Epigenetically Controls Behavioral Adaptations to Chronic Emotional Stimuli. *Neuron* **56**, 517–529 (2007).
143. Taniguchi, M. *et al.* HDAC5 and Its Target Gene, Npas4, Function in the Nucleus Accumbens to Regulate Cocaine-Conditioned Behaviors. *Neuron* **96**, 130–144.e6 (2017).
144. White, A. O. A. O. *et al.* BDNF rescues BAF53b-dependent synaptic plasticity and cocaine-associated memory in the nucleus accumbens. *Nat. Commun.* **7**, 11725 (2016).
145. Sun, H. S. *et al.* Regulation of BAZ1A and nucleosome positioning in the nucleus accumbens in response to cocaine. *Neuroscience* **353**, 1–6 (2017).
146. Huang, Y. Y., Kandel, D. B., Kandel, E. R. & Levine, A. Nicotine primes the effect of cocaine on the induction of LTP in the amygdala. *Neuropharmacology* **74**, 126–134 (2013).
147. Griffin, E. A. *et al.* Prior alcohol use enhances vulnerability to compulsive cocaine self-administration by promoting degradation of HDAC4 and HDAC5. *Sci. Adv.* **3**, (2017).
148. Tomasiewicz, H. C. *et al.* Proenkephalin mediates the enduring effects of adolescent cannabis exposure associated with adult opiate vulnerability. *Biol. Psychiatry* **72**, 803–810 (2012).
149. Ellgren, M., Spano, S. M. & Hurd, Y. L. Adolescent cannabis exposure alters opiate intake and opioid limbic neuronal populations in adult rats. *Neuropsychopharmacology* **32**, 607–615 (2007).
150. Watson, C. T. *et al.* Genome-Wide DNA Methylation Profiling Reveals Epigenetic Changes in the Rat Nucleus Accumbens Associated with Cross-Generational Effects of Adolescent THC Exposure. *Neuropsychopharmacology* **40**, 2993–3005 (2015).
151. Szutorisz, H. *et al.* Parental THC exposure leads to compulsive heroin-seeking and altered striatal synaptic plasticity in the subsequent generation. *Neuropsychopharmacology* **39**, 1315–1323 (2014).
152. Spano, M. S., Ellgren, M., Wang, X. & Hurd, Y. L. Prenatal Cannabis Exposure Increases Heroin Seeking with Allostatic Changes in Limbic Enkephalin Systems in Adulthood. *Biol. Psychiatry* **61**, 554–563 (2007).
153. Turner, K. J. *et al.* Afferent Connectivity of the Zebrafish Habenulae. *Front. Neural Circuits* **10**, 1–18 (2016).
154. Stamatakis, A. M. & Stuber, G. D. Activation of lateral habenula inputs to the ventral midbrain promotes behavioral avoidance. *Nat. Neurosci.* **15**, 1105–7 (2012).
155. Ramon y Cajal, S. *Histologie du Systeme Nerveux de l'homme et des Vertebres, Vol. 2.* (1911).
156. Savitz, J. B. *et al.* Habenula volume in bipolar disorder and major depressive disorder: A high-resolution magnetic resonance imaging study. *Biol. Psychiatry* **69**, 336–343 (2011).
157. Ranft, K. *et al.* Evidence for structural abnormalities of the human habenular complex in affective disorders but not in schizophrenia. *Psychol. Med.* **40**, 557–567 (2010).
158. Fakhoury, M. The dorsal diencephalic conduction system in reward processing: Spotlight on the anatomy and functions of the habenular complex. *Behav. Brain Res.* **348**, 115–126 (2018).
159. Kim, U. & Chung, L. -y. Dual GABAergic Synaptic Response of Fast Excitation and Slow Inhibition in the Medial Habenula of Rat Epithalamus. *J. Neurophysiol.* **98**, 1323–1332 (2007).
160. Choi, K., Lee, Y., Lee, C., Hong, S. & Lee, S. Optogenetic activation of septal GABAergic afferents entrains neuronal firing in the medial habenula. *Nat. Publ. Gr.* 1–10 (2016).
doi:10.1038/srep34800

161. Contestabile, A. & Fonnum, F. Cholinergic and GABAergic forebrain projections to the habenula and nucleus interpeduncularis: Surgical and kainic acid lesions. *Brain Res.* **275**, 287–297 (1983).
162. Kim, U. & Chang, S.-Y. Dendritic morphology, local circuitry, and intrinsic electrophysiology of neurons in the rat medial and lateral habenular nuclei of the epithalamus. *J. Comp. Neurol.* **483**, 236–50 (2005).
163. Morin, L. P. & Meyer-Bernstein, E. L. The ascending serotonergic system in the hamster: Comparison with projections of the dorsal and median raphe nuclei. *Neuroscience* **91**, 81–105 (1999).
164. Quina, L. A., Harris, J., Zeng, H. & Turner, E. E. Specific connections of the interpeduncular subnuclei reveal distinct components of the habenulopeduncular pathway. *J. Comp. Neurol.* **525**, 2632–2656 (2017).
165. Hamill, G. S., Olschowka, J. A., Lenn, N. J. & Jacobowitz, D. M. The subnuclear distribution of substance P, cholecystokinin, vasoactive intestinal peptide, somatostatin, leu α enkephalin, dopamine α β hydroxylase, and serotonin in the rat interpeduncular nucleus. *J. Comp. Neurol.* **226**, 580–596 (1984).
166. Lima, L. B. *et al.* Afferent and efferent connections of the interpeduncular nucleus with special reference to circuits involving the habenula and raphe nuclei. *J. Comp. Neurol.* **525**, 2411–2442 (2017).
167. Han, S. *et al.* Down-regulation of cholinergic signaling in the habenula induces anhedonia-like behavior. *Sci. Rep.* **7**, 900 (2017).
168. Sutherland, R. J. The dorsal diencephalic conduction system: A review of the anatomy and functions of the habenular complex. *Neurosci. Biobehav. Rev.* **6**, 1–13 (1982).
169. Aizawa, H., Kobayashi, M., Tanaka, S., Fukai, T. & Okamoto, H. Molecular characterization of the subnuclei in rat habenula. *J. Comp. Neurol.* **520**, 4051–4066 (2012).
170. Wagner, F., French, L. & Veh, R. W. Transcriptomic-anatomic analysis of the mouse habenula uncovers a high molecular heterogeneity among neurons in the lateral complex, while gene expression in the medial complex largely obeys subnuclear boundaries. *Brain Struct. Funct.* (2014). doi:10.1007/s00429-014-0891-9
171. Ouimet, C. C., LaMantia, a S., Goldman-Rakic, P., Rakic, P. & Greengard, P. Immunocytochemical localization of DARPP-32, a dopamine and cyclic-AMP-regulated phosphoprotein, in the primate brain. *J. Comp. Neurol.* **323**, 209–218 (1992).
172. Schalling, M. *et al.* Distribution and cellular localization of DARPP-32 mRNA in rat brain. *Brain Res. Mol. Brain Res.* **7**, 139–149 (1990).
173. Quina, L. A., Wang, S., Ng, L. & Turner, E. E. Brn3a and Nurr1 mediate a gene regulatory pathway for habenula development. *J. Neurosci.* **29**, 14309–14322 (2009).
174. Bétry, C. *et al.* Role of 5-HT₃ receptors in the antidepressant response. *Pharmaceuticals* **4**, 603–629 (2011).
175. Ichikawa, M. *et al.* Expression analysis of genes responsible for serotonin signaling in the brain. *Neurobiol. Dis.* **19**, 378–385 (2005).
176. Kinsey, A. M., Wainwright, A., Heavens, R., Sirinathsinghji, D. J. S. & Oliver, K. R. Distribution of 5-ht_{5A}, 5-ht_{5B}, 5-ht₆ and 5-HT₇ receptor mRNAs in the rat brain. *Mol. Brain Res.* **88**, 194–198 (2001).
177. Okamoto, H., Agetsuma, M. & Aizawa, H. Genetic dissection of the zebrafish habenula, a possible switching board for selection of behavioral strategy to cope with fear and anxiety. *Dev. Neurobiol.* **72**, 386–394 (2012).
178. Ogawa, S., Nathan, F. M. & Parhar, I. S. Habenular kisspeptin modulates fear in the zebrafish. *Proc. Natl. Acad. Sci.* **111**, 3841–3846 (2014).
179. Velasquez, K. M., Molfese, D. L. & Salas, R. The role of the habenula in drug addiction. *Front. Hum. Neurosci.* **8**, 174 (2014).
180. Fonck, C. *et al.* Demonstration of functional α 4-containing nicotinic receptors in the medial habenula. *Neuropharmacology* **56**, 247–253 (2009).

181. Hong, S., Zhou, T. C., Smith, M., Saleem, K. S. & Hikosaka, O. Negative reward signals from the lateral habenula to dopamine neurons are mediated by rostromedial tegmental nucleus in primates. *J. Neurosci.* **31**, 11457–11471 (2011).
182. Lammel, S., Lim, B. K. & Malenka, R. C. Reward and aversion in a heterogeneous midbrain dopamine system. *Neuropharmacology* **76 Pt B**, 351–9 (2014).
183. Hong, S. & Hikosaka, O. The Globus Pallidus Sends Reward-Related Signals to the Lateral Habenula. *Neuron* **60**, 720–729 (2008).
184. Proulx, C. D., Hikosaka, O. & Malinow, R. Reward processing by the lateral habenula in normal and depressive behaviors. *Nat. Neurosci.* **17**, 1146–1152 (2014).
185. Matsumoto, M. & Hikosaka, O. Lateral habenula as a source of negative reward signals in dopamine neurons. *Nature* **447**, 1111–5 (2007).
186. Bromberg-Martin, E. S. & Hikosaka, O. Lateral habenula neurons signal errors in the prediction of reward information. *Nat. Neurosci.* **14**, 1209–1218 (2011).
187. Shumake, J., Edwards, E. & Gonzalez-Lima, F. Opposite metabolic changes in the habenula and ventral tegmental area of a genetic model of helpless behavior. *Brain Res.* **963**, 274–281 (2003).
188. Jacinto, L. R., Mata, R., Novais, A., Marques, F. & Sousa, N. The habenula as a critical node in chronic stress-related anxiety. *Exp. Neurol.* **289**, 46–54 (2017).
189. Li, B. *et al.* Synaptic potentiation onto habenula neurons in the learned helplessness model of depression. *Nature* **470**, 535–541 (2011).
190. Yang, L. M., Hu, B., Xia, Y. H., Zhang, B. L. & Zhao, H. Lateral habenula lesions improve the behavioral response in depressed rats via increasing the serotonin level in dorsal raphe nucleus. *Behav. Brain Res.* **188**, 84–90 (2008).
191. Amat, J. *et al.* The role of the habenular complex in the elevation of dorsal raphe nucleus serotonin and the changes in the behavioral responses produced by uncontrollable stress. *Brain Res.* **917**, 118–126 (2001).
192. Meng, H. *et al.* Chronic deep brain stimulation of the lateral habenula nucleus in a rat model of depression. *Brain Res.* **1422**, 32–38 (2011).
193. Winter, C., Vollmayr, B., Djodari-Irani, A., Klein, J. & Sartorius, A. Pharmacological inhibition of the lateral habenula improves depressive-like behavior in an animal model of treatment resistant depression. *Behav. Brain Res.* **216**, 463–465 (2011).
194. Sartorius, A. *et al.* Remission of Major Depression Under Deep Brain Stimulation of the Lateral Habenula in a Therapy-Refractory Patient. *Biol. Psychiatry* **67**, e9–e11 (2010).
195. Morishita, T., Fayad, S. M., Higuchi, M., Nestor, K. A. & Foote, K. D. Deep Brain Stimulation for Treatment-resistant Depression: Systematic Review of Clinical Outcomes. *Neurotherapeutics* **11**, 475–484 (2014).
196. Mirrione, M. M. *et al.* Increased metabolic activity in the septum and habenula during stress is linked to subsequent expression of learned helplessness behavior. *Front. Hum. Neurosci.* **8**, 1–8 (2014).
197. Ressler, K. J., Paschall, G., Zhou, X. & Davis, M. Regulation of synaptic plasticity genes during consolidation of fear conditioning. *J. Neurosci.* **22**, 7892–7902 (2002).
198. Mathuru, A. S. & Jesuthasan, S. The medial habenula as a regulator of anxiety in adult zebrafish. *Front. Neural Circuits* **7**, 99 (2013).
199. Lee, A. *et al.* The habenula prevents helpless behavior in larval zebrafish. *Curr. Biol.* **20**, 2211–2216 (2010).
200. Zhang, J. *et al.* Presynaptic Excitation via GABAB Receptors in Habenula Cholinergic Neurons Regulates Fear Memory Expression. *Cell* **166**, 716–728 (2016).
201. Yamaguchi, T., Danjo, T., Pastan, I., Hikida, T. & Nakanishi, S. Distinct roles of segregated transmission of the septo-habenular pathway in anxiety and fear. *Neuron* **78**, 537–544 (2013).
202. Yo Otsu, A. *et al.* Functional Principles of Posterior Septal Inputs to the Medial Habenula. *Cell Rep.* **22**, 693–705 (2018).
203. Ohmura, Y., Tanaka, K. F., Tsunematsu, T., Yamanaka, A. & Yoshioka, M. Optogenetic

- activation of serotonergic neurons enhances anxiety-like behaviour in mice. *Int. J. Neuropsychopharmacol.* **17**, 1777–1783 (2014).
204. Marcinkiewicz, C. A. *et al.* Serotonin engages an anxiety and fear-promoting circuit in the extended amygdala. *Nature* **537**, 97–101 (2016).
 205. Marcinkiewicz, C. a., Dorrier, C. E., Lopez, A. J. & Kash, T. L. Ethanol induced adaptations in 5-HT_{2c} receptor signaling in the bed nucleus of the stria terminalis: Implications for anxiety during ethanol withdrawal. *Neuropharmacology* **89**, 157–167 (2015).
 206. Zohar, J. & Westenberg, H. G. Anxiety disorders: a review of tricyclic antidepressants and selective serotonin reuptake inhibitors. *Acta Psychiatr. Scand. Suppl.* **403**, 39–49 (2000).
 207. Kalén, P., Strecker, R. E., Rosengren, E. & Björklund, A. Regulation of striatal serotonin release by the lateral habenula-dorsal raphe pathway in the rat as demonstrated by in vivo microdialysis: role of excitatory amino acids and GABA. *Brain Res.* **492**, 187–202 (1989).
 208. Varga, V., Kocsis, B. & Sharp, T. Electrophysiological evidence for convergence of inputs from the medial prefrontal cortex and lateral habenula on single neurons in the dorsal raphe nucleus. *Eur. J. Neurosci.* **17**, 280–286 (2003).
 209. McCallum, S. E., Cowe, M. A., Lewis, S. W. & Glick, S. D. $\alpha 3\beta 4$ nicotinic acetylcholine receptors in the medial habenula modulate the mesolimbic dopaminergic response to acute nicotine in vivo. *Neuropharmacology* **63**, 434–440 (2012).
 210. Salas, R., Sturm, R., Boulter, J. & De Biasi, M. Nicotinic receptors in the habenulo-interpeduncular system are necessary for nicotine withdrawal in mice. *J. Neurosci.* **29**, 3014–3018 (2009).
 211. Glick, S. D. D., Kuehne, M. E. E., Maisonneuve, I. M. M., Bandarage, U. K. K. & Molinari, H. H. 18-Methoxycoronaridine, a non-toxic iboga alkaloid congener: Effects on morphine and cocaine self-administration and on mesolimbic dopamine release in rats. *Brain Res.* **719**, 29–35 (1996).
 212. Jackson, K. J., Sanjakdar, S. S., Muldoon, P. P., McIntosh, J. M. & Damaj, M. I. The $\alpha 3\beta 4^*$ nicotinic acetylcholine receptor subtype mediates nicotine reward and physical nicotine withdrawal signs independently of the $\alpha 5$ subunit in the mouse. *Neuropharmacology* **70**, 228–235 (2013).
 213. Toll, L. *et al.* AT-1001: A high affinity and selective $\alpha 3\beta 4$ nicotinic acetylcholine receptor antagonist blocks nicotine self-administration in rats. *Neuropsychopharmacology* **37**, 1367–1376 (2012).
 214. Harrington, L. *et al.* Role of $\beta 4^*$ Nicotinic Acetylcholine Receptors in the Habenulo-Interpeduncular Pathway in Nicotine Reinforcement in Mice. *Neuropsychopharmacology* **EPUB ahead**, 1–13 (2015).
 215. Fowler, C. D., Lu, Q., Johnson, P. M., Marks, M. J. & Kenny, P. J. Habenular Alpha5 nACh receptor signalling controls nicotine intake. *Nature* **471**, 597–601 (2011).
 216. Gorlich, A. *et al.* Reexposure to nicotine during withdrawal increases the pacemaking activity of cholinergic habenular neurons. *Proc. Natl. Acad. Sci.* **110**, 17077–17082 (2013).
 217. Pang, X. *et al.* Habenula cholinergic neurons regulate anxiety during nicotine withdrawal via nicotinic acetylcholine receptors. *Neuropharmacology* **107**, 294–304 (2016).
 218. Frahm, S. *et al.* Aversion to Nicotine Is Regulated by the Balanced Activity of $\beta 4$ and $\alpha 5$ Nicotinic Receptor Subunits in the Medial Habenula. *Neuron* **70**, 522–535 (2011).
 219. Ren, J. *et al.* Habenula ‘cholinergic’ neurons co-release glutamate and acetylcholine and activate postsynaptic neurons via distinct transmission modes. *Neuron* **69**, 445–52 (2011).
 220. Grady, S. R. *et al.* Rodent Habenulo-Interpeduncular Pathway Expresses a Large Variety of Uncommon nAChR Subtypes, But Only the $\alpha 3\beta 4$ and $\alpha 3\beta 3\beta 4$ Subtypes Mediate Acetylcholine Release. *J. Neurosci.* **29**, 2272–2282 (2009).
 221. Dao, D. Q., Perez, E. E., Teng, Y., Dani, J. a & De Biasi, M. Nicotine enhances excitability of medial habenular neurons via facilitation of neurokinin signaling. *J. Neurosci.* **34**, 4273–84 (2014).

222. Gardon, O. *et al.* Expression of mu opioid receptor in dorsal diencephalic conduction system: New insights for the medial habenula. *Neuroscience* **277**, 595–609 (2014).
223. Kitchen, I., Slowe, S. J., Matthes, H. W. & Kieffer, B. Quantitative autoradiographic mapping of mu-, delta- and kappa-opioid receptors in knockout mice lacking the mu-opioid receptor gene. *Brain Res* **778**, 73–88 (1997).
224. Mechling, A. E. *et al.* Deletion of the mu opioid receptor gene in mice reshapes the reward–aversion connectome. *Proc. Natl. Acad. Sci.* **113**, 11603–11608 (2016).
225. Hussain, R. J., Taraschenko, O. D. & Glick, S. D. Effects of nicotine, methamphetamine and cocaine on extracellular levels of acetylcholine in the interpeduncular nucleus of rats. *Neurosci. Lett.* **440**, 270–274 (2008).
226. Neugebauer, N. M. *et al.* Morphine dependence and withdrawal induced changes in cholinergic signaling. *Pharmacol. Biochem. Behav.* **109**, 77–83 (2013).
227. Darcq, E. *et al.* RSK2 signaling in medial habenula contributes to acute morphine analgesia. *Neuropsychopharmacology* **37**, 1288–1296 (2012).
228. Glick, S. D., Ramirez, R. L., Livi, J. M. & Maisonneuve, I. M. 18-Methoxycoronaridine acts in the medial habenula and/or interpeduncular nucleus to decrease morphine self-administration in rats. *Eur. J. Pharmacol.* **537**, 94–98 (2006).
229. Paris, J. M. & Cunningham, K. A. Habenula lesions decrease the responsiveness of dorsal raphe serotonin neurons to cocaine. *Pharmacol. Biochem. Behav.* **49**, 555–560 (1994).
230. McCallum, S. E. & Glick, S. D. 18-Methoxycoronaridine blocks acquisition but enhances reinstatement of a cocaine place preference. *Neurosci. Lett.* **458**, 57–59 (2009).
231. Khroyan, T. V., Yasuda, D., Toll, L., Polgar, W. E. & Zaveri, N. T. High affinity $\alpha 3\beta 4$ nicotinic acetylcholine receptor ligands AT-1001 and AT-1012 attenuate cocaine-induced conditioned place preference and behavioral sensitization in mice. *Biochem. Pharmacol.* **97**, 531–541 (2015).
232. Hammer Jr., R. P. & Cooke, E. S. Gradual tolerance of metabolic activity is produced in mesolimbic regions by chronic cocaine treatment, while subsequent cocaine challenge activates extrapyramidal regions of rat brain. *J Neurosci* **14**, 4289–4298 (1994).
233. Halawa, A. A., Damborsky, J. C., Slaton, G. S. & Winzer-Serhan, U. H. Activation of immediate early genes by nicotine after chronic neonatal nicotine exposure in brain areas involved in stress and anxiety responses. *Brain Res.* **1687**, 32–40 (2018).
234. James, M. H., Charnley, J. L., Flynn, J. R., Smith, D. W. & Dayas, C. V. Propensity to ‘relapse’ following exposure to cocaine cues is associated with the recruitment of specific thalamic and epithalamic nuclei. *Neuroscience* **199**, 235–42 (2011).
235. Mahler, S. V. & Aston-Jones, G. S. Fos Activation of Selective Afferents to Ventral Tegmental Area during Cue-Induced Reinstatement of Cocaine Seeking in Rats. *J. Neurosci.* **32**, 13309–13325 (2012).
236. Durkin, M. M., Gunwaldsen, C. a, Borowsky, B., Jones, K. a & Branchek, T. a. An in situ hybridization study of the distribution of the GABA(B2) protein mRNA in the rat CNS. *Brain Res. Mol. Brain Res.* **71**, 185–200 (1999).
237. Yamaguchi, M. *et al.* Repeated cocaine administration increases GABAB(1) subunit mRNA in rat brain. *Synapse* **43**, 175–180 (2002).
238. Rocha, B. A. *et al.* Cocaine self-administration in dopamine-transporter knockout mice. *Nat. Neurosci.* **1**, 132–137 (1998).
239. Carta, M., Allan, A. M., Partridge, L. D. & Valenzuela, C. F. Cocaine inhibits 5-HT₃receptor function in neurons from transgenic mice overexpressing the receptor. *Eur. J. Pharmacol.* **459**, 167–169 (2003).
240. Malvaez, M. *et al.* HDAC3-selective inhibitor enhances extinction of cocaine-seeking behavior in a persistent manner. *Proc. Natl. Acad. Sci. U. S. A.* **110**, 2647–52 (2013).
241. Mueller, D. & Stewart, J. Cocaine-induced conditioned place preference: Reinstatement by priming injections of cocaine after extinction. *Behav. Brain Res.* **115**, 39–47 (2000).
242. Pfaffl, M. W. *et al.* Real-time RT-PCR quantification of insulin-like growth factor (IGF)-1, IGF-1

- receptor, IGF-2, IGF-2 receptor, insulin receptor, growth hormone receptor, IGF-binding proteins 1, 2 and 3 in the bovine species. *Domest. Anim. Endocrinol.* **22**, 91–102 (2002).
243. Pfaffl, M. W. A new mathematical model for relative quantification in real-time RT-PCR. *Nucleic Acids Res.* **29**, 2003–2007 (2001).
244. Mittelstaedt, T. *et al.* Differential mRNA expression patterns of the synaptotagmin gene family in the rodent brain. *J. Comp. Neurol.* **512**, 514–28 (2009).
245. Wang, D. O. *et al.* A quick and simple FISH protocol with hybridization-sensitive fluorescent linear oligodeoxynucleotide probes. *Rna* **18**, 166–175 (2012).
246. Gomez, J. L. *et al.* Chemogenetics Revealed: DREADD Occupancy and Activation Via Converted Clozapine. *Science (80-.)*. **507**, 503–507 (2017).
247. Manvich, D. F. *et al.* The DREADD agonist clozapine N-oxide (CNO) is reverse-metabolized to clozapine and produces clozapine-like interoceptive stimulus effects in rats and mice. *Sci. Rep.* **8**, 1–10 (2018).
248. Padovan-Hernandez, Y. & Knackstedt, L. A. Dose-dependent reduction in cocaine-induced locomotion by Clozapine-N-Oxide in rats with a history of cocaine self-administration. *Neurosci. Lett.* **674**, 132–135 (2018).
249. Zhu, H. & Roth, B. L. Silencing Synapses with DREADDs. *Neuron* **82**, 723–725 (2014).
250. Lee, H.-M., Giguere, P. M. & Roth, B. L. DREADDs: novel tools for drug discovery and development. *Drug Discov. Today* **19**, 469–73 (2014).
251. Dong, S., Allen, J. A., Farrell, M. & Roth, B. L. A chemical-genetic approach for precise spatio-temporal control of cellular signaling. *Mol. Biosyst.* **6**, 1376–80 (2010).
252. Alexander, G. M. *et al.* Remote control of neuronal activity in transgenic mice expressing evolved G protein-coupled receptors. *Neuron* **63**, 27–39 (2009).
253. Rogan, S. C. & Roth, B. L. Remote control of neuronal signaling. *Pharmacol. Rev.* **63**, 291–315 (2011).
254. Armbruster, B. N., Li, X., Pausch, M. H., Herlitze, S. & Roth, B. L. Evolving the lock to fit the key to create a family of G protein-coupled receptors potently activated by an inert ligand. *Proc. Natl. Acad. Sci. U. S. A.* **104**, 5163–8 (2007).
255. Dong, S., Rogan, S. C. & Roth, B. L. Directed molecular evolution of DREADDs: a generic approach to creating next-generation RASSLs. *Nat. Protoc.* **5**, 561–73 (2010).
256. Vogel-Ciernia, A. & Wood, M. a. Examining object location and object recognition memory in mice. *Curr. Protoc. Neurosci.* **69**, 8.31.1-8.31.17 (2014).
257. Mumby, D. G. Perspectives on object-recognition memory following hippocampal damage: lessons from studies in rats. *Behav. Brain Res.* **127**, 159–181 (2001).
258. Mumby, D. G., Gaskin, S., Glenn, M. J., Schramek, T. E. & Lehmann, H. Hippocampal damage and exploratory preferences in rats: memory for objects, places, and contexts. *Learn Mem* **9**, 49–57 (2002).
259. Assini, F. L., Duzzioni, M. & Takahashi, R. N. Object location memory in mice: Pharmacological validation and further evidence of hippocampal CA1 participation. *Behav. Brain Res.* **204**, 206–211 (2009).
260. Dere, E., Huston, J. P. & De Souza Silva, M. a. The pharmacology, neuroanatomy and neurogenetics of one-trial object recognition in rodents. *Neurosci. Biobehav. Rev.* **31**, 673–704 (2007).
261. Winters, B. D., Saksida, L. M. & Bussey, T. J. Object recognition memory: Neurobiological mechanisms of encoding, consolidation and retrieval. *Neurosci. Biobehav. Rev.* **32**, 1055–1070 (2008).
262. Ennaceur, a. One-trial object recognition in rats and mice: Methodological and theoretical issues. *Behav. Brain Res.* **215**, 244–254 (2010).
263. Haettig, J., Sun, Y., Wood, M. a & Xu, X. Cell-type specific inactivation of hippocampal CA1 disrupts location-dependent object recognition in the mouse. *Learn. Mem.* **20**, 139–46 (2013).
264. Lambert, N. a, Borroni, a M., Grover, L. M. & Teyler, T. J. Hyperpolarizing and depolarizing

- GABAA receptor-mediated dendritic inhibition in area CA1 of the rat hippocampus. *J. Neurophysiol.* **66**, 1538–1548 (1991).
265. Arai, A., Silberg, J. & Lynch, G. Differences in the refractory properties of two distinct inhibitory circuitries in field CA1 of the hippocampus. *Brain Res.* **704**, 298–306 (1995).
 266. Kügler, S., Kilic, E. & Bähr, M. Human synapsin 1 gene promoter confers highly neuron-specific long-term transgene expression from an adenoviral vector in the adult rat brain depending on the transduced area. *Gene Ther.* **10**, 337–47 (2003).
 267. Grover, L. M. & Yan, C. Blockade of GABAA receptors facilitates induction of NMDA receptor-independent long-term potentiation. *J. Neurophysiol.* **81**, 2814–2822 (1999).
 268. Chapman, C. a, Perez, Y. & Lacaille, J. C. Effects of GABA(A) inhibition on the expression of long-term potentiation in CA1 pyramidal cells are dependent on tetanization parameters. *Hippocampus* **8**, 289–98 (1998).
 269. Mayford, M. *et al.* Control of memory formation through regulated expression of a CaMKII transgene. *Science* **274**, 1678–1683 (1996).
 270. Dittgen, T. *et al.* Lentivirus-based genetic manipulations of cortical neurons and their optical and electrophysiological monitoring in vivo. *Proc. Natl. Acad. Sci. U. S. A.* **101**, 18206–18211 (2004).
 271. Scheyltjens, I. *et al.* Evaluation of the expression pattern of rAAV2/1, 2/5, 2/7, 2/8, and 2/9 serotypes with different promoters in the mouse visual cortex. *J. Comp. Neurol.* **523**, 2019–2042 (2015).
 272. White, M. D., Milne, R. V. J. & Nolan, M. F. A Molecular Toolbox for Rapid Generation of Viral Vectors to Up- or Down-Regulate Neuronal Gene Expression in vivo. *Front. Mol. Neurosci.* **4**, 1–15 (2011).
 273. Winters, B. D. Double Dissociation between the Effects of Peri-Postrhinal Cortex and Hippocampal Lesions on Tests of Object Recognition and Spatial Memory: Heterogeneity of Function within the Temporal Lobe. *J. Neurosci.* **24**, 5901–5908 (2004).
 274. Winters, B. D. Transient Inactivation of Perirhinal Cortex Disrupts Encoding, Retrieval, and Consolidation of Object Recognition Memory. *J. Neurosci.* **25**, 52–61 (2005).
 275. Balderas, I. *et al.* The consolidation of object and context recognition memory involve different regions of the temporal lobe. *Learn. Mem.* **15**, 618–624 (2008).
 276. Bermudez-Rattoni, F., Okuda, S., Roozendaal, B. & McGaugh, J. L. Insular cortex is involved in consolidation of object recognition memory. *Learn. Mem.* **12**, 447–449 (2005).
 277. Rossato, J. I. *et al.* On the role of hippocampal protein synthesis in the consolidation and reconsolidation of object recognition memory. *Learn Mem* **14**, 36–46 (2007).
 278. Otto, T., Eichenbaum, H., Wible, C. G. & Wiener, S. I. Learning-related patterns of CA1 spike trains parallel stimulation parameters optimal for inducing hippocampal long-term potentiation. *Hippocampus* **1**, 181–192 (1991).
 279. Mathew, S. S. & Hablitz, J. J. Calcium release via activation of presynaptic IP3 receptors contributes to kainate-induced IPSC facilitation in rat neocortex. *Neuropharmacology* **55**, 106–16 (2008).
 280. Takahashi, A., Mikami, M. & Yang, J. Hydrogen peroxide increases GABAergic mIPSC through presynaptic release of calcium from IP3 receptor-sensitive stores in spinal cord substantia gelatinosa neurons. *Eur. J. Neurosci.* **25**, 705–16 (2007).
 281. Sik, a, Penttonen, M., Ylinen, a & Buzsáki, G. Hippocampal CA1 interneurons: an in vivo intracellular labeling study. *J. Neurosci.* **15**, 6651–6665 (1995).
 282. Klausberger, T. GABAergic interneurons targeting dendrites of pyramidal cells in the CA1 area of the hippocampus. *Eur. J. Neurosci.* **30**, 947–957 (2009).
 283. Gerlai, R., Henderson, J. T., Roder, J. C. & Jia, Z. Multiple behavioral anomalies in GluR2 mutant mice exhibiting enhanced LTP. *Behav. Brain Res.* **95**, 37–45 (1998).
 284. Kaksonen, M. *et al.* Syndecan-3-deficient mice exhibit enhanced LTP and impaired hippocampus-dependent memory. *Mol. Cell. Neurosci.* **21**, 158–172 (2002).
 285. Vaillend, C., Billard, J. M. & Laroche, S. Impaired long-term spatial and recognition memory and

- enhanced CA1 hippocampal LTP in the dystrophin-deficient Dmdmdx mouse. *Neurobiol. Dis.* **17**, 10–20 (2004).
286. Migaud, M. *et al.* Enhanced long-term potentiation and impaired learning in mice with mutant postsynaptic density-95 protein. *Nature* **396**, 433–439 (1998).
287. Nakauchi, S. *et al.* Early postnatal nicotine exposure causes hippocampus-dependent memory impairments in adolescent mice: Association with altered nicotinic cholinergic modulation of LTP, but not impaired LTP. *Neurobiol. Learn. Mem.* **118**, 178–188 (2015).
288. Nosten-Bertrand, M. *et al.* Normal spatial learning despite regional inhibition of LTP in mice lacking Thy-1. *Nature* **379**, 826–829 (1996).
289. Brakebusch, C. *et al.* Brevican-Deficient Mice Display Impaired Hippocampal CA1 Long-Term Potentiation but Show No Obvious Deficits in Learning and Memory Brevican-Deficient Mice Display Impaired Hippocampal CA1 Long-Term Potentiation but Show No Obvious Deficits in Learning an. **22**, 7417–7427 (2002).
290. Fowler, C. D. & Kenny, P. J. Habenular signaling in nicotine reinforcement. *Neuropsychopharmacology* **37**, 306–7 (2012).
291. Tuesta, L. M. *et al.* GLP-1 acts on habenular avoidance circuits to control nicotine intake. *Nat. Neurosci.* **20**, 708–716 (2017).
292. Antolin-Fontes, B., Ables, J. L., Görlich, A. & Ibañez-Tallon, I. The habenulo-interpeduncular pathway in nicotine aversion and withdrawal. *Neuropharmacology* (2014). doi:10.1016/j.neuropharm.2014.11.019
293. Lopez, A. J. *et al.* Promoter specific effects of DREADD modulation on synaptic plasticity and hippocampal learning. *J. Neurosci.* **36**, 3588–3599 (2015).
294. Harris, J. a. *et al.* Anatomical characterization of Cre driver mice for neural circuit mapping and manipulation. *Front. Neural Circuits* **8**, 1–16 (2014).
295. Kerstetter, K. A. *et al.* Corticostriatal Afferents Modulate Responsiveness to Psychostimulant Drugs and Drug-Associated Stimuli. *Neuropsychopharmacology* **41**, 1128–1137 (2016).
296. Mahler, S. V *et al.* Designer receptors show role for ventral pallidum input to ventral tegmental area in cocaine seeking. *Nat. Neurosci.* 1–11 (2014). doi:10.1038/nn.3664
297. Ferguson, S. M. *et al.* Transient neuronal inhibition reveals opposing roles of indirect and direct pathways in sensitization. *Nat. Neurosci.* **14**, 22–4 (2011).
298. Scofield, M. D. *et al.* Gq-DREADD selectively initiates glial glutamate release and inhibits cue-induced cocaine seeking. *Biol. Psychiatry* **78**, 441–451 (2015).
299. Augur, I. F., Wyckoff, A. R., Aston-Jones, G., Kalivas, P. W. & Peters, J. Chemogenetic Activation of an Extinction Neural Circuit Reduces Cue-Induced Reinstatement of Cocaine Seeking. *J. Neurosci.* **36**, 10174–80 (2016).
300. Hsu, Y.-W. a *et al.* Role of the dorsal medial habenula in the regulation of voluntary activity, motor function, hedonic state, and primary reinforcement. *J. Neurosci.* **34**, 11366–84 (2014).
301. Qin, C. & Luo, M. Neurochemical phenotypes of the afferent and efferent projections of the mouse medial habenula. *Neuroscience* **161**, 827–37 (2009).
302. Tuesta, L. M., Fowler, C. D. & Kenny, P. J. Recent advances in understanding nicotinic receptor signaling mechanisms that regulate drug self-administration behavior. *Biochem. Pharmacol.* **82**, 984–95 (2011).
303. Guettier, J.-M. *et al.* A chemical-genetic approach to study G protein regulation of cell function in vivo. *Proc. Natl. Acad. Sci.* **106**, 19197–19202 (2009).
304. Werme, M., Ringholm, A., Olson, L. & Brene, S. Differential patterns of induction of NGFI-B, Nor1 and c-fos mRNAs in striatal subregions by haloperidol and clozapine. *Brain Res.* **863**, 112–119 (2000).
305. Filip, M., Bubar, M. & Cunningham, K. Contribution of serotonin (5-hydroxytryptamine; 5-HT) 5-HT2 receptor subtypes to the hyperlocomotor effects of cocaine: acute and chronic pharmacological analyses. *J. Pharmacol. ...* **310**, 1246–1254 (2004).
306. Kwapis, J. L. *et al.* Context and Auditory Fear are Differentially Regulated by HDAC3 Activity in

- the Lateral and Basal Subnuclei of the Amygdala. *Neuropsychopharmacology* **42**, (2017).
307. Michelhaugh, S. K. *et al.* Dopamine neurons express multiple isoforms of the nuclear receptor nurr1 with diminished transcriptional activity. *J. Neurochem.* **95**, 1342–1350 (2005).
 308. Hemstedt, T. J., Bengtson, C. P., Ramírez, O., Oliveira, A. M. M. & Bading, H. Reciprocal Interaction of Dendrite Geometry and Nuclear Calcium–VEGFD Signaling Gates Memory Consolidation and Extinction. *J. Neurosci.* **37**, 6946–6955 (2017).
 309. Finegersh, A. & Homanics, G. E. Chromatin immunoprecipitation and gene expression analysis of neuronal subtypes after fluorescence activated cell sorting. *J. Neurosci. Methods* **263**, 81–88 (2016).
 310. Alaghband, Y. *et al.* Distinct roles for the deacetylase domain of HDAC3 in the hippocampus and medial prefrontal cortex in the formation and extinction of memory. *Neurobiol. Learn. Mem.* **145**, (2017).
 311. Sun, Z. *et al.* Deacetylase-Independent function of HDAC3 in transcription and metabolism requires nuclear receptor corepressor. *Mol. Cell* **52**, 769–782 (2013).
 312. Bannon, M. J. *et al.* Decreased expression of the transcription factor NURR1 in dopamine neurons of cocaine abusers. *Proc. Natl. Acad. Sci. U. S. A.* **99**, 6382–6385 (2002).
 313. Alberini, C. M., Ghirardi, M., Metz, R. & Kandel, E. R. C/EBP is an immediate-early gene required for the consolidation of long- term facilitation in Aplysia. *Cell* **76**, 1099–1114 (1994).
 314. Taubenfeld, S. M., Milekic, M. H., Monti, B. & Alberini, C. M. The consolidation of new but not reactivated memory requires hippocampal C/EBPbeta. *Nat. Neurosci.* **4**, 813–818 (2001).
 315. Robert, I., Sutter, A. & Quirin-Stricker, C. Synergistic activation of the human choline acetyltransferase gene by c-Myb and C/EBPbeta. *Brain Res. Mol. Brain Res.* **106**, 124–35 (2002).
 316. Malvaez, M. *et al.* Habits Are Negatively Regulated by Histone Deacetylase 3 in the Dorsal Striatum. *Biol. Psychiatry* 1–10 (2018). doi:10.1016/j.biopsych.2018.01.025